"GENETIC MAPPING AND MOLECULAR CHARACTERIZATION OF *tbr1* MUTANT IN *ARABIDOPSIS THALIANA*"

Dissertation

Zur Erlangung des akademischen Grades
Doktor der Naturwissenschaften (Dr. rer. nat.)
der Mathematisch-Naturwissenschaftlichen Facultät
der Universität Potsdam

A thesis submitted for the degree of Doctor of Philosophy (PhD) to
the University of Potsdam

ANA-SILVIA NITA

Potsdam, June 2005

ACKNOWLEDGEMENTS

I would like to thank and express my gratitude to Prof. Dr. Mark Stitt, Director of Max-Planck-Institute of Molecular Plant Physiology (MPIMP), Golm, for reviewing my thesis and opportunity to accomplish my thesis in the institute.
I would like to thank to my direct supervisor the leader of Molecular Genomics Group, Dr. Wolf-Rüdiger Scheible, for his supervision during my thesis work.
My very special thanks and gratitude to Prof. Dr. Thomas Altmann for closely following the project, for valuable suggestions and his kindness to review my work progress reports over the three years and the final thesis work.
Many thanks also to Dr. Markus Pauly, for his comments and suggestions, as one of the additional supervisors to follow the project progress.
I would like to thank all the members (present and former) of Molecular Genomics Group –, Dr. Daniel Osuna, Dr. Jens-Hölger Dieterich, Ms. Grit Rubin, Ms. Uta Deiting, Ms. Dana Schindelasch, Mr. Volker Bischoff, Ms. Bhavani Sundaram, Mr. Bikram Datt Pant, Ms. Franczeska Colle, Ms Magdalena Musialak, Ms. Christine Majer, and Ms. Dana Hoser and especially to Dr. Rajendra Bari and Dr. Andrej Kochevenko, for their cooperation and good working environment in the lab.
Thanks to Dr. Kim Larsen for gas-chromatography analyses (Plant cell wall group).
I would like to thank Dr. Nicolai Obel and Veronica Erben (Plant cell wall group) for their kindness to help with MALDI-TOF analyses.
I am grateful to Anja Kuschinsky, for help regarding cell wall polysaccharides immunolabeling experiment.
Thanks to Dr. Manfred Pinnow,(Fraunhofer Institute), for the scanning electron microscopy analysis.
I also want to thank to the Gardeners team, especially Mr. Torsten Schülze and Mr. Frank Hühn, for the very good care of the plants in the green house.

I thank so much and I am very grateful to my dear family, my father-Ion and my mother-Maria, for their help and forever support and understanding, to Bogdan Nicola and my sister-Veronica for all her love and daily e-mails to keep me up-dated.

I take the chance to thank and express my gratitude to my friends for their encouragements, advices and understanding: Ljubisa Jovanovic, Cristian Munteanu, Lucian & Monica Postelnicu, Laura Olariu, Florin Vladescu, Mihaela & Viorel Rusu.
As long as I had to always speak English in the institute and write my thesis in English, I definitely need to thank to my dear English teacher, Daniela Bordei; she did a good job.

TABLE OF CONTENTS

1. CHAPTER: INTRODUCTION

Plant cells are usually enclosed by a more or less rigid cell wall, which contains mostly cellulose. As the outermost layer of the plant cell, the wall has important roles in adhesion, cell-cell signalling, transport and distribution of water and minerals, and in defence act (Darvill *et al*., 1980). It also maintains the internal turgor pressure (Bacic *et al*., 1998), and participates in numerous growth and differentiation processes. As a natural product, the plant cell wall provides the raw material for production of paper, textiles, lumber, and a wide variety of polymers used to make films, plastics, coatings, adhesives, and thickeners in numerous final products (Lapasin and Pricl, 1995). Cellulose is the most abundant polymer in the plant cell wall, which is the major source for cellulose production (Brown, 1996). As the most abundant reservoir of organic carbon in the biosphere, the plant cell wall greatly impacts many ecological processes (Cosgrove, 1997).

1.1 CELL WALL STRUCTURE AND FUNCTION

The main components of the cell wall are: cellulose, hemicellulose, pectic polysaccharides, lignin, suberin, wax, cutin, proteins and water. The general cell wall structure consists of two to three different layers: (1) a middle lamella, which is the outermost layer, composed primarily of pectic polysaccharides, (2) a primary wall comprised of cellulose, hemicellulose, pectic polysaccharides and proteins, and (3) in cells of some tissues, a secondary cell wall that is deposited onto the primary cell wall, and consists mainly of cellulose.

The middle lamella forms the interface between the primary walls of neighbouring cells. The primary cell wall is able to expand, allowing cell growth and thus increasing the surface area of the cells. Some cells deposit additional layers inside the primary cell wall to form the secondary cell wall. This occurs after growth stops or when the cells begin to differentiate. This secondary wall is usually much thicker than the primary wall, and its role is mostly for support. It is comprised mainly of cellulose and lignin and it cannot expand due to its high lignin content, the presence of other cross-linking components, such as ferulic acids and elevated levels of cellulose. It develops by successive encrustation and deposition of cellulose fibrils and other components (Figure 1). The secondary wall may completely

surround a cell or may be formed only in localized regions producing, for example, spirally thickened tracheary elements (Mc Cann *et al*., 1990).

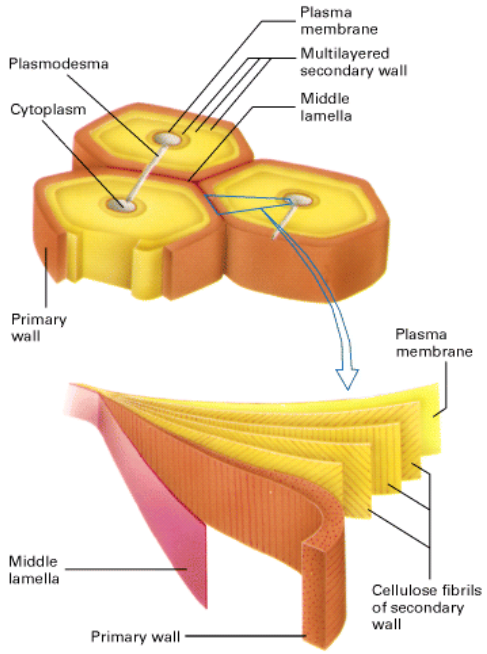

Figure 1: **The structure of the secondary cell wall, built up of a series of layers of cellulose**. The cell wall between two cells comprises three distinct layers: the middle lamella, the primary cell wall and the secondary cell wall. Cellulose fibrils of the secondary wall are paralleloriented to each other and the orientation changes from layer to layer. The connection between two neighbour cells is made by plasmodesma (reproduced from Lodish *et al.,* 2000).

The primary wall structure is the same in nearly all cell types and species. In contrast, in the case of secondary cell walls, there are differences based on the cell type and species-specificity. In both, the primary and secondary cell walls there are cellulose microfibrils, embedded in an amorphous substance, called the matrix. Matrix materials are heteropolymers that are generally grouped into two families of polysaccharides: pectins and hemicelluloses (Figure 2).

Cellulose chains form crystalline structures, the microfibrils. During the development of the secondary wall they are deposited in layers (as lamellae), and the microfibrils of each layer are parallel to each other (parallel texture). However, their orientation changes from layer to layer (Mc Cann *et al*., 1990).

Cell wall expansion is generally well coordinated with wall polymer synthesis and secretion. For instance, the rate of wall deposition in young stems and roots is highest in the zone of maximal cell expansion (Silk, 1984).

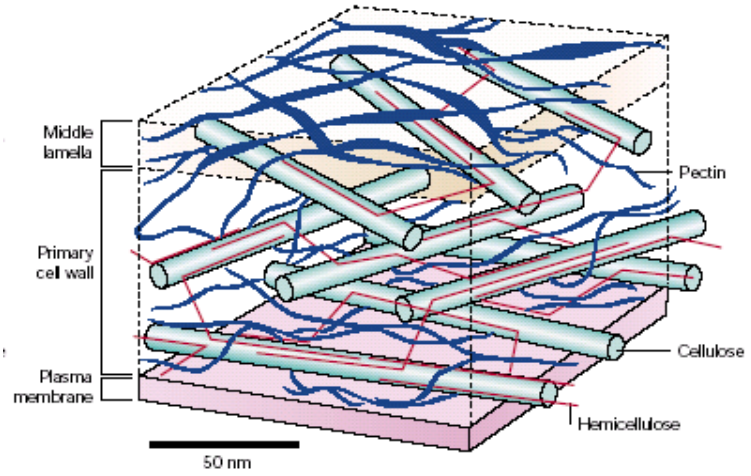

Figure 2: Plant cell wall structure, a model showing the main structural components and their arrangement. Cellulose fibrils are embedded in the matrix materials consisting mainly of pectins and hemicelluloses (reproduced from McCann *et al.,* 1990).

The predominant polysaccharide of the cell wall is cellulose (30%), which is present as long, unbranched fibrils, composed of approximately 30 to 36 hydrogen bounded chains of β-1,4-glucose (Figure 3).

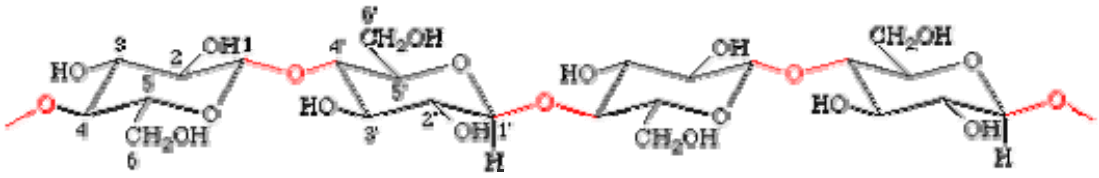

Figure 3: Cellulose molecular model

In microfibrils, the multiple hydroxyl groups are hydrogen bond with each other, holding the chains firmly together and contributing to their high tensile strength. This strength is important in cell walls, where they are meshed in the carbohydrate matrix, helping to maintain rigidity and support the plants.

Cellulose is an excellent fibre. Wood, cotton, and hemp rope are all made of fibrous cellulose. Cellulose contains (1, 4)-β-glucopyranose residues associated in glucan chains, and can exist in a crystalline or non-crystalline state. Crystalline cellulose has at least two distinct allomorphs: cellulose I and cellulose II. In the first type, the glucan chains are exclusively oriented parallel to each other, and this form is thermodynamically metastable. Cellulose II is the form most commonly found in nature and it is the more thermodynamically stable

allomorph. Glucan chains are oriented in an antiparallel manner. The chains may or may not be folded.
Cellulose I can be converted directly to cellulose II, but not vice versa. Plants produce mainly cellulose I (http://www.lsbu.ac.uk/water/hycel.html).

Hemicelluloses, which tipically comprise 30% of the cell wall, are branched polysaccharides containing backbones of neutral sugars that can form hydrogen bonds with the surface of cellulose fibrils (Carpita and Gibeaut, 1993). Xyloglucans (XGs) are major components of the hemicelluloses. Xyloglucan has a backbone composed of 1,4-linked β-D-glucose-pyranosyl residues. Up to 75% of these residues are substituted at O6 with mono-, di-, or triglycosyl side chains containing xylose, galactose, or fucose. A convention has been adopted to describe certain ubiquitous side chains of XG in which the entire side chain including the glucan backbone residues is designed by a single letter code on the basis of its terminal sugar (Figure 4).

Code letter	Represented structure
G (Glucose)	-ß-D-Glc*p*-
X (Xylose)	α-D-Xyl*p*-(1→6)┐ -ß-D-Glc*p*-
L (gaLactose)	ß-D-Gal*p*-(1→2)-α-D-Xylp-(1→6)┐ -ß-D-Glc*p*-
F (Fucose)	α-L-Fuc*p*-(1→2)-ß-D-Gal*p*-(1→2)- α-D-Xyl*p*-(1→6)┐ -ß-D-Glc*p*-

Figure 4: One-letter codes for the differently substituted backbone β-D-glycosyl residues in xyloglucans present in *Arabidopsis thaliana*. There are additional letter codes for xyloglucans (XGs) (not shown here) occurring in different plant species; *p*- denotes the pyranose form of the sugar (Fry *et al.*, 1993).

The typical structures of the subunits in these xyloglucans are shown below (Figure 5).

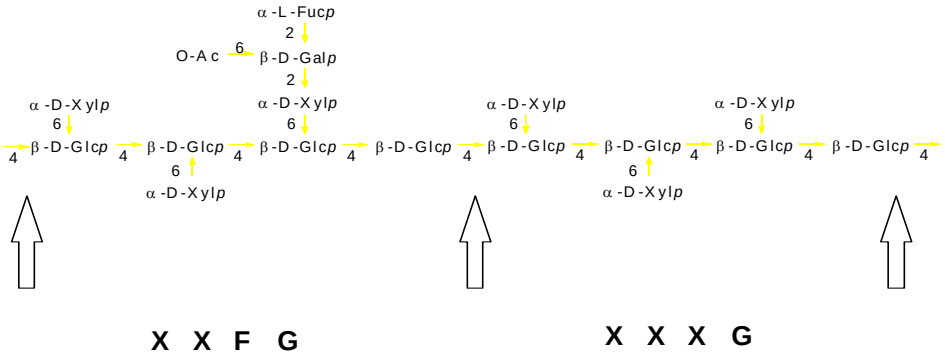

Figure 5: General structure of xyloglucan (XG). The one letter XG nomenclature for each of the substituted β-D-glucosyl residues is shown below the structure. XGs can be depolymerised with endoglucanase, which hydrolyses the XG-backbone at the unsubstituted β-glucosyl residues (see arrows), yielding XG-oligosaccharides (XGOs).

Cellulose is relatively stable in growing cells and exhibits only a slight turnover, whereas xyloglucan turnover is significant (Nishitani and Matsuda, 1982).

In addition to xyloglucan, other hemicelluloses, such as: xylans, arabinoxylans, and mannans may bind to cellulose.

In the primary wall of dicotyledonous plants, the most abundant hemicellulose is xyloglucan. Monocotyledonous plants are divided into two classes: commelinoid and non-commelinoid. The commelinoid cell walls have glucuronoarabinoxylans as the major non-cellulosic polysaccharides. The primary cell wall of the grasses differ from other commelinoid cell walls in containing branched arabinoxylans and mixed-link β-glucans, as the most abundant non-cellulosic polysaccharides (Carpita and Gibeaut, 1993). In contrast, the composition of the primary cell walls of the non-commelinoid monocots is similar to that of the primary cell walls of most dicots (Harris *et al.,* 1997).

Coexisting with the cellulose-hemicellulose network in the cell wall structure, there is another interweaving polymer network, which consists of pectins (35%). Pectins are a heterogeneous group of polysaccharides that are rich in glucuronic acid (GlcA) and 1,4 linked α-D-galacturonic acid (GalA) residues. The pectic polysaccharides include: homogalacturonan (HGA), rhamnogalacturonan I (RG-I) and rhamnogalacturonan II (RG-II). Homogalacturonans are homopolymers of 1,4-α-D-GalA with occasional branching of β-D-Xyl linked to GalA residues, forming a xylogalacturonan. The rhamnogalacturonan I backbone contains repeats of the disaccharide 1,2-α-L-Rha-1,4-α-D-GalA, with rhamnose residues further substituted with other linear and branched polysaccharides such as 1,5-α-L-arabinans and 1,4-β-D-

arabinogalactans. Rhamnogalacturonan II is a substituted galacturonan with a backbone of 1,4-α-D-GalA residues that has four structurally different oligosaccharides side chains at different locations (Ridley *et al.,* 2001).

In the cell wall, cellulose is associated with hemicelluloses via a mixture of hydrogen and hydrophobic bonding and physical entrapment, whereas pectins form a gel around the cellulose-hemicellulose network (Carpita and Gibeaut, 1993).

Polysaccharide synthesis can be divided into four distinct stages: 1) the production of activated nucleotide-sugar donors, 2) the initiation of polymer synthesis, 3) polymer elongation, and 4) the termination of synthesis (Delmer and Stone, 1988). The key enzymes in cell wall biogenesis are the polysaccharide (glycan) synthases and glycosyl transferases (GT) that catalyse formation of the bonds between adjacent monosaccharides from activated nucleotide-sugar donors.

The sugar units used for the synthesis of polysaccharides derive from nucleotide sugars made in the cytoplasm. There are two alternative pathways for nucleotide sugar production that can function: 1) the salvage pathway, which recycles sugars released from the wall during assembly and turnover by the sequential action of monosaccharide kinases and nucleotide sugar pyrophosphorylases (Feingold and Avigad, 1980); and 2) the myo-inositol pathway, in which myo-inositol is oxidised to glucuronic acid (GlcA), then activated to UDP-GlcA. The epimerization of UDP-GlcA results in UDP-GalA, the activated precursor for incorporation of galacturonic acid (GalA) into the backbone of pectic polysaccharides. UDP-GlcA is also the precursor in the synthesis of UDP-Xylose and UDP-Arabinose (Feingold and Avigad, 1980).

Complex (branched) non-cellulosic and pectic polysaccharides are synthesized within the endoplasmic reticulum and Golgi apparatus (Gibeaut and Carpita, 1994). The plant Golgi apparatus has a dynamic organization. The functional unit is the individual dictyosome, which displays a distinct *cis*-to-*trans* polarity, its associated trans-Golgi network, and the Golgi matrix that surrounds both structures (Staehelin and Moore, 1995). The Golgi apparatus is responsible for synthesis of wall matrix polysaccharides that bind to and surround cellulose microfibrils. Antibodies to carbohydrate epitopes have been used to locate xyloglucans in the *trans*-Golgi cisternae and *trans*-Golgi network, and unesterified pectin in the *cis* and medial Golgi cisternae. Methyl-esterified pectin was found in medial and *trans* cisternae, suggesting that backbone synthesis is initiated in the *cis* and medial Golgi cisternae and methyl esterification takes place in the other cisternae.

In addition to these polysaccharides, the plant cell wall also contains a range of proteins (1-5%) which are implicated in the organisation and metabolism of the cell wall. The structural proteins can be classified into five main families: 1) extensins rich in hydroxyproline (HRGP), 2) proteins rich in glycine (GRP) (Ringli *et al*., 2001), 3) proteins rich in proline (PRP), 4) lectins, and 5) proteins associated with arabinogalactans (AGP). It is worth noting that structural proteins vary greatly in their abundance, depending on the cell type, developmental stage, and environmental stimuli. Wounding, pathogen attack, and treatment with elicitors increase the expression of many of these proteins, and wall structural proteins are often localized to specific cell and tissue types (Showalter, 1993). Studies of HRGPs suggest that these proteins are involved in protection against pathogens and desiccation, and in structural strengthening of walls (Tire *et al.,* 1994). AGPs show specific binding to pectins, and are therefore thought to be involved in cell adhesion. AGPs are also implicated in the growth, nutrition, and guidance of pollen tubes through stylar tissues (reviewed by Cosgrove, 1997).

Numerous enzymes may be found associated with cell walls. Cell wall enzymes can also be grouped into families, according to their function: (1) peroxidases that participate in the lignification processes of the cell wall; (2) transglycosidases that catalyse the breaking and forming of glycosidic bonds in the cell wall; (3) a large number of hydrolases (glycosidases, glucanases, cellulases, polygalacturonases, etc.) and, just as important, (4) esterases, a group of enzymes which are necessary for the efficient degradation of the cell wall; (5) "expansins", the proteins capable of breaking the hydrogen bonds between cellulose microfibrils and xyloglucans (Showalter, 1993).

1.2 CELLULOSE SYNTHASES IN *ARABIDOPSIS THALIANA*

In the native cellulose biogenesis, the microfibril shape, size, and also the direction of the microfibril assembly, appear to be determined by a multimeric enzyme complex that resides in the plasma membrane. This complex, known as a terminal complex (TC), or rosette was discovered through electron microscopy of freeze fracture replicas (Brown *et al*., 1996; Kimura *et al*., 1999), and it is one of the largest protein complexes known in plants. It can be observed in mosses, ferns, algae and vascular plants (Brown, 1996; Delmer, 1999). There are six particles, arranged in a hexagonal shape, constituting the terminal complex (TC), (~25 nm in diameter), and each particle in turn is believed to consist of six catalytic cellulose synthase subunits (Figure 6) and additional, as yet unknown, protein components (Delmer, 1999). They are named CesA, as accepted term for all catalytic subunits within the complex. Although the

complex resides in the plasma membrane, rosettes are assembled in the Golgi apparatus and then transported to the plasma membrane (Haigler and Brown, 1986).

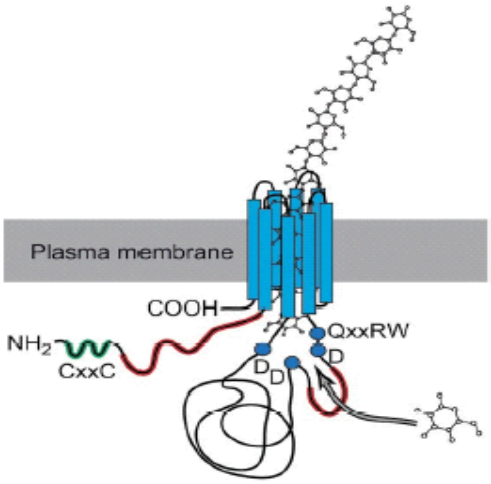

Figure 6: **Suggested topology of a cellulose synthase catalytic subunit**. The transmembrane helices of the CesA protein are thought to form a pore in the plasma membrane through which the growing glucan chain passes. The large central domain folds in a way to bring together the conserved regions containing the 3-D (invariant region) residues and the QxxRW motif (where X is any aminoacid), which are believed to be important for substrate binding and catalysis. The conserved regions (CR-P) and hypervariable (HVP) plant specific regions are placed in the cytoplasm where they may interact with other proteins (reproduced from Richmond T., 2000; Delmer, 1999).

As cellulose is a major component of all higher plant cell walls, CesA proteins are expressed in all tissues and cell types of the plant. They are required for both, the formation of short cellodextrins primers as well as long cellulose chains, suggesting that *CesA* genes may have different functions (Peng *et al.*, 2002). Recently, genetic approaches have been used successfully to show that the cellulose synthase subunits in a single particle are not all derived from the same *CesA* gene, but rather from two or three genes (Taylor *et al.*, 2000; Scheible *et al.*, 2001; Taylor *et al.*, 2003). Each subunit may require three dimers for its formation and they may be necessary for the assembly of six glucan chains.

It is thought that CesA is member of this protein complex which appears to consist of six large subunits, arranged in a hexagonal pattern. In order to generate a cellulose microfibril, known to contain at least 36 glucan chains, all six subunits of the rosette terminal complex would need to be specifically associated with one another (D. Delmer, 1999).

1.3 CELLULOSE SYNTHESIS MECHANISM

Cellulose is made at the cell surface. In contrast to other cell wall polysaccharides, which are synthesized in two steps in the endoplasmic reticulum and the Golgi apparatus, and afterwards carried to the cell surface by transporting vesicles (Staehelin *et al.*, 1995; Perrin *et al.*, 2001), cellulose is thought to be synthesized by the plasma membrane bound complex-rosette. Cellulose biosynthesis proceeds in at least two stages, first, polymerization and second -crystallization. The first stage is catalyzed by the enzyme cellulose synthase, and the second stage is dependent on the organization of the cellulose synthases, possibly with other proteins, such that the glucan chains are assembled in their final, crystalline form.

The catalytic subunit is a transmembrane protein with a number of transmembrane regions. It is generally accepted that uridine 5'diphosphate (UDP)-glucose is the donor for glucose in the polymerizing reaction to finally form cellulose. UDP-D-glucose is produced from sucrose by the action of sucrose-synthase (SuSy) (Amor *et al.*, 1995). This enzyme plays an important role in cellulose metabolism during rapid secondary cell wall biogenesis, providing the substrate directly to cellulose synthase. The catalytic subunit has to bind to the substrate, UDP-glucose, and to the end of the growing glucan chain. During polymerization, two UDP-glucose molecules simultaneously bind adjacent to each other, but at 180 degrees orientation, resulting in a double addition of two glucose residues for each catalytic cycle.

Further metabolic studies have led the authors to propose a biosynthetic pathway for cellulose that starts with the transfer of a glucose residue from the soluble cytoplasmic substrate, uridine 5'diphosphate (UDP)- glucose onto sitosterol, to form sitosterol β-glucoside (SG) on the inner side of the plasma membrane (Delmer 1999; Cantatore *et al.*, 2000). Sitosterol-glucoside then acts as a primer, initiating the polymerization of glucan chains, catalyzed by CesA proteins of the cellulose synthase complex. The result is the formation of cellodextrins (sitosterol-cellodextrins (SCD)), that are lipid linked oligosaccharides (Peng *et al.*, 2002; Perrin *et al.*, 2001). The cellodextrins may be cleaved from the sitosterol primer by Korrigan endocellulase/IRX2 (Nicol *et al*., 1998; His *et al*., 2001; Szyjanowicz *et al*., 2004), the active site of which is predicted to be located on the outer face of the plasma membrane. Further elongation of the cellodextrins, catalyzed by the same or different CesA proteins, produces the glucan chains of cellulose, which then form the microfibrils (Figure 7).

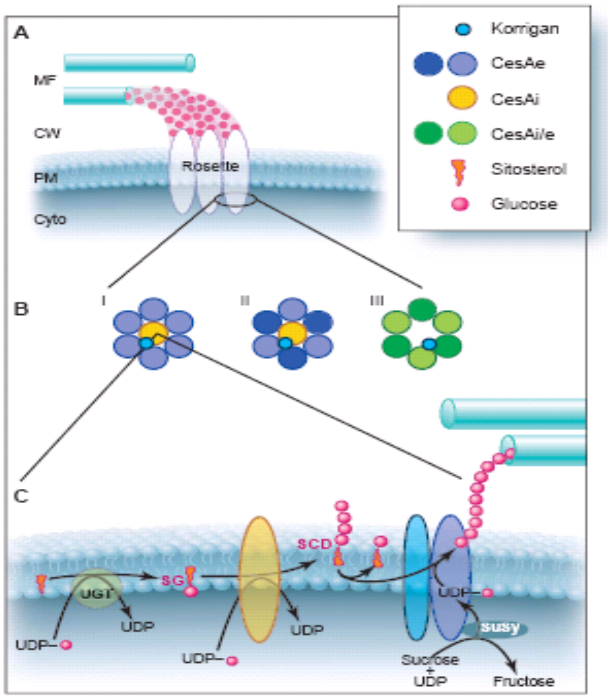

Figure 7: Cellulose synthesis mechanism. The cellulose synthase rosette is located in the plant cell plasma membrane. (A) Longitudinal view of the rosette, composed of six elementary particles, during elongation of cellulose microfibrils (MF). Sucrose synthase (SuSy) on the cytoplasmic face of the plasma membrane (PM) may channel UDP-glucose to the 36 growing glucan chains, which are extruded into the plant cell wall where they coalesce to form microfibrils. (B) Possible substructures within one elementary particle of the rosette. (i) The particle contains six elongating polypeptides (CesAe), one initiating polypeptide (CesAi), and one copy of Korrigan cellulase. (ii) The particle contains three copies each of two types of elongating polypeptide (CesAe), one initiating polypeptide (CesAi), and one copy of Korrigan cellulase. (iii) The particle contains three copies each of two types of polypeptide that both initiate synthesis and promote chain elongation (CesAi/e), and one copy of Korrigan cellulase. (C) Initiation of cellulose synthesis. UDP-glucosyl transferase (UGT) transfers a glucose residue onto a sitosterol molecule on the cytoplasmic face of the plasma membrane, forming sitosterol-β-glucoside (SG). The short glucose chain is extended with UDP-glucose by an initiating CesAi subunit to form an sitosterolcellodextrins (SCD), which "flips" to the outer face of the plasma membrane. The cellodextrin chain is then cleaved by Korrigan cellulase, binds to the elongating CesAe, and is extended into a glucan chain by addition of UDP-glucose provided by sucrose synthase (Steve M. Read and Tony Bacic, 2002, adapted principally from Scheible *et. al.,* 2001 and R. M. Brown and I. M. Saxena, 2000).

In contrast, several other studies showed that no exogenous primer was required to initiate cellulose synthesis *in vitro*, raising doubts about the proposed involvement of sterol β-glucoside as a primer (Peng *et al.,* 2002). However, the discrepancy between *in vivo* and *in vitro* requirements for cellulose in bacterial cellulose synthesis, highlights the notion that *in vitro,* the conditions may not accurately reflect the *in vivo* situation (Somerville *et al.*, 2004). Several *CESA* genes appear to be expressed throughout plants (Scheible *et al.*, 2001), even though cellulose synthesis is thought to be largely confined to expanding cells. This raises the possibility that cellulose synthesis is controlled posttranscriptionally (Somerville *et al*., 2004).

Although generally considered a plant material, cellulose is also produced by some bacteria. A model system to study microfibril formation is represented by *Acetobacter xylinum*, which normally forms large, highly ordered cellulose microfibrils. A typical single cell can convert up to 108 glucose molecules per hour into cellulose. In the bacterium, the enzyme cellulose synthase is present on the cytoplasmic membrane, and unlike higher plant cellulose synthases, the bacterial synthases remain active when isolated. The cellulose product is obtained extracellularly and is much purer then the one synthesized by higher plants.
The cellulose synthesizing bacterium, *Acetobacter xylinum*, has linear TCs composed of a row of particles on the plasma membrane. On the surface of the bacterial cell, rows of pores characteristically secrete mini-crystals of glucan chains which extrude and then coalesce into microfibrils. Clusters of microfibrils result in a compound structure known as the ribbon, and the ribbons, synthesized by many cells, aggregate, resulting in the formation of a gel-like sheet. This bacterium is widely used as a model system of cellulose biosynthesis and its crystallization, because it can be easily maintained in culture and the synthesized cellulose is directly influenced by many types of reagents added to the medium (Brown, 1996). When *Acetobacter xylinum* produces cellulose in the presence of materials that bind to β-1,4-glucans, the resulting microfibrils are altered in shape, being more fragmented and frayed (Saxena *et al.*, 1994; Haigler *et al.*, 1982; Hayashi *et al.*, 1987), and give X-ray diffraction patterns that appear to resemble more closely those of microfibrils synthesized by land plants (Atalla *et al*., 1993). Such result suggests that hemicellulose entrapment in muro, significantly alters microfibril morphology. This is also consistent with the fact that cotton fibres have low hemicellulose content and highly crystalline cellulose.

Homologues (*CelA*) of bacterial cellulose synthase genes have been also identified in cotton (Pear *et al.*, 1996). *CelA* contains UDP-glucose binding domains characteristic of glucosyl transferase catalytic sites, and its pattern of expression during cotton fibre development, coincides with the pattern of cellulose deposition.

1.4 MUTANTS IN THE *ARABIDOPSIS THALIANA* CELLULOSE SYNTHASE GENES

The family of (true) cellulose synthase (*CesA*) genes is composed of ten members in *Arabidopsis thaliana*. *CesA* family genes have 10–14 exons and are distributed across all five chromosomes. They contain the conserved D,D,D,QXXRW motif, which is characteristic of

processive β-glycosyltransferases (Saxena *et al.*, 1995), eight membrane spanning regions, and a putative zinc-binding domain that may be involved in protein-protein interaction. There are already some general characteristics known regarding *CesA* expression: 1) the family members are expressed to varying levels, for example, *AtCesA1* is much more highly expressed than *AtCesA9* (Turner and Somerville 1997; Taylor *et al.*, 1999; M. Doblin, unpublished); 2) they are also expressed in multiple tissues that relate to their expression in specific cell types, common to these tissues. For instance, *AtCesA7* mutant -*irx3*- shows a collapsed xylem phenotype throughout the plant, within leaves hypocotyls, stem and root (Turner and Somerville, 1997; Taylor *et al.*, 1999; Arioli *et al.*, 1998; Willimson *et al.*, 2001); 3) multiple *CesA* genes are expressed in the same cell type. It was shown that *AtCesA 1, 3*, and *6*, all exhibit a very similar expression pattern, being expressed in cells undergoing expansion in tissues such as the root and hypocotyl among others (Arioli *et al.*, 1998; Fagard *et al.*, 2000; Scheible *et al.*, 2001; Williamson *et al.*, 2001).

The new work raises the possibility that plants contain many *CesA* genes, thus one CesA protein could catalyze chain initiation on the SG (sitosterol-glucoside) primer, whereas another could catalyze the elongation step. Alternatively, different CesA proteins might be required for assembly of the rosette complex, or for the elongation reaction itself (Steve M. Read and Tony Bacic, 2002).

Plants with mutations in a particular *CesA* gene show reduced cellulose synthesis only in particular cell types or at specific life-cycle stages, resulting in distinct phenotypes.

Classical genetic mutants in several of these genes have already been isolated based on their strong phenotypes. For example, the *rsw1* mutant displays a severe, conditional (temperature dependent) radially swollen root phenotype. Based on this phenotype, the *RSW1* gene was positionally cloned and shown to encode the highly and almost ubiquitously (roots, leaves, flowers, seeds) expressed *CesA1* gene, that is required for primary cellulose biosynthesis throughout the plant. Epidermal cells of all plant organs are affected in the mutant. The *rsw1-1* mutation is believed to cause disassembly of the plasma membrane rosette complex (Turner and Somerville, 1997; Arioli *et al.*, 1998).

Specific mutations in the highly expressed *CesA3* gene of *Arabidopsis thaliana* (1) have been shown to confer resistance to the cellulose synthesis inhibitor isoxaben in the *ixr1-1* and *ixr1-2* mutants (Scheible *et al.*, 2001), being expressed highly in roots and shoots, (2) reveal a link between cellulose synthesis and jasmonate (JA) and ethylene responses in the *cev1* mutant (Ellis *et al.*, 2002), therefore leading to constitutive expression of stress response genes and

enhanced resistance to fungal pathogens. The respective plants show an increased production of jasmonate (JA) and ethylene. The *cev1* mutant phenotype could be reproduced by treating wild type plants with cellulose biosynthesis inhibitors. Studying the particular behaviour of the cellulose synthesis mutants, it was found out that the expression of defence-related genes in the *eli1* mutant, in cellulose synthase inhibitor-treated plants and in other mutations affecting cellulose synthesis suggested that reduced cellulose synthesis invokes a wide variety of cellular responses, some of which are regulated via JA- and ethylene-mediated pathways (Ellis *et al.*, 2002). Defence genes expression is certainly an indirect effect of reduced cellulose synthesis. Several mutants with altered cell wall synthesis were shown to exhibit ectopic lignin deposition, suggesting a possible link between the phenotypes (Cano-Delgado *et al.*, 2000). Lignification occurs during normal development of secondary walls of tracheids and other cell types of the vascular system and is also induced during defence responses inhibiting pathogen ingress (Vance *et al.*, 1980).

In addition, (3) the *eli*1 mutations of *CesA3* clearly showed that cellulose and lignin synthesis are linked (Cano-Delgado *et al.*, 2003). It was observed that the *eli1* mutant produces large amounts of lignin in cells that do not normally lignify (especially root xylem cells). These studies suggest that there may be a close link between pathogens and altered cell wall properties.

The *procuste1 (prc1),* an AtCesA6 mutant, has been identified by mutation in a cellulose synthase required for normal cell elongation, specifically in roots and dark-grown hypocotyls (Fagard *et al.*, 2000).

The irregular xylem 3 gene -*IRX3*- encodes the AtCesA7 gene, a cellulose synthase component that is specifically required for secondary cell wall synthesis (Taylor *et al.*, 1999). The xylem elements in the mutant have weakened walls due to a severe deficiency in secondary cell wall cellulose deposition, and collapse upon themselves. It is clear that *IRX3* belongs to a small subfamily of cellulose synthase genes, including *RSW1* and the cotton *CELA1*, but shows distant relationships to a large number of other cellulose synthase related genes. The mutation in the *irx3* mutant leads to the loss of the last 168 amino acids of the mature protein structure. This portion contains four membrane- spanning domains and several other features conserved in RSW1 and CELA1; therefore the *irx3* mutation appears to be a null mutation (Taylor *et al.*, 1999).

Similarly, the *irx1* (AtCesA8) mutant shows a deficiency in cellulose deposition in the secondary cell wall and a very specific expression of the *IRX1* gene in developing vascular tissues.

IRX1 and IRX3 define two distinct classes of catalytic subunits, both of which are required for cellulose synthesis, in the same cell type to give normal levels of cellulose deposition in the secondary cell wall (Taylor *et al.*, 2000). They are responsible for cellulose deposition in the secondary cell walls of xylem elements. The *irx1* and *irx3* mutants exhibit a very similar characteristic collapsed xylem phenotype, being indistinguishable in the xylem (Turner and Somerville, 1997).

1.5 OTHER COMPONENTS INVOLVED IN THE CELLULOSE BIOSYNTHESIS

Up to date, no other genes encoding verified cellulose synthase subunits have been identified. Other proteins, besides the catalytic subunits of cellulose synthase, are also required for normal cellulose synthesis in plants.

Sucrose synthase (SuSy), an enzyme catalyzing the formation of UDP-glucose from sucrose, is thought to associate with the cellulose synthase complex itself, or at least with the plasma membrane (Amor *et al*.,1995; Salnikov *et al*., 2001).

The cytoskeleton plays an important role in cellulose biosynthesis. Many studies indicate that the cortical microtubule (MT) network adjacent to the membrane is involved in aligning the orientation of cellulose microfibrils as they are deposited into the wall (Emons *et al.*, 1992; Baskin, 2001). Actin plays a role in setting the pattern of cortical microtubules, which in turn directs the pattern of cellulose microfibril deposition (Delmer and Amor, 1995).

Korrigan is a mutant that was identified as an extreme dwarf with pronounced alterations in the primary cell wall showing a defect in the elongation (Nicol *et al*., 1998; His *et al*., 2001; Szyjanowicz *et al*., 2004). The correspondent gene encodes a plasma membrane endo 1,4-β-glucanase that probably cleaves the cellodextrins from the sitosterol primer during cellulose synthesis.

Kobito mutant also shows a dwarf phenotype with short hypocotyls and roots, short inflorescence stem with some internodes, floral organs present a miniature morphology. The corresponding gene encodes a plasma membrane protein of yet unknown function (Pagant *et al.,* 2001, 2002).

Lipid-linked cellodextrins participate in cellulose synthesis in *Agrobacterium tumefaciens* and sitosterol-β-glucosides have been proposed to act as a primer for cellulose synthesis (Peng *et al.,* 2002). UDP-glucose and sitosterol produce sitosterol-β-glucoside under

UDP-glucose:sterol glycosyltransferase (SG), encoded by two genes in *Arabidopsis thaliana*. T-DNA-insertion double mutants *sg1 sg2* display a level of sitosterol-β-glucoside that is over 30-fold reduced compared to wild type plants.

A GTPase, *RAC13*, has been implicated in the regulation of cellulose synthesis. *RAC13* gene expression increase in the transition phase from primary to secondary wall synthesis in cotton fibres (Delmer *et al.,* 1995). This coincides with the production of hydrogen peroxide (H_2O_2) which has been shown to stimulate cellulose synthesis during fibre differentiation (Potikha *et al.,* 1999).

A few mutations affecting genes involved in N-glycans either synthesis, or modification, also lead to reduced levels of cellulose accumulation. Embryos of the *cyt-1* mutant of *Arabidopsis thaliana* have strongly reduced levels of cellulose, and show a radial swelling and alterated cell wall structures (Nickle and Meinke, 1998; Lukowitz *et al.,* 2001). A second embryo-lethal mutation, *knf,* also produces radially swollen embryos and have strongly reduced cellulose content (Mayer *et al.,* 1991; Gilmor *et al.,* 2002). *KNF* encodes α-glucosidase I, an enzyme that removes terminal glucose from the N-linked glycan precursor $Glc_3Man_9GlcNAc_2$. Mutant phenotypes indicate that N-glycosylation has a role at some stages in the process of cellulose synthesis (Lukowitz *et al.,* 2001).

1.5.1 The *tbr1* (trichome birefringence) mutant

Another mutant, named *trichome birefringence 1* (*tbr1*) (Potikha and Delmer, 1995) lacks the strong birefringence of leaf trichomes under polarized light, which is characteristic of plant cells that contain highly ordered cellulose in their secondary cell walls. Stem trichomes lack the birefringence, as well. Xylem birefringence is also somewhat reduced, but not so drastically as that observed for trichomes. Cellulose content in isolated trichomes is strongly reduced in *tbr1* (about 18% of the level found in wild type). Moreover, *tbr1* leaves also display a reduced number (about 30% less) of trichomes, as compared to wild-type. These data strongly suggest that *tbr1* trichomes are heavily impaired in their ability to synthesize a secondary wall cellulose. The small amount of remaining cellulose is presumably due to normal deposition in the shape-determining primary cell wall. This conclusion is supported by the observation that, in the very early stages of trichome development in wild type, the developing trichomes lack birefringence, and thus resemble those seen in *tbr1*. Only later, after trichome shape is established, the birefringence appears (Potikha and Delmer, 1995).
Total leaf cellulose content was reduced in mutant plants by 20-30%. No major differences in stem cellulose content were found between wild-type and *tbr1*.

In general, it seems that primary wall cellulose synthesis is not inhibited because of the mutation. Examination of callus tissue, consisting almost exclusively of cells with just primary cell walls, shows no difference in cellulose content between mutant and wild type.

Trichome shape is normal in *tbr1* mutants, indicating that its ability to organize the cytoskeleton is not affected. There are other differences observed between mutant and wild type trichomes. The base of *tbr1* trichomes is swollen, compared to wild type; the structure of the ring of subsidiary cells at the base of the trichome appears to be deformed in the mutant; the knob-like projections characteristic of wild type are missing in the mutant and the stomata appear to be much thicker and protrude further from the surface of the leaf. In the ring of subsidiary cells at the base of the trichome, *tbr1* deposit callose, in contrast to wild type. It was also observed an excess of callose deposition in the vascular system (phloem). Measurements of callose synthase activity in the mutant leaves showed normal to somewhat elevated levels of activity (Potikha and Delmer, 1995).

The *tbr1* (trichome birefringence) mutant was selected by screening EMS-mutagenized M2 seedlings of Arabidopsis thaliana ecotype Columbia (Col-0). A rosette leaf of each M2 seedling was excised and prepared to examine for birefringence. Seed was collected from the mutant showing the described phenotype and propagated. Plants from the M4 generation were used as the male parent in backcrosses with either ecotype Columbia or Landsberg erecta. Backcrossing was repeated three successive times with Col-0.

The *tbr1* mutation was only detected once in a screen of approximately 7000 M2 seedlings. The mutation is constitutive and the plants otherwise appear phenotypically normal, with the trichomes exception, showing no birefringence, but germination percentage is somewhat lower for *tbr1* compared with wild type (Potikha and Delmer, 1995).

A rough genetic map position of the *tbr1* mutation was previously established by Ravit Eshed (Lab of D. Delmer, UC Davis, USA) in a bulk segregant analysis, and the mutation was localized between CIW50 and BstNI markers, on chromosome V of *Arabidopsis thaliana*.

1.6 TRICHOME DEVELOPMENT AND IMPORTANT KNOWN MUTANTS IN *ARABIDOPSIS THALIANA*

1.6.1 Trichome development

The trichomes of *Arabidopsis thaliana* are unicellular hairs, often branched, that are normally found on the leaves, sepals, petioles and stems. During development, the epidermal

cells perceive different signals and respond through intracellular signalling pathways, initiating cell differentiation and adopting a specific cell fate. Other cell types present in the epidermis include unspecialized epidermal cells, stomatal guard cells and root hairs. Trichome cells differentiate while epidermal pavement cells are still dividing, and it synthesizes more DNA, but cell division is arrested. After three rounds of endoreduplication, the cell expands outwards from the leaf surface as a single cone. This is followed by another round of endoreduplication after which branches are initiated (Oppenheimer *et al.,* 1997). DNA contents of trichome cells ranging from 4C to 64C have been reported, with an average of 32C. At least three genes, *TTG (TRANSPARENT TESTA GLABRA), GL1 (GLABROUS1)*, and *TRY (TRYPTICON)* are involved in the patterning of *Arabidopsis thaliana* trichomes (Hülskamp *et al.*, 1994).

The mature leaf trichome is a large, polarized cell, with two branch positions and a large nucleus located at the lower branch point. Their walls may be strengthened by silicate, calcium carbonate or other encrustations giving the respective hairs a bristle-like appearance. During trichome maturation, the cell wall thickens to approximately 5 μm, and the surface becomes covered with papillae. In addition, the epidermal cells around the base of a trichome acquire a distinct rectangular shape (Hülskamp *et al.*, 1994). Exceptionally long (1-6 cm), single-celled and unbranched hairs, consisting of nearly pure cellulose, surround the seeds of *Gossypium* (cotton).

The functions that are attributed to trichomes range from protecting the plants against herbivores and UV light, to reducing transpiration, control the heat exchange and increasing tolerance to freezing. The process of trichome formation in *Arabidopsis thaliana* is considered to be a relatively simple model system to study the complex mechanisms that control gene expression during cellular differentiation. When compared with other cell types, the development of trichomes is an attractive model system for two reasons. First, the process can be easily monitored because it occurs on the accessible outer surface of the plant. Second, morphological mutants can be readily isolated and characterized because trichomes are not essential for the survival of the plant (Haughn and Somerville, 1988).

1.6.2 Important known mutants involved in trichome development in *Arabidopsis thaliana*

There are many known trichome mutants and they have been grouped into several phenotypic classes: (1) initiation mutants, (2) mutants with a increased or decreased branch number, (3) mutants incapable of epidermal outgrowth, (4) mutants presenting a distorted

appearance, and (5) mutants affecting cell wall maturation. Most trichome mutations affect all of the trichomes on a plant (Hülskamp *et al.*, 1994).

Trichome initiation is impaired by mutations affecting the *GLABROUS 1 (GL1)* gene or the *TRANSPARENT TESTA GLABRA (TTG)* gene. GL1 encodes a Myb-like protein, a transcription factor, and the *gl1* mutation appears to affect trichome development, mutant leaves being glabrous (Herman and Marks, 1989)**,** while the *ttg* mutation has additional developmental consequences. Mutant *ttg* plants lack anthocyanin pigments and the seeds lack the polysaccharide mucilage that accumulates in the outer layer of the testa. Both mutants form only a few trichomes on the margins of the rosette and cauline leaves.

The *GLABRA2 (GL2)* gene is required for normal trichome morphogenesis (Koornneef *et al.*, 1982; Rerie *et al.*, 1994). In *gl2* plants, expansion of the trichomes is affected.

Mutations in the *GLABRA3 (GL3)* gene have effects on trichome development, leading to a reduced trichome initiation process and smaller trichomes due to fewer rounds of endoreduplication (Koornneef *et al.*, 1982). In the *trypticon* (*try*) mutants, trichomes are overdeveloped, producing four to six branches and contain a large nucleus, undergoing extra endo-cycles. *TRY* also affects trichome patterning.

Several other recessive mutations seem to reduce trichome branching without affecting initiation. Architecture mutants with reduced branching define four loci (*angustifolia*, *stachel, stichel* and *zwichel*) (Hülskamp *et al.*, 1994). *GL3* and *TRY* genes control trichome branch number through cell volume, while "architecture" genes organize the number and the relative positions of branching points on the growing cell (Folkers *et al.*, 1997).

Two genes, *STACHEL (STA)* and *ANGUSTIFOLIA (AN)* are required for the specification of both, the primary and the secondary branching events, respectively. The two branching events are specified separately by *AN* and *STA*. The trichomes on *sta* mutants appear to have skipped primary but not secondary branching. *AN* mediates the secondary branching. The double mutant *an sta* develops unbranched trichomes.

The *STICHEL (STI)* gene was described to play a role in the initiation of branching. (Hülskamp *et al.*, 1994). The respective mutants do not develop any branch points. In contrast, mutations in the *NOEK (NOK)* gene result in glassy trichomes with an increased branch point number. The *nok* trichomes are normal in size, (by nuclear size), but produce up to seven branches.

Mutations in *STI* and *NOK* result in opposite phenotypes: fewer branch points or, on the contrary, supernumerary branch points, respectively.

The *ZWICHEL (ZWI)* gene encodes a kinesin motor protein with a calmodulin-binding domain, indicating that microtubule-based transport is important for branch formation (Oppenheimer *et al.*, 1997).

General trichome expansion is affected by mutations in eight different genes. These recessive mutations include *distorted dis1* and *dis2* as well as *gnarled (grl)*, *klunker (klk)*, *spirrig (spi)*, *wurm (wrm)*, *crooked (crk)*, and *alien (ali)* (Hülskamp *et al.*, 1994).

Several recessive mutations appear to alter the final stage of trichome development. The *under developed trichome (udt)* mutation results in trichomes that are more slender than in wild type plants and produce underdeveloped papillae toward the tips of the branches (Haughn and Somerville, 1988). Three other mutations, *chablis (cha), chardonnay (cdo)*, and *retsina (rts)* result in trichomes that lack the rough papillae surface of wild-type mature trichomes (Hülskamp *et al.*, 1994).

The mutant, named *trichome birefringence1* (*tbr1*), which lacks the strong birefringence of leaf trichomes under polarized light (Potikha and Delmer, 1995), could be classified as a maturation mutant, lacking the trichome secondary cell wall of normal trichomes (Hülskamp *et al.*, 1994).

Aim of the thesis

Cellulose is the earth's major biopolymer and is of tremendous economic globally importance. It is the major constituent of cotton (over 94%) and wood (over 50%). Traditionally, cellulose is harvested from plant resources. With the ever increasing human population and continued demand for cottons, wood or other cellulose derived products, more land is required to meet the global demand. This has a direct impact on the earth's carbon cycle. The carbon cycle on earth is a vast interplay between the carbon dioxide of the atmosphere and its fixation via photosynthesis into organic products, among which cellulose is the most abundant macromolecule on earth. Cellulose can be thought of as a giant carbon deposit, because carbon incorporated into cellulose remains in the product for a rather long time (Brown, 1996).

In this context, we need to understand cellulose biosynthesis in terms of the global carbon cycle as well as its use by humans. One way to gain more insights into the function of the cell wall polysaccharides, in particular cellulose, is to generate plants or identify mutants, that contain defined structural alterations. Once these plants have been identified, their impact on the plant life cycle can be assessed.

In this thesis the aim was to identify and characterize a new gene involved in cellulose synthesis complex process, using forward genetics approaches. The phenotype of the identified mutant *–tbr1–* is expressed in trichomes, considered as model cells due to their size, localization (epidermal cells), and easiness to work with.

Previous characterization of *tbr1* mutant (Potikha and Delmer, 1995) suggested an effect on secondary cell wall synthesis, process that is still poorly understood. The detailed analysis of this mutant and corresponding gene gives us a better understanding of this physiologically and economically important process in plants.

2. CHAPTER: MATERIALS AND METHODS

2.1 MATERIALS

2.1.1 Equipments

Mini spin Centrifuge	Eppendorf, Germany
Table touch centrifuge 5415 D	Eppendorf, Germany
Centrikon T-124 ultra-centrifuge	Kontron Bio-tech, Neufahrn, Germany
Vibratome VT1000S	Leica, Bensheim, Germany
Retchmill	Retsch, Haan, Germany
Microscopes	Olympus, Leica, Germany
Polarizer	Olympus, Leica, Germany
Thermal cyclers:	
Programmable thermal controller PTC-100	MJ Research Inc.
Peltier thermal cycler PTC-200	MJ Research Inc.
Real-time PCR machine Geneamp 5700	PE Apllied Biosystems, Darmstadt, Germany
Thermomixer compact	Eppendorf, Germany
Vortexer	Heidoph, Germany
Electric balances (AB104-S, PB10502-S)	Mettler, Toledo, Germany
Incubator	Binder, Germany
Hybridization oven (Hybridizer HB-1D)	Techne, Germany
Nucleic acids electrophoresis apparata	
Mini gel chamber	Hoefer, Germany
Standard gel chamber	Life Technologies, Biorad Germany
Standard gel apparatus	Life Technologies, Biorad Germany
Biophotometer	Eppendorf, Germany
Pipettes	
HandyStep multirepeter	Brand, Germany
Multipipette plus	Eppendorf, Germany
Multichannel (12 channels)	Eppendorf, Germany
Pipettes (2 µl, 20 µl, 200 µl, 1000 µl)	ABImed, Germany
Gene pulser	Bio-rad, Germany
Particle Delivery System	PDS-100/He Biolistic® Bio-rad, Germany
Gas Chromatograph	6890N Network GC system, Agilent
MALDI-TOF spectrometer	Voyager De-Pro, Applied Biosystems, Weterstadt, Germany

2.1.2 Enzymes, chemicals and reaction kits

Enzymes

Taq-polymerase	Invitrogen, Karlsruhe, Germany
Pfu-polymerase	Stratagene, Heidelberg, Germany
Restriction enzymes	Roche, Manheim, Germany
RNase I,	Roche, Manheim, Germany
DNase I	Sigma Aldrich, Germany
Reverse Transcriptase	Invitrogen, Karlsruhe, Germany
T4 DNA ligase	Promega, Manheim, Germany
GATEWAY™ BP clonase	Invitrogen, Karlsruhe, Germany
GATEWAY™ LR clonase	Invitrogen, Karlsruhe, Germany
Xyloglucanase	Novozyme, Bagsvaerd Denmark

Chemicals

Digoxigenin	Roche, Manheim, Germany
Lysosim	Sigma, Aldrich, Germany
Lactic acid	Sigma, Aldrich, Germany
Phenol:Chloroform	Roth, Karlsruhe, Germany
Silwet L-77	Helena Chemical, Fresno, USA
Trizol reagent	Invitrogen, Karlsruhe, Germany
Triton X-100	Serva, Heidelberg, Germany
X-gal	Duchefa, Haarlem, the Netherlands
X-gluc	Duchefa, Haarlem, the Netherlands

Reaction kits

High Speed Plasmid Purification kit	Qiagen, Hilden, Germany
Nucleospin Plasmid Purification kit	Macherey Nagel, Dueren Germany
Nucleospin Extract kit	Macherey Nagel, Dueren Germany
QIAquick PCR purification kit	Qiagen, Hilden, Germany
pENTR_SD/D_TOPO Cloning kit	Invitrogen, Karlsruhe, Germany
DNAse I (RNAse free) kit	Sigma, Epicentre, Germany
Non-radioactive labelling and detection kit	Roche, Manheim, Germany
SYBR Green Master Mix	Applied Biosystems, Darmstadt, Germany
GATEWAY™ directional Cloning system	Invitrogen, Karlsruhe, Germany

2.1.3 Synthetic oligonucleotides

Primers for the genetic markers used in the *tbr1* mapping process:

NGA158-F:	ACCTGAACCATCCTCCGTC
NGA158-R:	TCATTTTGGCCGACTTAGC
NGA249-F:	GGATCCCTAACTGTAAAATCCC
NGA249-R:	TACCGTCAATTTCATCGCC
CIW14-F:	CATGATCCATCGTCTTAGT
CIW14-R:	AATATCGCTTGTTTTTGC
CIW50-F:	CAACATCAATGGTCTTAGTC
CIW50-R:	GATGCACAGAAAGGTCATG
MHFD-F:	AAAAACCCAAACTTTCTATTTATAC
MHFD-R:	ACTTCGCTTCAAGTAAAGAGG
MBK20AFLIII-F:	ACAGGAGTATGGCAGTAGCGACTAA
MBK20AFLIII-R:	GACGACCAAGGATAGACCGAAAT
BSTN1CAPS-F:	GTGAACTGTGCAGGCATAAG
BSTN1CAPS-R:	CACAAGATTGCATCCTTTGAC
K18J17.1-F:	AGAAAATTGTTTATACGAATC
K18J17.1-R:	GGAAATCCTCAGACTGG
K18J17.1B-F:	CGTAACAATTCAAAACCGA
K18J17.1B-R:	GGCGAGTGACTTTTATTATAGA
MOJB-F:	TGAAAGATTTTAGGAGGACAA
MOJB-R:	GTAGGAGAAGGGGACAAGTT
EMC-F:	AACAGATCGGAAAATCGTCG
EMC-R:	AATGACGACGAGACGCTCTT
CIW18-F:	AACACAACATGGTTTCAGT
CIW18-R:	GCCGTTTGTCTCTTCAC
CIW16-F:	TGGTTAGATTTGCTGTT
CIW16-R:	ATTCTGCATTATTAGTTGTC
CIW15-F:	TCCAAAGCTAAATCGCTAT
CIW15-R:	CTCCGTCTATTCAAGATGC
NGA225-F:	TCTCCCCACTAGTTTTGTGTCC
NGA225-R:	GAAATCCAAATCCCAGAGAGG
TAQ1 CAPS1-F:	GGTACTGTTGGCATCATTGGAT
TAQ1 CAPS1-R:	AGTTTGTGGCAGTTTATGGG
TAQ1 CAPS2-F:	GCATAATTAGCGGTGGTACTGT
TAQ1 CAPS2-R:	CGGCTTGTTGATGGGTATT
TAS I CAPS1-F:	GAGACATCTCCATTGCCGTATT
TAS I CAPS1-R:	TCGTCGAAGCAAGTAAGTGAAC
TAS I CAPS2-F:	TGGCCATGAGGATAAGTAAAT
TAS I CAPS2-R:	GGAGCATTCAACTTCATATCTG

MPH151-F:	ACGCCTCATATGCACATTAAC
MPH151-R:	AGCAACTAGTCGAATCGCTTAG
MPH15 2A-F:	ACGATTATAGAGCAACCGAAGA
MPH 15 2A-R:	CAACATGTACCATGCGTGAATA
MPH15 2B-F:	GAGTCAGCGTGAAAATCGAAA
MPH15 2B-R:	ACAACATGTACCATGCGTGAAT
PDM I DCAPS-F:	ATTTTTGTTTGGCGATTGAG
PDM I DCAPS-R:	CAACTCTTTTCTGCAGAAAAGTTT
MOJ9 SSLP3-F:	TGGGGTGACTCTAGATGTATAA
MOJ9 SSLP3-R:	TGCCAAAACCTACCTATTTC
MPH151-1-F:	AGGCCATAGCGTAAGCAC
MPH151-1-R:	GATTTCATTCATTTCCGTCA
MPH151- 2-F:	AACTCTCCACTGCGATCTGA
MPH151- 2-R:	GACGCTTGACCAAGGATAGAA
MPH151- 3-F:	GCTCATGCGAATACGGTTCTT
MPH151- 3-R:	ACATTTAGCAACGGAAAACGG

Primers used for *TBR* gene sequencing:

PROTEIN 1 F:	ATTTCCGGATAATTTAGTTAGA
PROTEIN 1 R:	ATATTGTATTCGTCGTGACA
PROT1 SEQ1:	AACGAGGGGTATTTTAATTTGA
PROT1 SEQ2:	CCGGATCTCAGTTCTCTTCAAT
PROT1 SEQ3:	CACCGAAAAAGCAGACTAAAAC
PROT1 SEQ34:	GGTATGGTTTGCGGAGCCTA
PROT1 SEQ4:	TCCGTGGGGAGGCTGAGTAC
PROT1 SEQ5:	AAGAATGTGAATCCGGCAAAGT
PROT 1 SEQ6:	GCCAAACACAACGAAAAACTTA
PROT 1 SEQ7:	ATAATGTGAACGCAAGAATTTG

Primers used for developing a genetic marker for *tbr1-1* allele:

HPA2 CAPS-F:	ATACGGTTTAGTTTCGGTTCA
HPA2 CAPS-R:	CCAATTTTAGCCCGATATTT

Primers used for sequencing of other candidate genes:

THIORED-1F:	AACAAAGCTCAATCTCGACGAAA
THIORED- 1R:	TAGCACATCGTTGGCATTGTC
THIORED SEQ 1:	TTACCGAAATGTTTCCACGTTT
THIORED SEQ 2:	ATGATCTTGCGACTTGCGAGAA
THIORED SEQ 3:	TGACCTCCCAAGCTTTTCATTA
THIORED4:	CAATCTCGACGAAAAGAAAAA
TUBULIN F:	AATTCAAACATTATTTTTCTCCGTT
TUBULIN R:	AGCGGTTAGTGAAAGACGTAGATA
TUB SEQ 1:	ACTACTCTCTTCACTCGCCCAAAC
TUB SEQ 2:	AATGGGCTCTTGTTTATTTGCTTA
TUB SEQ 3:	GATGTGGGAACTGTTGGGCAAGC
TUB SEQ 4:	CAGCAATGCTTCCATCTTTTAT
TUB SEQ 5:	GAGGCAAGGGTTCCATTAGATA
TUB SEQ 6:	GAAGTACCTCAACGCCATTGTT

Primers used for T-DNA insertion lines analysis:

SALK069441R:	TGATTTCGACGGTGACGGA
SALK069441F:	GCGTCACAAAACAGTGGCATT
SALK065990R:	GCCACAAAGAAACAGAACCGAT
SALK065990F:	TGGCTACAATCTTGGTGACTCA
SALK020184R:	GTCGCATTTGCTTCAAGGGTAT
SALK020184F:	CTAAGAAGATGGACTCGTCGAAGAA
SALK135222R:	CAAATGGGACAACGGACACA
SALK135222F:	TTGACCCAATCTCCCTCGAA
SALK058509R:	CTGTGGCGTCACTGGATCTATT
SALK058509F:	CGCCGTTAAGTATATGCCAATC
SALK-LBb1:	GCGTGGACCGCTTGCTGCAACT
SAIL F:	TTCAGAAATGGATAAATAGCCTTG
SAIL R :	GAAATGGATAAATAGCCTTGC

Primers used for RT-PCR analysis:

Ubiquitin (Ubq10)-F:	CACACTCCACTTGGTCTTGCGT
Ubiquitin (Ubq10)-R:	TGGTCTTTCCGGTGAGAGTCTTCA
Tbr RTF**:**	AATGTGAATCCGGCAAAGTCC
Tbr RTR:	GGTCTGCGTTTACCTGAAATGG
TBR RT2F:	AATAATCAGTCACGGACCACCGCCG
TBR RT2R:	AAACCAAACAACATCTCCGGC
At1RTfor:	ATGGCCCTCCTCTGAAGTGTGT
At1gRTrev:	AACATCGACCGCAGTCAAACC
At3gRTfor:	TTCCCCGTCACATTTCAGC
At3gRtrev:	CTGTTTCATCATCGCATGCTC
ActinF:	ACTTTCATCAGCCGTTTTGA
ActinR:	ACGATTGGTTGAATATCATCAG

Primers for gene promoter-GUS fusion analysis:

TBR F:	CAATGTGGACGGAAGATGAGTTGGACAATGC
TBR R:	CAATGGATCCGCATATACTTAACGGCGTCTG
At3g F:	CAATGTCGACTTTCGGAGTTTCTAGTCTGGA
At3g R:	CAATGGATCCTTCAGGCAATGCGTAATCTAT
At1g F:	CAATGTCGACCCATTTGTATCAATCTCCCCC
At1g R:	CAATCCCGGGAATGAAGCACACGGAAAGTGA

Primers used for *tbr1* complementation:

tbrpBinF:	CAATGGATCCCAACCCTAAAACCACTCGTC
tbrpBinR:	CAATGTCGACTTGGAGAGAAACCTCGATTTA
tbrpBin2F:	CAATGGATCCCTTAAGGCTCTGAAATCTAAT
tbrpBin2R:	CAATGTCGACGATCAAACAAGTATTGGG

Primers used for GFP fusion:

ENTRYcDNA5F: CACCATGGCGTCAGACGCCGTTAAG
ENTRYcDNA5R: AGTTTTTCGTTGTGTTTGGCTG
ENTRYcDNAstopR: TTAAGTTTTTCGTTGTGTTTGGCTG

2.1.4 Plasmids:

Plasmids	Source
pENTR/SD/D_TOPO	Invitrogen Gmbh
pK7FWG2	GATEWAY (Karimi *et. al.,* 2002)
pK7WGF2	GATEWAY (Karimi *et. al.,* 2002)
pGWB17/18	Inst. for Molecular Genetics, Shimane University, Japan
pBI101.1	Clontech, USA (Jefferson *et al*., 1987, 1986)
pBINAR	Institute of Genebiology research, Berlin, Germany, (Stockhaus *et al.,* 1987)
pBIC20	(Meyer *et al.*, 1994)

2.1.5 Plant material and growth conditions

Arabidopsis thaliana Columbia (Col-0)- NASC, N1093); Landsberg (Ler)- NASC, N8581; Ws- NASC, N1603, *tbr1* mutant, *irx1*, *irx3*, *sgt*.

All *A. thaliana* plants were grown in environmental chambers under standard conditions (120 µmol m-2 s-1 light, 60% relative humidity, 21^0C), continuous light or in the greenhouse, on soil. The cultivation on plates was done on AMOZ medium, containing MS salt (2.45 g/l, MES (0.6 g/l), Select agar (7g/l), for 1 l distilled H_2O, pH 5.7-5.8 (adjusted with KOH) and sterilized by autoclaving before use. Sucrose 0.5%, final concentration, was added to the medium after autoclaving. In the case of selective growth, the medium was supplemented with the appropriate antibiotic.

2.1.6 Plant Transformation

A colony of transformed *A. tumefaciens* was inoculated and a pre-culture of 5 ml YEB, pH 7.0 (Bacto-tryptone (5 g/l), Bacto-yeast-extract (1 g/l), Bacto-peptone (1 g/l), sucrose (5 g/l) in 1 l H_2O) supplied with rifampicin (25 µg/ml) and the specific selection for the vector was prepared. The mixture was incubated at 28^0C for two days. 2 ml of the preculture were further inoculated in 400 ml YEB selective medium and again incubated at 28^0C overnight. The bacterial cells were harvested by centrifugation at 8000 rpm for 10 min., at 4^0C and resuspended in 200 ml infiltration medium (sucrose (50 g/l), MS-Medium (2.2 g/l), MES (0.05 g/l), 10 µl BAP (benzamine-aminopurine) in H_2O, pH 5.7). The bacterial solution (200 ml) was

added to 1 ml Silwet L-77. The plants inflorescences were dipped for 10 sec. in this solution and dried overnight (Clough and Bent, 1998).

2.1.7 Seed surface sterilization

As a first step, the seeds are washed with 70% ethanol (v/v). Ethanol is discarded and a second washing step is required with bleach solution containing 1/3 NaHClO (12%) + 2/3 sterile distilled water + 0.1% Triton X100, for 15 min. The seeds are collected by centrifuging and supernatant is discarded. After washing three times with sterile distilled water, the seeds are resuspended in 0.15% sterile agar solution (in distilled water), being ready for cultivation on sterile agar plates, using a sterile Pasteur pipette.

2.1.8 Bacterial strains and cultivation conditions

E. coli DH5α (Invitrogen) DeoR endA1 gyrA96 hsdR17(r k- m k-) recA1 relA1 supE44 thi-1 Δ (lacZYA-argFV169)ϕ 80 δ lacZ Δ M15 F^- λ^-.

E. coli Top 10- Gateway, Invitrogen, GmbH, Germany.

Cultivation was usually performed in LB medium as described by Sambrook *et al*., (1989).

LB-Medium (Luria-Bertani Medium) contains: Bacto-tryptone (20 g/l), Bacto-yeast-extract (5 g/l) and NaCl (0.5 g/l) added to 950 ml H_2O. The pH was adjusted to 7.0 and the volume was filled up to 1l.

Agrobacterium tumefaciens pGV 3101 pmp90

Agrobacterium tumefaciens strain *GV3101* is based on the C58 and pMP90 genotypes that have proven to be productive in use with *A. thaliana* marker gene gentamicin, opine: nopaline (Koncz and Schell, 1986). *A. tumefaciens* cells were grown in YEB medium (Yeast Extract Broth) containing: Bacto-tryptone (5 g/l), Bacto-yeast-extract (1 g/l), Bacto-peptone (1 g/l), sucrose (5 g/l) in 950 ml H_2O. The pH was adjusted to 7.0 with 5 M NaOH and the volume was brought to 1l). The solution was sterilized by autoclaving and after that, $MgSO_4$ (20 g/l) and 10 ml $MgCl_2$ (50 mM) were added. For preparing medium plates, Bacto Agar (15 g/l) was added.

2.1.9 Antibiotics

Antibiotic	Final concentration	Antibiotic	Final concentration
Ampicillin	100 μg/ml	Spectinomycin	100 μg/ml
Hygromycin	20 μg/ml	Streptomycin	10 μg/ml
Kanamycin	50 μg/ml	Tetracyclin	10 μg/ml
Rifampicin	25 μg/ml		

2.1.10 Stock solutions

Denaturation solution
0.5 N NaOH, 1.5 M NaCl

Neutralization solution
M Tris-HCl, pH=7.5; 1.5 M NaCl

20 x SSC buffer
3 M NaCl, 300 mM sodium citrate, pH=7

Proteinase K
2mg/ml Proteinase K in 2 X SSC buffer

Prehybridization solution
(Standard buffer)
5 x SSC, 0.1% (w/v) N-lauroyl sarcosine
0.02% (w/v) SDS, 1% Blocking reagent

Standard buffer + 50% formamide
50% formamide deionized, 5 x SSC,
0.1% (w/v) N-lauroyl sarcosine,
0.02 %(w/v) SDS, 1% blocking reagent

2 x Wash solution
2 x SSC, containing 0.1% SDS

0.5 x Wash solution
0.5% SSC, containing 0.1% SDS

Maleic acid buffer
100 mM maleic acid, 150 mM NaCl, pH=7.5

Washing buffer 1 (dilute 1:10 with H_2O) 1.0
100 mM maleic acid, 150 mM NaCl
pH=7.5; 0.3% Tween 20

Blocking solution
(1:10 in 1 x maleic acid buffer)

Detection buffer
(dilute 1:10 with H_2O)
100 mM Tris-HCl, 100 mM NaCl: pH=9.5

TE buffer
10 mM Tris, 1 mM EDTA; pH=8.0

Anti-Digoxigenin-AP
1:5000 dilution in 1x blocking solution

NBT (nitrobluetetrazolium) **solution**
75 mg/ml NBT in 70% (v/v) DMF

BCIP (5-bromo-4-chloro-3-indolyl phosphate)
50 mg/ml BCIP (toluidinium salt) in 100% DMF.

DEPC-H_2O (1l)
DEPC was added to H_2O to a final concentration of 0.1%. The solution was stirred overnight at room temperature (RT) in a hood and sterilized by autoclaving.

PBS (Phosphate-Buffered Saline) (1l)
NaCl (8 g/l), KCl (0.2 g/l), Na_2HPO_4 (1.44 g/l) and KH_2PO_4 (0.24 g/l) were added to 800 ml H_2O and the pH was adjusted to 7.4. The volume was finally filled up to 1l.

TBE Buffer [5 x], (Tris-Borate-EDTA buffer) (1l)
Tris (54 g/l), 27.5 g boric acid (27.5 g/l), 0.5 M EDTA (pH 8.0) were added to H_2O.

TE Buffer [1 x], (Tris-EDTA buffer) (1l)
0.1 M Tris-HCl (pH 8.0) and 0.25 M EDTA were added to H_2O.

2.2 METHODS

2.2.1 DNA cloning methods

2.2.1.1 Amplification of DNA fragments via polymerase chain reaction (PCR)

DNA fragments used for cloning or sequencing were amplified by PCR using proof reading polymerase (*Pfu*) or a mixture of *Taq* and *Pfu* (10:1) enzymes.

A standard PCR mixture (50 µl volume) comprises:

10X PCR reaction buffer…….5 µl
$MgCl_2$ (25 mM stock solution)……....5 µl
dNTP mixture (stock of 10 mM each)…….2 µl
Primers mixture (forward and reverse, 10 pmol each)….2,2 µl
DNA template/plasmid…….100 ng plant DNA or 1 ng plasmid DNA
Taq (*Pfu*) polymerase (5U/ µl stock)……1 µl
Sterile H_2O……up to 50 µl

A standard programme for a PCR reaction:

1) Initial denaturation……95^0C for 3 min
30-39 cycles from step 2 to 4:
2) Denaturation……..95^0C for 50 seconds
3) Annealing……...50 $(55)^0$C for 1min.
4) Primer extension……72^0C for 2minutes

5) Final extension……...72^0C for 10 min.

Standard cloning methods were performed as described by Sambrook and Russell (2001). Isolated plasmids DNA were checked by restriction analysis and when identified, also sequenced to confirm the identity.

2.2.1.2 Preparation of *E. coli* ultra-high competent cells

E. coli DH5α competent cells were prepared as described by Inoue *et al.,* (1990).
Bacterial cells are cultivated on LB-agar plate, at 37^0C, for overnight. 10-12 colonies are picked-up and inoculated in 250 ml LB medium in 1 l flask, grown at 19^0C with vigorous shaking until the culture reach OD=0.5 (normally it takes 24-36 hours). Then, the flask is placed on ice for 10 min. The cells are harvested by spinning at 5000 rpm for 10 min. at 4^0C, then, gently resuspended in 80 ml ice-cold TB solution (10 mM PIPES, 15 mM $CaCl_2$, 250 mM KCl, pH 6.7 adjusted with KOH or HCl, then 55 mM $MnCl_2$ is added) and placed on ice for 10 more min. After that, pellet cells is harvested by centrifuging at 5000 rpm for 10 min, at 4^0C and resuspended in 20 ml ice-cold TB and 1.4 ml DMSO (DMSO, need to be stored at –20^0C before use) and aliquoted 100 µl for transformation and kept at –80^0 C.

2.2.1.3 Genetic transformation of *E. coli* chemical competent cells

Transformation of *E. coli* was performed as described by Hanahan *et al*., (1983). The ligation product (5-10 µl) is mixed with an aliquot of 100 µl competent cells in an 1.5 ml sterile tube and placed on ice for 30 min. The cells are then heated at 42^0C for 45 sec. and immediately cooled on ice for 3 min. 900 µl sterile LB medium with no antibiotic selection is added and the transformed cells are incubated at 37^0C for 1 h, shaking. Then the cells are plated out on LB

selective agar plates (containing the appropriate antibiotic) and incubated at 37^0C, overnight, for colonies selection.

2.2.1.4 Preparation of *Agrobacterium tumefaciens* electrocompetent cells

(Nagel *et al.,* 1990)

To prepare competent cells of *Agrobacterium tumefaciens,* an overnight culture was grown in 200 ml YEB medium. The cells are incubated at 28^0C for 3 hours and then centrifuged at 5000 rpm for 10 min. at 4^0C. The cells were washed once in 10 ml pre-cooled TE-buffer and resuspended in 20 ml fresh YEB buffer. The cells aliquots of 50 µl each were kept frozen, at -80^0C.

2.2.1.5 Transformation of *Agrobacterium tumefaciens* by electroporation (Mersereau *et al.*, 1990)

About 100 ng of DNA was mixed with an aliquot of competent *A. tumefaciens* cells (50 µl of *GV3101 pMP90*) on ice and the mixture was transferred to a cold cuvette for the incorporation of the DNA into the cells by electroporation. The electroporation was carried out with a 2 mm cuvette, under the following conditions: capacitance: 25 µF, voltage: 1.8 kV, resistance: 200 Ohm, and pulse length: 5 msec. in the electroporation apparatus. After that, 900 µl of YEB medium (no antibiotic selection) was added to the cells and they were allowed to regenerate at 28^0C for 2-3 h. Then, 200 µl of the cells were plated on each YEB selective plate with antibiotics and incubated for two days at 28^0C.

2.2.1.6 Genetical mapping of *tbr1* mutation.

2.2.1.6.1 Map-based cloning general introduction

Cloning genes by their map position (positional cloning) is a method of isolating genes for which only a mutant phenotype is known. In contrast to gene tagging, positional cloning is an essentially indirect approach; mapping will narrow down the genetic interval containing a mutation by successively excluding all other parts of the genome. There are some main steps to follow in a mapping process: 1)-mapping the gene; 2)-generating recombinants; 3)-chromosome walk- making a contig spanning the gene; 4)-identifying the gene from the region of interest.

1. Mapping the gene. Mapping with a high resolution requires a high density of genetic markers distributed on the respective chromosome . As a first step in the mapping process, the mutant is out-crossed to another ecotype (Columbia-0 (Col-0) or Landsberg (Ler)). The most

commonly used combination for mapping purposes is Ler x Col-0. The resulted F2 population is used for fine-resolution mapping.

The molecular markers most widely used in mapping experiments at present, are simple sequence length polymorphisms (SSLPs), cleaved amplified polymorphic sequences (CAPS) and derived CAPS (dCAPSs). They are PCR-based and can be analyzed on agarose gels, which makes them easy to use. Utilizing flanking markers, a large mapping population of plants is screened for recombinants in the vicinity of the mutation. Finally, the genetic interval containing the mutation is narrowed down as much as possible, by analyzing closer markers in the region (Brookes, 1999; Lukowitz, 2000; Jander *et al.,* 2002; Scheible *et al*., 2004).

2. Generating recombinants. It is important to have a fair number of plants with recombination breakpoints very close to the gene of interest, based on the available genetic markers in that region.

3. Chromosome walk. Once a genetic interval has been defined for the respective gene, it is necessary to identify molecular clones covering the whole corresponding chromosomal interval by chromosome walking. In *A. thaliana*, a physical map of the complete genome (mostly BACs) is already available.

4. Identifying the gene of interest. Mutant complementation is the least ambiguous way to identify the gene. The region is split into overlapping fragments of between 5 and 50 kb, and each fragment in turn is introduced into the mutant plants for transformation. Only the fragments containing the entire gene will rescue the mutant phenotype. By choosing overlapping fragments, those fragments that do not contain the gene can be easily excluded. To further confirm that the correct gene has been isolated, there is need to sequence it from both, mutant and wild type, expecting to see a difference. Positional cloning will result in identifying the gene responsible for the observed phenotype
(http:// fp.bio.utk.edu/botany/Botany_courses/botany404/Lablecture).

More than 2100 F2 plants of *tbr1*xLer were cultivated in the greenhouse conditions, in 96 well trays. Alkaline lysis DNA (Klymuk *et al.*, 1993) was prepared from flowers (it provides higher DNA yield) of individual plants and used as template for PCR screening with flanking genetic markers.

PCR was set-up in a 22 µl final volume.

10X PCR reaction buffer…….2,2 µl
$MgCl_2$ (25 mM stock solution)……...2,2 µl
dNTP mixture (stock of 10 mM each)…….0,5 µl
Primers mixture (forward and reverse, 10 pmol each)….1,1 µl
Taq (*Pfu*) polymerase (5U/ µl stock)…….0,5 µl

DNA template……2 µl
Sterile H_2O…….up to 22 µl

Programme used for amplification:
1) Initial denaturation……94^0C for 1 min.
39 cycles from step 2 to 4:
2) Denaturation……..94^0C for 20 sec
3) Annealing……...48-55^0C for 20 sec
4) Primer extension……72^0C for 30 sec

5) Final extension……...72^0C for 2 min.

Resulted PCR products, short in length were run on a high resolution agarose gels (4%), in TBE buffer.

In the case of CAPS markers, the PCR product was further digested with the appropriate enzyme and the products analyzed on high resolution agarose gels to identify homozygous and heterozygous plants, respectively.

2.2.1.7 *TBR* gene sequencing

The identified putative protein was amplified from wild type Col-0 CTAB-DNA template and four different *tbr1* mutant plants, using flowers material to yield more DNA , by following PCR programme:

1) Initial denaturation……94^0C for 1 min.
39 cycles from step 2 to 4:
2) Denaturation……..94^0C for 50 sec
3) Annealing……...55^0C for 30 sec
4) Primer extension…….72^0C for 3 min.

5) Final extension……...72^0C for 10 min.

The primers used for amplification and sequencing are given in the oligonucleotides section of the material and methods chapter. The respective PCR product was 2828 bp length.

2.2.1.8 Cosmid complementation of *tbr1* mutant

A genomic wild type Col-0 library inserted in *E. coli NM 554* cells (Meyer *et al.,* 1994) was screened with digoxigenin (DIG) labelled DNA probes.

The DNA probes were DIG labelled in a 50 µl PCR reaction mixture containing:

10 x PCR buffer……5 µl
$MgCl_2$ (25mM stock)……5 µl
DNTP's (10mM each)……..1 µl
Primers mix (F+R)……2 µl
Taq polymerase (5U/µ)…… 1 µl
WT col DNA template……..2 µl

DIG……2 µl
H_2O……up to 50 µl

The resulted PCR products were analysed by electrophoresis on 2% agarose gel, cleaned from the PCR mixture and eluted in TE buffer; DNA amount was spectrophotometrically quantified. Therefore, probe A contained 116 ng/µl DNA, probe B -91 ng/µl DNA, the product corresponding to probe C had 83 ng/µl DNA and D -88 ng/µl DNA.

The bacterial cells contain pBIC20 binary vector (25 kb). pBIC20 provides resistance to tetracycline in *E. coli,* to tetracycline and kanamycin in *A. tumefaciens*, and to kanamycin in plants (Meyer *et al.,* 1994). The library contains 4.7 x 10^4 recombinant clones with an average insert size of 14 kb. More than 95% of the clones in the library are recombinant. *E. coli* cells stock containing the genomic library was diluted 1:300 and 200 µl from this were plated on LB-agar plates (10 cm diameter) containing tetracycline (25 µg/ml medium), as selection marker, then grown at 37^0 C for overnight. Bacterial colonies were transferred to a nylon membrane. A consecutive alkaline treatment serves to lyse the colonies. The denatured DNA is then immobilized on the membrane, followed by a proteinase K treatment to digest the interfering proteins. Detection is carried out with colorimetric detection reagents: NBT/BCIP (according to hybridization manual, Roche, Manheim, Germany).

The selected hybridization spots from the nylon filters were identified with the corresponding colonies on the LB-plates of cells containing the genomic library. The interesting colonies were isolated and plated on fresh, selective LB plates to obtain single-cell colonies for PCR screening, using the same primers to amplify the original DNA probes (A, B, C, D). Thus, each bacterial colony was PCR screened with the four pairs of primers.

E. coli colonies that amplify DNA probes A, B, C, D, or two of them consecutively, were identified. The selected cosmids were isolated and *tbr1* plants were transformed with the different cosmid clones by *Agrobacterium tumefaciens GV3101*. Resistant plants were selected on AMOZ medium agar plates including 0.5% saccharose and kanamycin (50 µg/ml).

2.2.1.9 GATEWAY cloning technology

GATEWAY cloning technology is a novel universal system for cloning and subcloning DNA sequences, facilitating gene functional analysis and protein expression. The GATEWAY cloning system uses phage lambda-based site-specific recombination instead of restriction endonucleases and ligase. This recombination system is used by λ during the switch between the lytic and lysogenic pathways. The key DNA recombination sequences (*att* sites) and

proteins that mediate the recombination reactions are the foundation of Gateway cloning technology (Weisberg and Landy, 1983; Landy, 1989).

2.2.2 DNA/ RNA analyses

2.2.2.1 Plasmid DNA isolation from *E. coli* and *A. tumefaciens* cells

DNA plasmid was isolated using Nucleospin Plasmid kit from Macherey-Nagel.

Overnight bacterial culture resulted from one single colony grown in 5 ml selective LB (YEB for *A. tumefaciens)* medium was used. The cells were harvested by short centrifugation and resuspended in 250 µl solution A1 (50 mM TrisHCl, 10 mM EDTA, pH 8.0, 100 µg/ml RNAse). Then cells lysation is achieved by mixing with 250 µl solution A2 (200 mM NaOH, 1% SDS). A3 buffer (3 M KOAc, pH 5.5) is added for neutralization. The supernatant resulted by centrifuging at 12000 rpm for 10 min. is loaded onto a provided column, then centrifuged briefly again. The flow is discarded and then the column is washed with A4 buffer, containing ethanol. DNA plasmid can be eluted from the column, by adding TE elution buffer and centrifuging at high speed (12000 rpm) for 1 min. DNA concentration was measured spectrophotometrically.

2.2.2.2 Spectrophotometric determination of DNA or RNA concentration

DNA (RNA) concentration and purity was measured spectrophotometrically at 260-280 nm wavelengths. 2 µl DNA sample is dissolved in 98 µl sterile H_2O (the same for RNA sample). The ratio between the values obtained at 260 and 280 nm allows an estimation of nucleic acid purity. Pure DNA (RNA) preparations have OD_{260}/OD_{280} ratios of 1.8 and 2.0 respectively (Sambrook *et al.,* 1989).

2.2.2.3 DNA isolation from *Arabidopsis thaliana* plants

CTAB- DNA extraction (Lukowitz *et al.,* 2000)

The method yields relatively clean, high molecular weight DNA. A single rosette leaf or an inflorescence provides sufficient starting material. The tissue can be used fresh or stored at -20^0C before processing. A small amount of plant material is well grinded in a 1.5 ml reaction tube. 300 µl of 2 x CTAB buffer (2% cetyl-trimethyl-ammonium bromide containing 1.4 M NaCl, 100 mM TrisHCl, pH 8.0 and 20 mM EDTA) is added and the sample is incubated at 65^0C for at least 10 min (up to several hours). After cooling down, 300 µl of chloroform is added and mixed by vortexing. The two phases are separated by centrifuging briefly in a microfuge. The upper, aqueous phase is transferred to a fresh tube and mixed well with 300 µl

2- propanol. The pellet DNA is obtained by centrifuging 5 min, 10000 rpm. The supernatant is discarded and the white pellet is washed with 500 µl of 70% ethanol, then spinned down again. Ethanol is removed and the pellet is allowed to air-dry, being dissolved at the end in 100 µl TE buffer (10 mM Tris-HCl, pH 8.0, 1 mM EDTA). 1-2 µl of DNA is necessary for a PCR reaction. DNA prepared in this way can be kept few weeks at 4^0C, or at -20^0C, for several months.

Alkaline lysis DNA preparation (Klimyuk *et al.,* 1993).

Alkaline lysis method is quick and yields a roughly clean DNA. Typically, this protocol is used to process a large number of tissue samples in a microtiter plate format. A 96-wells plate for use in a termocycler is ideal for the purpose. The plate can be placed on ice. Using the round end of flexible polyethylene stirring rods that exactly fit into the wells of the microtiter plate, several tissue samples can be mashed simultaneously. Part of a young rosette leaf or a small inflorescence provides sufficient material. The tissue can be used fresh or stored at -20^0C prior to processing. Using significantly higher amount of tissue may lead to problems with PCR amplification due to the presence of inhibiting substances in the lysate. A small amount of plant tissue is harvested and placed in the plate's wells. The tissue is mashed in 50 µl 0.25 N NaOH then incubated for 30 seconds at 96^0C. First, 50 µl 0.25 N hydrochloric acid is added, and second, 25 µl 0.5 M Tris HCl pH 8.0 / 0.25% (v/v IGEPAL CA-630). 2 min. incubation at 96^0C is necessary. 1-2 µl from this crude lysate can be used in a PCR reaction as template. The obtained crude lysate allows PCR amplification of small DNA fragments, such as SSLP markers.

2.2.2.4 DNA purification methods

PCR products purification and DNA fragments elution for cloning purposes were done using QIAquick PCR purification kit (Qiagen), or Nucleospin Extract (Macherey-Nagel), following the provided manuals instruction.

2.2.2.5 DNA sequencing

All DNA sequencings, either isolated plasmids DNA, or PCR products, were performed by MWG-Biotech (Ebersberg, Germany), or AGOWA GmbH (Berlin, Germany).

2.2.2.6 Total RNA isolation from *Arabidopsis thaliana*

RNA was isolated using Trizol reagent. The plant material has to be harvested and immediately placed on liquid N_2. The material is grinded very well in a porcelain pot, in liquid N_2 all the

time, to keep the material frozen. 100 mg plant material is necessary in order to obtain a high concentration of RNA. The grinded material is mixed very well with 1 ml Trizol. 200 ml cloroform is added over, then the sample is vortexed and incubated 5 min. at room temperature. The two phases are separated by spinning for 10 min. at 13000 rpm, at 4^0C. The resulted aqueous phase is transferred into a fresh, sterile tube (around 500-600 µl), mixed well with 500 µl isopropanol and left 10 min. at room temperature. After centrifuging at 13000 rpm for other 10 min., the obtained white pellet is washed with 1 ml 70 % ethanol and then centrifuged again at 13000 rpm for 5 min. The pellet appears now clear and almost gelatinous. After few minutes of air-dry, 50 µl sterile water is added to dissolve the pellet. A DNA digestion step is necessary, taking into consideration that a small DNA amount is present also in the pellet. The typical yield is between 500-700 µg RNA per 100 mg of mature leaf material.

2.2.2.7 DNA-se treatment of isolated RNA

To avoid any DNA contamination in the isolated RNA, and further interferences in the sensitive analyses (as RT-PCR), a DNA-ase enzyme digestion is needed. In a 1 ml RNA-ase free sterile tube is added 1-5 µg of RNA, 1 µl sterile H_2O, 1 µl 10X reaction buffer and 1 µl of DNA-ase I, (1 unit/µl, Sigma product) and DNA digestion occurs at room temperature, for 15 min. The reaction is stopped by adding 1 µl of stop solution (50 mM EDTA) to bind Ca and Mg ions to inactivate DNA-ase I and heating at 70^0C for 10 min. to denature both, DNA-ase I and RNA hairpins. More sterile water is added over the sample up to 200 µl and other 200 µl of 4 M LiCl to reprecipitate RNA overnight, at 4^0C. RNA is collected after a centrifugation step at 12000 rpm, for 10 min., then the pellet is washed in 1 ml 70% ethanol and air-dried. RNA is dissolved in 50 µl sterile water. The typical yield is between 500-700 µg RNA per 100 mg of mature leaf material. RNA can be now used for further sensitive analyses.
DNA contamination can be checked after DNA-ase treatment by performing a PCR reaction using enzyme treated sample as template, and a pair of primers which amplifies a specific product on genomic DNA (actin gene product, 160 bp in length on cDNA template, and 616 bp in length on genomic DNA template).

2.2.2.8 First strand cDNA synthesis

The cDNA synthesis was performed according to Invitrogen description. The following 20 µl reaction volume can be used for 10 pg-5 µg of total RNA, DNA-ase treated previously to avoid DNA contamination. In a nuclease free microcentrifuge tube the following components are added: 1 µl of oligo (dT) (50 µM); 10 pg-5 µg of total RNA; 1 µl 10 mM dNTP mix (10 mM

each dATP, dGTP, dCTP and dTTP at neutral pH); sterile distilled water up to 13 µl. The mixture is heated to 65^0C for 5 min. and then incubated on ice for at least 1 min. In the same tube is added 4 µl 5X first-strand buffer; 1 µl 0.1 M DTT; 1 µl RNA-ase OUT™ recombinant RNA-ase inhibitor (40 units/µl; 1 µl of superscript III RT (200 units/µl). The components are well mixed bx pipetting, then incubated at 50^0C for 30-60 min. The reaction is inactivated at 700C for 15 min. The resulted cDNA can be used as a template for PCR amplification.

2.2.2.9 Real-Time RT-PCR analysis

PCR reactions were performed in a 96-well plate using an ABI PRISM® 7900 HT Sequence Detection System (Applied Biosystems, Foster City, CA, USA). SYBR® Green was used to monitor double strand (ds) DNA synthesis. The reactions were set in 10 µl volume, containing 5 µl 2X SYBR® Green Master Mix Reagent (Applied Biosystems), 1.0 ng cDNA, 200 nM of each gene-specific primer (forward and reverse), and sterile H_2O up to 10 µl.

A standard thermal profile reaction programme was used for amplification: 50^0C for 2 min; 95^0C for 10 min.; 40 cycles of 95^0C for 15 sec and 60^0C for 1 min. The resulted data were analysed using the SDS 2.0 software (Applied Biosystems). All amplification plots were analysed with a threshold of 0.2 to obtain Ct (threshold cycle) values. The Ct values were first normalized to the Ct values of ubiquitin 10 (Ubq10-At4g05320) housekeeping gene, in order to compare the results from different PCR runs or cDNA samples. PCR efficiency was calculated using the program LinRegPCR (Ramakers *et al.,* 2003).

2.3 BIOCHEMICAL METHODS

2.3.1 *tbr1* mutant plant selection

tbr1 mutant plants can be selected by observing individual treated plant leaves, under a microscope in the presence of polarized light. The first step in the leaf preparation is washing with methanol, for 15-20 minutes to decolorize, then heating at 98-100^0C in lactic acid (85%) for one hour to complete discoloration. After rinsing a few times with water, the material is ready for visual observation under the microscope, in the presence of polarized light (described by Potikha and Delmer, 1995).

2.3.2 GUS activity assay

Transgenic plants carrying gene promoter-GUS fusion constructs were checked for the GUS activity using X-GLUC (5-bromo-4 chloro-3-indolyl β-D-glucuronic acid) (Jefferson *et al.,*

1987). The plants were immersed in fresh prepared GUS staining solution (1 mg/ml X-GLUC, 10 mM EDTA, 0.1% Triton X-100, and 50 mM sodium phosphate buffer, pH 7.2) and then incubated at 37^0C overnight. The next day the plants were washed several times in ethanol until chlorophyll was completely removed, for a better GUS staining observation. The pictures were taken under the microscope.

2.3.3 Stem cross-sections

The stem cross-sections from wild type and *tbr1* plants were made using the vibratome (Leica, Bensheim, Germany). They were stained in toluidine blue 0,1% for 3 min., then observed under the microscope.

2.3.4 Isolation of cell wall material

Cell wall material necessary for biochemical analysis (GC and MALDI-TOF) was isolated as follows. Fresh plant material was harvested and snap-frozen in liquid nitrogen. The frozen material was grinded in methanol using either a retch-mill (Retsch, Haan, Germany) for small amounts (~2 mg scale). Afterwards, the material was extracted with a 1:1 (v/v) methanol, chloroform mixture until no more green pigments could be extracted form the plant material. Finally, the material was washed once with acetone and left to dry overnight or alternatively subjected to vacuum for 30 min.

Leaf trichomes were harvested by shaving individual leaves (described in the section 2.3.7).

2.3.5 Cell wall polysaccharides antibodies immunolabeling

With the aid of a raser-blade, fine leaf sections were made from wild type and *tbr1* plants, then washed in an eppendorf tube with 800 µl antibody solution, by shaking for 2 h. The antibody solution was prepared in PBS (phosphate buffered saline) (NaCl, KCl, Na_2HPO_4, pH 4.8) containing 3% (w/v) non fat dry milk. After antibody wash, the sections are rinsed five times in PBS buffer, then a second solution, containing a 100 fold dilution of anti-rat/mouse IgG linked to FITC (fluoresceinthiocyanat, green fluorescent label) in PBS/milk) is added and incubated for 1 h by gently shaking. PBS washes (five times) are necessary afterwards. At the end, the material is fixed on glass slides, and observed under the microscope for fluorescence labelling.

2.3.6 GFP-protein fusion transient expression

Microcarriers of gold particles can be used for leaves bombardment with protein-GFP fusion constructs. 30 mg of dry gold particles (1 µm size, Bio-rad, Germany) are washed with 1 ml of

100 % ethanol then precipitated by a 5 min. centrifugation. The washing step is repeated three times. After that, 0.5 ml of sterile distilled water is added and the particles resuspended by vortexing. Aliquots of 50 µl each are prepared for bombarding. The particles can be stored at -20^{0}C for few weeks. DNA plasmid (protein-GFP fusion construct) is isolated using Nucleospin Plasmid kit (Macherey Nagel). 5 µl of DNA plasmid (1 µg/µl) is necessary for one bombarding, prepared in the following way. In one sterile 1.5 ml tube is added under continuous vortexing: 5 µl DNA plasmid, 50 µl of sterile 2.5 M $CACl_2$ and 20 µl of 0.1 M spermidine (free base, tissue culture grade). The microcarriers are centrifuged at 10000 rpm for 10 sec. and then the supernatant has to be removed as much as possible. 250 µl of 100 % ethanol is added for washing by vortexing, then centrifuged again and the supernatant discarded. At the end, the microcarrierrs are resuspended in 50 µl of 100 % ethanol and kept on ice. The rapture discs used for bombarding were 1100 psi (Bio-rad, Germany)

The *A. thaliana* wild type leaves have to be placed one by one on sterile MS agar-medium plates, with the adaxial side touching the medium. The plates with the bombarded leaves are kept for 1-2 days at 25^{0}C to develop the signal, then observed under confocal microscope.

2.3.7 Scanning electron microscopy analysis of wild type Col-0 and *tbr1* mutant trichomes

Leaf trichomes were used for the analysis. The trichomes were harvested by shaving individual leaves. First, the leaf is fixed on a glass slide, then kept in liquid N_2 until frozen. The frozen trichomes can be shaved using a sharp forceps, then placed in a 1.5 ml eppendorf tube containing water. The material is harvested by centrifuging briefly to high speed. For scanning electron microscopy, the trichomes were deposited on holders with Carbon foil gold sputtering.

2.4 DATABASES AND INTERNET LINKS

Arabidopsis Biological Resources Center	http://aims.cps.msu.edu/
Arabidopsis thaliana Insertion Database	http://atidb.org/cgi-perl/index
ClustalW	http://www.ebi.ac.uk/clustalw/
dCAPS Finder	http://helix.wustl.edu/dcaps/
Munich Information Center for Protein Sequences	http://mips.gsf.de/projects/plants/
Plant Cis Acting Regulatory Elements	http://intra.psb.ugent.be:8080/PlantCARE/
The Arabidopsis Information Resource	http://www.arabidopsis.

T-DNA Express	http://signal.salk.edu/cgi-bin/tdnaexpress
The ExPASy server	http://www.expasy.org/
The TIGR Arabidopsis thaliana Database	http://www.tigr.org/tdb/e2k1/ath1/

3. CHAPTER : RESULTS

3.1 INITIAL CHARACTERIZATION OF THE TBR1 MUTANT

3.1.1 Trichomes phenotype

Seeds from *tbr1* mutant plants were first grown in the greenhouse to check the presence of the previously described phenotype (Potikha and Delmer, 1995) when isolated the mutant, lacking the trichome birefringence under polarized light (Figure 8).

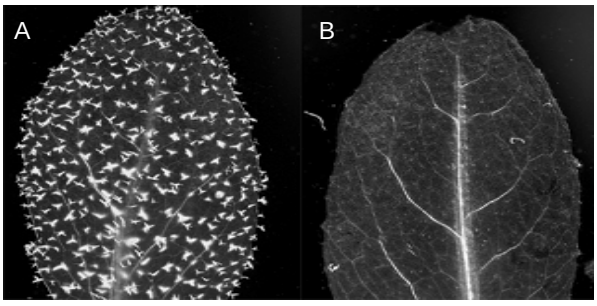

Figure 8. Phenotype of *tbr1* trichomes observed under polarized light. The pictures were taken from individually treated 25 day old leaves, with a light microscope under polarized light, using a Leica polarizer. A) –Wild type Col-0 leaf reveals the strong trichome birefringence under polarized light; B) –*tbr1* mutant leaf display no trichome birefringence when compared to wild type.

Consistent with the previous description of the phenotype (Potikha and Delmer, 1995), individual mutant trichomes have a normal shape and size (Figure 9).

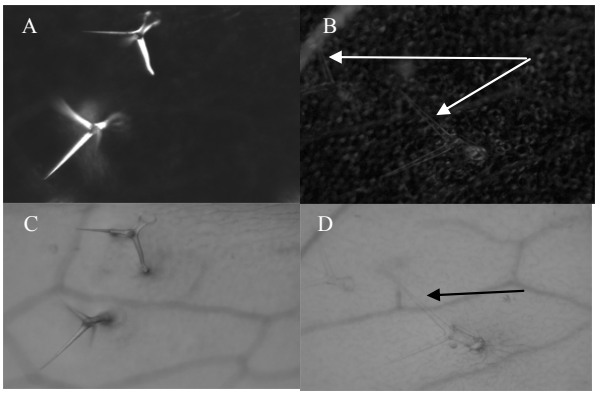

Figure 9. Individual *tbr1* trichome phenotype observed in the presence and absence of polarized light. Leaves of 25 days old plants were observed and pictures were taken from leaf trichomes under the light microscope, using a Leica polarizer. A) –Wild type Col-0 trichomes seen under polarized light B) –*tbr1* trichomes (indicated with the white arrows) observed under polarized light; C) –Wild type Col-0 trichomes observed in non polarized light; D) –*tbr1* trichomes (indicated with the black arrow) in non polarized light. Mutant trichome shape and size are essentially the same as those of wild type trichomes.

3.1.2 Growth phenotype

When looked at the growing *tbr1* plant population in the greenhouse, an additional phenotypic feature was observed, namely a large variation in growth, from dwarf plants up to plants comparable to wild type in size (Figure 10).

Figure 10. Variation in growth of *tbr1* mutant plants compared with wild type Col-0, when grown in the greenhouse conditions. The plants were five weeks old. *tbr1* plants display a large variation in developmental state.

3.1.3 Leaf phenotype

The mutant also exhibits a leaf phenotype having smaller leaves than the wild type, with shorter petioles and a softer surface (perhaps because of the smaller number of trichomes), and being rather round in shape than oval, as in the wild type (Figure 11).

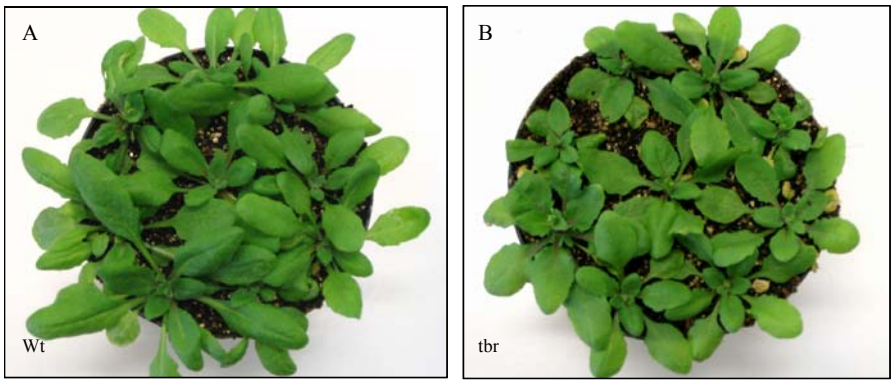

Figure 11. Leaf phenotype of *tbr1* plants; The plants were grown for 20 days in the greenhouse. (A) – Wild type Col-0; (B) –*tbr1* plants. *tbr1* leaves are smaller, softer, and they have a more rounded shape and shorter petioles compared to wild type plants.

3.1.4 Stem phenotype

When grown in the greenhouse, the mutant plants develop a thinner and shorter stem compared with wild type. It is possible that this phenotype is connected to a lower level of secondary cellulose deposition, in which case it might be possible to detect some of the morphological changes known for the characterized secondary cell wall mutants, *irx 1* and *3* (*irregular xylem*) (Taylor *et al.*, 2000; Turner *et al.,* 1999; Turner and Somerville, 1997) in *tbr1* plants. Therefore, stem diameter was measured, at the upper part and at the lower part, and stem cross-sections were observed under the microscope to reveal any difference in tissue development and/or morphology. The sections were stained with toluidine blue (0.1%) and observed under the microscope.

From the stem measurements, it can be seen that the mutant plants have significantly smaller diameters, at both measured points (upper and lower stem part, respectively) (Figure 12).

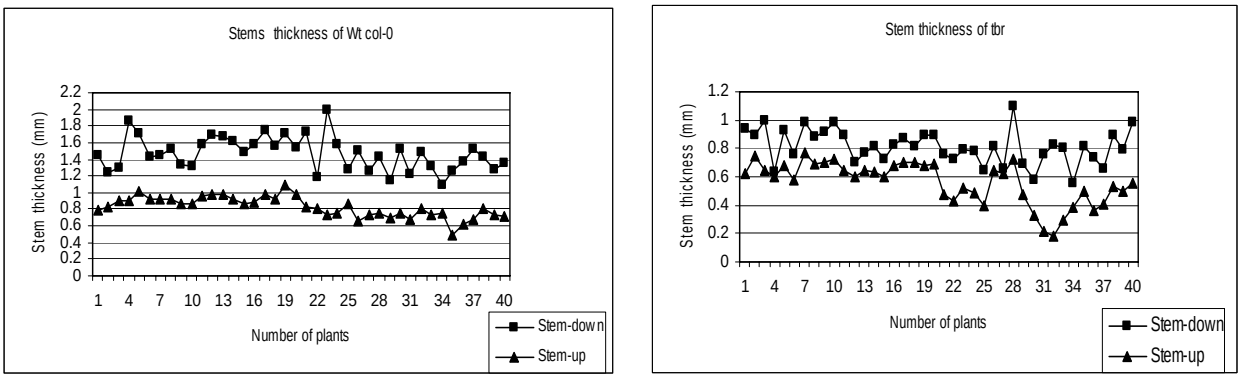

Figure 12. Stem thickness measurements of wild type and *tbr1* plants. The diameter of 40 mature growing plant stems, having the same age (25 days old in the greenhouse) were measured in wild type and *tbr1* plants at both, the upper and lower parts of the stem.

Despite the variation in stem diameter, no remarkable morphological differences were detected in the stained stem cross-sections of mutant plants compared to wild type (Figure 13). This is also consistent with previous analysis of the cellulose content in *tbr1* stems, which showed no significant difference when compared with wild type (Potikha and Delmer, 1995).

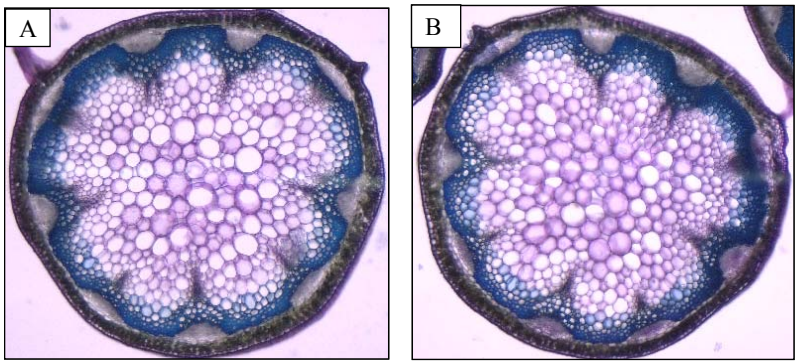

Figure 13. Stem cross-sections of wild type (A) and *tbr1* (B) plants. The stem sections were made from 25 days old plants, using a vibrotome, then stained with toluidine blue (0.1%) and observed under the microscope. A) –Wild type Col-0 stem cross-section; B) –*tbr1* stem cross-section. No morphological difference was observed in the mutant plants when compared to wild type.

3.1.5 Comparison of the *tbr1* phenotype with other secondary cell wall mutants

Trichome birefringence is a phenotypic characteristic of the *tbr1* mutant, that has been described as a secondary cell wall deficiency mutant (Potikha and Delmer, 1995).

The *irregular xylem* (*irx*) mutants of *Arabidopsis thaliana* exhibit a collapsed xylem phenotype that is caused by a deficiency in secondary cell wall deposition, and a decreased cellulose content in the secondary cell wall. Both the *irx1* and *irx3* mutations affect exactly the same cell types and are caused by mutations in the *AtCesA8* and *AtCesA7* genes (Turner and Somerville, 1997; Taylor *et al.,* 1999). Leaves from *irx* mutant plants were individually treated to observe their trichome birefringence phenotype under the microscope, in the presence of polarized light.

Neither *irx1* nor *irx3* plants displayed a lack of trichome birefringence, which is characteristic for *tbr1* mutant (Figure 14, panel B and C). The shape and size of the trichomes are not modified in the *irx1* and *irx3* mutants, either (Figure 15, panel B and C).

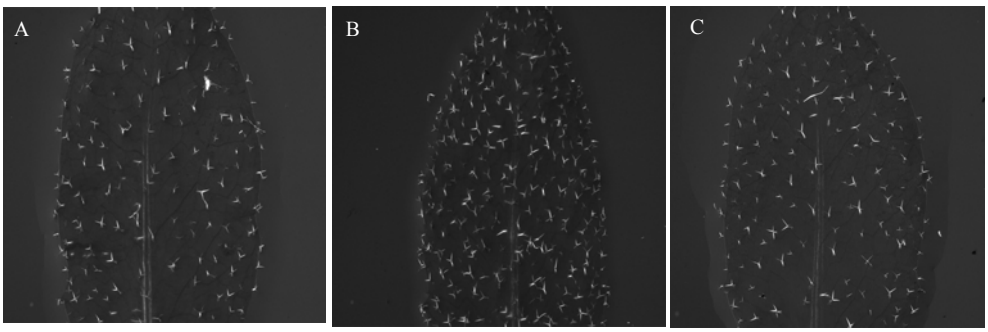

Figure 14. Trichome birefringence phenotype under polarized light of other secondary cellulose deficient mutants. The mutant leaves were three weeks old and they were individually treated for phenotype observation. The pictures were taken under polarized light, using a light microscope and a Leica polarizer. A) –Wild type Col-0 trichome birefringence; B) –*irx1* mutant; C) –*irx3* mutant. The *irx1* and *irx3* mutant plants show normal trichome birefringence under polarized light.

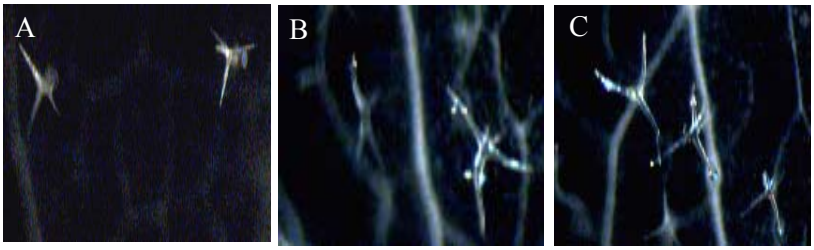

Figure 15. Individual trichomes birefringence phenotype of secondary cellulose deficient mutants, observed under polarized light**.** A) –Wild type trichomes; B) –*irx1* mutant trichomes; C) –*irx3* mutant trichomes. Mutant trichome shape and size are similar to wild type.

3.2 POSITIONAL CLONING OF THE *TBR* GENE

3.2.1 Genetic mapping of the *tbr1* mutant

A rough genetic map position of the *tbr1* mutation was previously established by Ravit Eshed (Lab of D. Delmer, UC Davis, USA) in a bulk segregant analysis, and the mutation was localized between the CIW50 and BstNI markers, on chromosome V of *Arabidopsis thaliana*.

The F2 seeds from a *tbr1* x Ler mapping cross, were used for fine mapping process. More than 2100 F2 plants were analysed by PCR with different genetic markers. A high throughput assay was available in our laboratory, in which the F2 population plants were grown in 96-well trays (with individual plant locus). Plant material was harvested for preparation of the alkaline DNA from individual plants by alkaline lysis, in a corresponding 96-well plate, and the DNA was used as a template for PCR reactions performed in a 96-well plate.

Molecular markers involved in the mapping experiment were either simple sequence length polymorphisms (SSLPs), or cleaved amplified polymorphic sequence (CAPS) markers, all of them localized on chromosome V. Some of the used markers were available in the *Arabidopsis thaliana* collection database, while others were developed based on information available from the Cereon *Arabidopsis* Polymorphism Collection (for instance, MPI100) (Jander *et al.,* 2002). All the selected markers were first checked by PCR using two types of isolated DNA template, a high purity yield (CTAB-DNA (CTAB: cetyl-trimethyl-ammonium bromide buffer)) and a low quality template (alkaline lysis extracted DNA), from wild type Col-0, Ler, a mixture of Col and Ler, and Ws, in different PCR conditions: various magnesium concentrations and a range of annealing temperatures (Table 1).

Table 1. Genetic markers used for *tbr1* positional cloning and the selected optimal conditions required for PCR amplification, Mg concentration and PCR annealing temperature.

No.	Marker name	Marker type			PCR product length (bp)		Mg concentration (mM)	PCR Annealing temperature (^{0}C)
		InDel	**SNP**	**CAPS**	**Col**	**Ler**		
1	**MPI100**	**19**			**175**	**156**	**2.5**	**55**
2	**MHFD**		**SNP**		**124**	**114**	**2.5**	**55**
3	**TasI**			**CAPS**	**269**	**105+164**	**2.5**	**52**
4	**PdmI**			**CAPS**	**129+19**	**148**	**2.5**	**52**
5	**MPH15.1**	**12**			**205**		**2.5**	**50**
6	**MOJB**		**SNP**		**174**	**154**	**2.5**	**50**
7	**MOJ9**		**SNP**		**159**	**148**	**2.5**	**48**
8	**EMC**		**SNP**		**131**	**135**	**2.5**	**50**

These initial checking steps were necessary in order to make sure that the markers were robust enough, offering reliable results under optimal PCR conditions and yielding the correct, specific product from alkaline lysis DNA template, which is easier to obtain when working with a large number of plants subjected to screening (Figure 16).

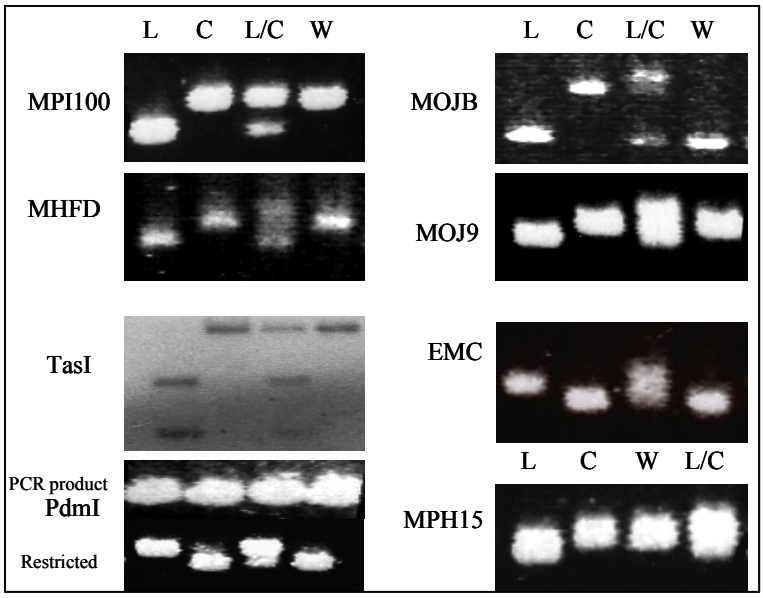

Figure 16. Genetic molecular markers used for *tbr1* fine mapping. The markers were tested by PCR on different DNA templates isolated from Landsberg (L), Columbia-0 (C), a mixture of Landsberg and Columbia (L/C) and Wassilewskija (W) ecotype.

The PCR products were analysed on high-resolution agarose gels (4%) to identify the recombinants in the vicinity of the mutation, based on the PCR screening. PCR products from two 96-well plates were run at once in a large gel chamber. In this way it was easier and faster, to select recombinants from each 96-well tray of plants, screened with two flanking markers, by analyzing on the same agarose gel both PCR products of one plant DNA sample.

A total of 107 recombinants was selected based on PCR screening with two flanking markers, choosing the plants that gave a signal, either as homozygous or heterozygous, respectively, for the two analyzed markers (Figure 17).

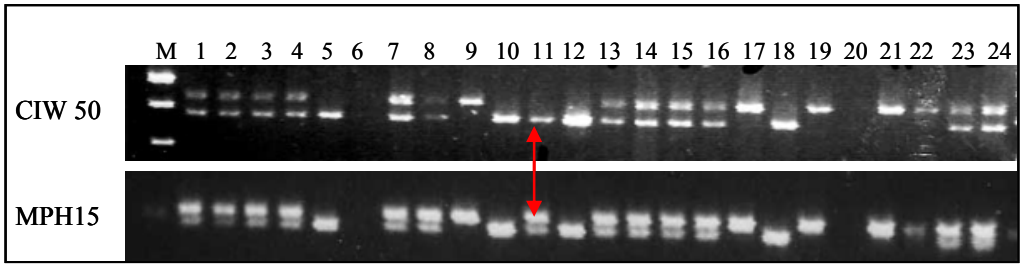

Figure 17. PCR screening of F2 plants *tbr1* x Ler (mapping population) with two flanking genetic markers (for example, CIW50 and MPH15 shown here) to identify recombinants (as indicated by red arrow), based on PCR screening.

For these recombinants, high purity CTAB-DNA was prepared and analyzed by PCR with further genetic markers available from the chromosomal area. In this way, the number of recombinants was reduced step by step and the genetic interval of interest was progressively narrowed down, by using closer and closer markers in the region. F2 plants that showed a wild type phenotype but had different genotypes for the flanking markers, were also phenotyped using the F3 progeny (24 of the F3 plants were checked for each of the selected F2 plant). By correlating the PCR marker screening results with recombinant phenotyping, in the end, the genetic interval containing the mutation was restricted to 45 kb, between the PdmI and MPH15 markers, on BAC clone MPH15 of chromosome V (Figure 18).

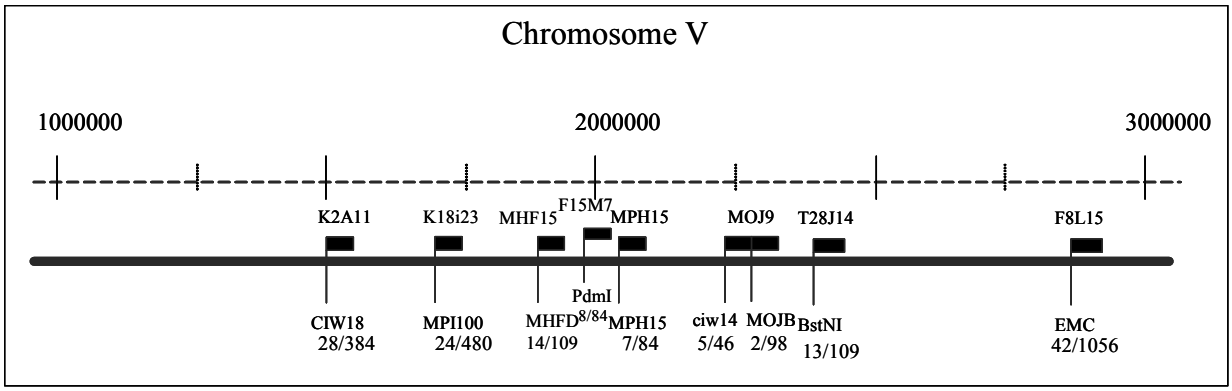

Figure 18. Positional cloning of the *TBR* gene. A scale representation of important genetic markers used for *tbr1* mapping, localized on top of chromosome V. Black boxes represent the BAC clones names on which the respective markers are situated . The number of recombinants identified out of the number of analyzed plants for each genetic marker is indicated below the marker name.

3.2.2 Cosmid complementation of *tbr1* mutant

To determine the identity of the *TBR* gene, a mutant complementation experiment using bacterial colony hybridization approach was performed. Initially, four evenly distributed specific DNA probes were designed (placed at every 10-15 kb distance), so that they cover the entire selected genetic interval containing the mutation (45 kb in size). The first probe, A, was chosen close to the end of BAC F15M7, position 72081 bp. The second DNA probe -B- is located on the next BAC clone, BAC MPH15, position 16890 bp. Probe C, is situated on BAC MPH15 as well, position 32662 bp. The last probe, D, is also on BAC MPH 15 at position 44420(Figure 19). The resulted PCR products vary in size from 301 to 505 bp. (Table 2).

The genomic sequences of DNA probes used for the cosmid complementation of *tbr1* mutant experiment are given in Appendix I.

Table 2. DNA probes designed for *tbr1* complementation.

No.	DNA probe name	Primers	Length (bp)	Genomic position	Flanking genes
1	A	Forward: GATTCTGGATTCTTAGCTCGT Reverse: TACATTGCTGAGGATATGACC	403	Bac F15M7: 72081	At5g06660 At5g06670
2	B	Forward: AGGCCATAGCGTAAGCAC Reverse: GATTTCATTCATTTCCGTCA	301	Bac MPH15: 16890	At5g06700 At5g06710
3	C	Forward: AACTCTCCACTGCGATCTGA Reverse: GACGCTTGACCAAGGATAGAA	357	Bac MPH15: 32662	At5g06730 At5g06740
4	D	Forward: GCTCATGCGAATACGGTTCTT Reverse: ACATTTAGCAACGGAAAACGG	505	Bac MPH15: 44420	At5g06780

A genomic wild type Col-0 cosmid library inserted in *E. coli NM554* cells (Meyer *et al.*, 1994) was screened with digoxygenin (DIG)-labelled DNA probes, using a colony hybridisation approach, and overlapping cosmid clones were identified and isolated (Figure 19).

E. coli NM554 bacterial cells contain the pBIC20 binary vector (Meyer *et al.*, 1994), which has a cloning range of 10-25 kb, with inserts cloned in the unique *HindIII* site. *A. thaliana tbr1* mutant plants were transformed with the identified cosmid clones- A, B, BC, CD and D (Figure 19), using *Agrobacterium tumefaciens* strain *GV3101* and the floral dip (infiltration) method (Clough and Bent, 1998).

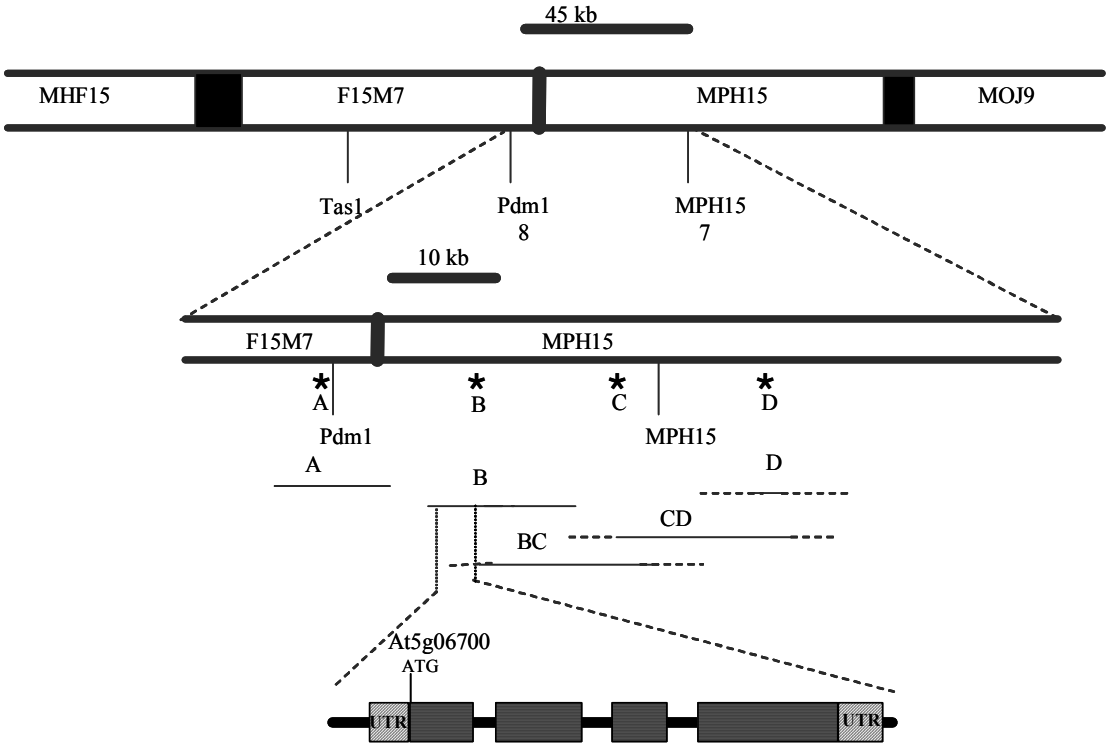

Figure 19. Cosmid complementation of the *tbr1* mutant. The genetic interval of interest is selected between the PdmI and MPH15 markers. The BAC clones MHF15, F15M7, MPH15, and MOJ9, respectively, are indicated as white boxes, showing the overlapping parts as black boxes in between. The DNA probes chosen for the colony hybridization are indicated in the enlarged view, as black asterisks (A, B, C, and D), right under the BAC clone name, and, further below, the positions and lengths of the identified cosmid clones for the selected interval (A, B, BC, CD, and D) are shown. The continuous lines indicates the extents of the selected cosmid clones and this was confirmed by end sequencing. The doted lines mark the end of the cosmid clones as indicated by the presence of *HindIII* sites on the BAC. The structure (not to scale) representation and also gene code annotation of the identified *TBR* gene is shown at the bottom of the figure, together with the annotated open reading frame.

The kanamycin-resistant T1-progeny were selected on agar plates, and resistant seedlings were transferred to soil. Only the *tbr1* mutant seedlings, that were transformed with the cosmid clone hybridizing to DNA probe B displayed a wild type phenotype, i.e. trichome birefringence, thus showing complementation of the mutant. In contrast, plants transformed with the other cosmid clones showed no trichome birefringence of the treated leaves, and thus still exhibited the mutant phenotype.

From the end sequencing result of the cosmid clones hybridizing DNA probes A and B, it could be concluded that the cosmid hybridizing to DNA probe B contains three entire gene sequences, which might be considered as candidates (unknown protein -At5g06700; homeobox protein -At5g06710 and a pseudogene) (Table 3). The neighbouring cosmid clone hybridizing to DNA probe BC contains the full sequences of two (homeobox protein-At5g06710 and pseudogene sequence) (Table 3) of the three potential candidates, but it did not complement the

tbr1 mutant plants. A *HindIII* site (single cloning site of pBIC20 vector) is situated at position 15512 bp on BAC MPH15, inside the gene sequence At5g06700, annotated as an unknown protein in the database. That is the start site of cosmid clone BC. Therefore, the full sequence of the unknown protein (gene-At5g06700), on the cosmid hybridizing to DNA probe B, complemented the mutant, and could be considered as the best candidate gene responsible for the *tbr1* mutation.

Table 3. Gene annotations and positions on the genetic interval of BAC MPH15 analyzed by *tbr1* cosmid complementation. The details for the gene which complemented the mutant and considered as candidate gene responsible for the *tbr1* mutation are marked with bold characters.

Start	End	Type	Code	Description
1	81277		contig	MPH15
6994	9622	Gene/Protein	At5g06680	Gamma-tubulin interactin protein-like
10904	12131	Gene/Protein	At5g06690	Thioredoxin-like 5
13891	16063	Gene/Protein	At5g06700	Unknown protein
18558	20537	Gene/Protein	At5g06710	Homeobox protein
22224	22641	Pseudogene	MPH15 7	
27820	29110	Gene/Protein	At5g06720	Peroxidase
30460	31874	Gene/Protein	At5g06730	Peroxidase
34347	36305	Gene/Protein	At5g06740	Lectin-like protein kinase

Twenty-four progeny (T2) from each transformed plant (T1) were also analysed for the presence of the phenotype, in the next generation. The progeny of plants complemented with B segregated as expected: three plants out of twenty four showed the mutant phenotype, while the other twenty-one revealed trichome birefringence, i.e. the wild type phenotype. The T2 plants transformed with the other cosmids, all had the mutant phenotype.

3.2.3 *TBR* gene sequencing

Subsequently, At5g06700 and some neighbouring genes situated on the restricted mapping interval were considered for sequencing: a gamma-tubulin interactin protein-like gene (At5g06680), thioredoxin-like 5 (At5g06690), and the putative protein (At5g06700). The respective genes were PCR amplified from *tbr1* mutant DNA and also from wild-type Col-0 DNA template, using a proofreading DNA polymerase (*Pfu*), and were sequenced.

Only the sequencing of gene At5g06700, encoding a putative protein of unknown function, revealed a point mutation in *tbr1* plants, compared to wild type DNA (Figure 20).

The sequences of the two other genes (gamma-tubulin interactin protein-like gene, thioredoxin-like 5) were unchanged in *tbr1* plants. Three further independent DNA samples from individual mutant plants were subsequently sequenced and they all confirmed the mutation: a guanine residue present in the wild-type At5g06700 gene is changed to an adenine in the mutant DNA sequence. This transition leads to an amino acid change in the corresponding protein sequence: a glycine residue is replaced by glutamic acid.

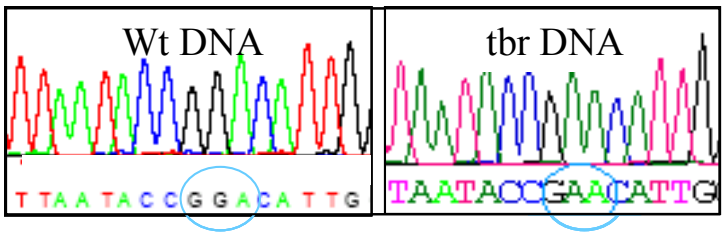

Figure 20. Wild type Col-0 and *tbr1* DNA sequencing chromatograms indicating the point mutation.

The sequencing results were consistent with the results of the complementation experiments. The cosmid clone B, which complemented the *tbr1* mutation was also end-sequenced (to both, left and right side) and shown to contain the entire At5g06700 gene, annotated as a putative protein, in which the point mutation was found.

By these mapping and complementation experiments described, the *TBR* gene was identified as corresponding to gene At5g06700, located on BAC MPH15 of chromosome V of *Arabidopsis thaliana*.

3.2.4 Development of a CAPS marker for the *tbr1-1* allele

To enable *tbr1* mutant alleles to be detected by PCR, a CAPS marker was developed. CAPS markers (Cleaved Amplified Polymorphic Sequences) exploit DNA single nucleotide changes, resulting in different restriction pattern for the analysed types. In this way, a marker can be developed, that allows a mutant plant to be easily identified by a PCR reaction, without phenotypic analysis. Such a marker was designed for *tbr1*. An *HpaII* (*MspI*) restriction site is present in the wild type PCR product, but not in the mutant.

Seeds harvested from complemented plants were grown in liquid culture for three days, and high quality CTAB-DNA (cetyl-trimethyl-ammonium bromide buffer) was isolated and used as the template for PCR amplification. The *tbr1* mutant (T1 generation), that was phenotypically complemented by the B probe, showed a heterozygous signal, as expected,

when the resulting PCR product was digested with *HpaII* enzyme (three bands on the agarose gel) (Figure 21). All the others gave the signal of the unrestricted PCR product, corresponding to the mutant allele (one PCR product band on the agarose gel).

Wild type DNA sequence containing *HpaII* enzyme restriction site (CCGG):

GGTTGGATTTGGTTGGGAAGTCCTCTGAGCAGTACAAAGGAGCTGATGTTATTGTCTTTAATA**CCGG**ACATTGG
HpaII
TGGACTCATGAGAAAACATCCAAAGGgtactaaaatctctctcaatctactggaatatttgctctgtctttgtttg
tgttgtataatgtagaactgattttggagtttgtttcatagGGAGGATTATTATCAAGAAGGAAGTAATGTTTATC
ATGAACTCGCTGTTCTTGAAGCTTTTCGTAAAGCTTTGACTACATGGGGTCGATGGGTTGAGAAGAATGTGAATCC
GGCAAAGTCC**CTCGTTTTCTTTCGGGG**

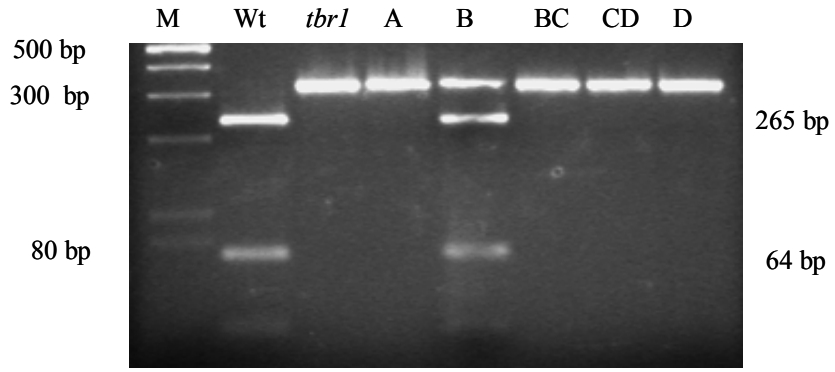

Figure 21. Development of a CAPS marker for the *tbr1-1* allele. The DNA sequence containing an *HpaII* restriction site (marked with red color and underlined in the sequence fragment) is given. The forward and reverse primers used to amplify the DNA fragment are marked as bold flanking sequences. The capital letters denote the exon sequence, while the small letters denote the intron DNA sequence. PCR products (corresponding to wild type, *tbr1*, and *tbr1* mutant plants transformed with A, B, BC, CD, and D) were restricted with *HpaII* and then run on a high resolution agarose gel (4%). The product corresponding to cosmid B, that complemented the *tbr1* mutant, gives the expected heterozygous signal (three bands on the agarose-gel).

3.2.5 The *TBR* gene structure

The annotation of the *TBR* in the publicly available database comprises four exons and three introns, and has a genomic length of 1.5 kb (Figure 22).

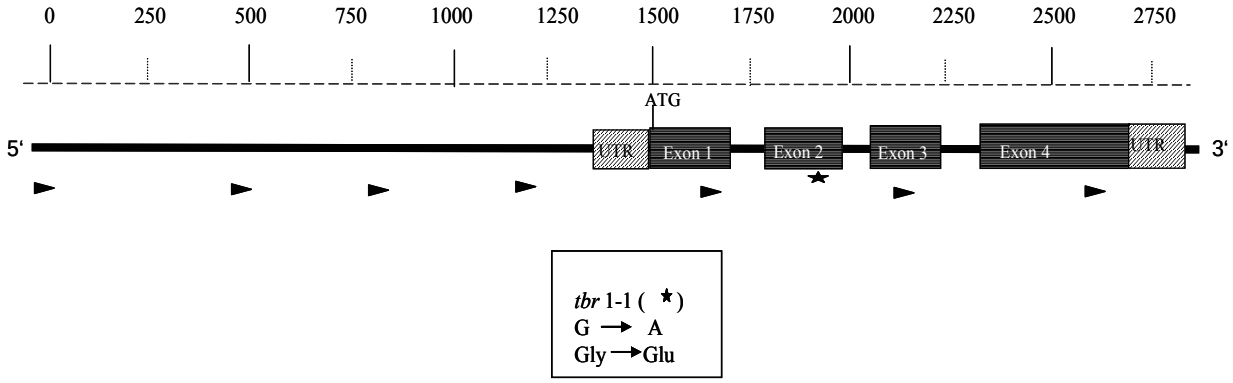

Figure 22. Structure of the *TBR* gene, showing exons (dark boxes) and introns (spaces in between the boxes), as annotated in the *Arabidopsis thaliana* public database. The positions of the sequencing primers used are indicated by small black arrows. The position of the mutation found in the *tbr1* mutant DNA sequence is marked with a black asterisk.

There were some indications suggesting that the *TBR* gene has a larger size than the one annotated in the public database, at the time of identification. Three cDNA clones were available for the *TBR* transcript: 179N15, G4A3 and RAFL16-77-N09. All three clones were obtained, the respective plasmids were isolated and they were sent for DNA sequencing. The third clone, RAFL16-77-N09 contained the full-length cDNA, which indicates that the expressed part of the *TBR* gene extends with an additional 5' region. Another independent indication was that the N-terminal part of *TBR* protein sequence showed a very high similarity with a homologous gene sequence (annotated as -At3g12060).

The proposed *TBR* gene, including the segment that is missing from the gene sequence annotation, consists of 2.2 kb; it contains five exons and five introns, with a long fragment in front, annotated as an untranslated region (UTR) in the database (Figure 23). The transcript length is 1.8 kb. There were two more open reading frames present in the extended fragment, very close to each other (21 bp in between), in the same reading frame as each other, and with the ATG- translation initiation codon annotated as start in the database.

The long gene structure was confirmed by the sequence of the available cDNA clone-RAFL16-77-N09 and furthermore, two different complementation experiments were performed, involving either the database annotated, or the suggested longer gene fragment to rescue the mutant phenotype (details in the section 3.3).

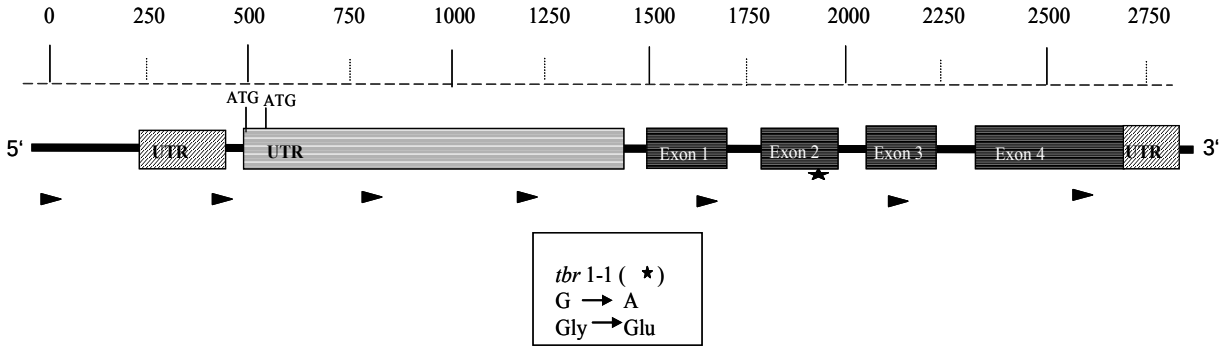

Figure 23. Suggested structure of the *TBR* gene. Exons are indicated as dark boxes, introns- the segments between exons. The extended part of TBR protein is marked as a long UTR in the database (grey horizontal shading). The black asterisk shows the position of the mutation identified in the *tbr1* mutant. The positions of the sequencing primers used are indicated by small black arrows.

3.2.6 The *TBR* gene and its homologues in *Arabidopsis thaliana*

The TBR protein is a member of a novel plant specific gene/protein family containing more than 20 members, and designated as TBL-trichomes birefringence like. None of the proteins in this family has an attributed biochemical or biological function (Figure 24, panel A). The identified mutation in the *TBR* sequence introduces a negatively charged residue into a highly conserved motif among family members, which is characterized by the presence of uncharged amino acid residues defining a hydrofobic region (Figure 24, panel B).

TBR is predicted to be a membrane-spanning protein (transmembrane region between amino acid residues 39 and 56, based on computer program analysis (SwissProt)). One of the closest homologues is a segmental duplicated twin (*TBL1*/gene At3g12060) of *TBR*, located on chromosome III of *Arabidopsis thaliana* (Figure 25).

A

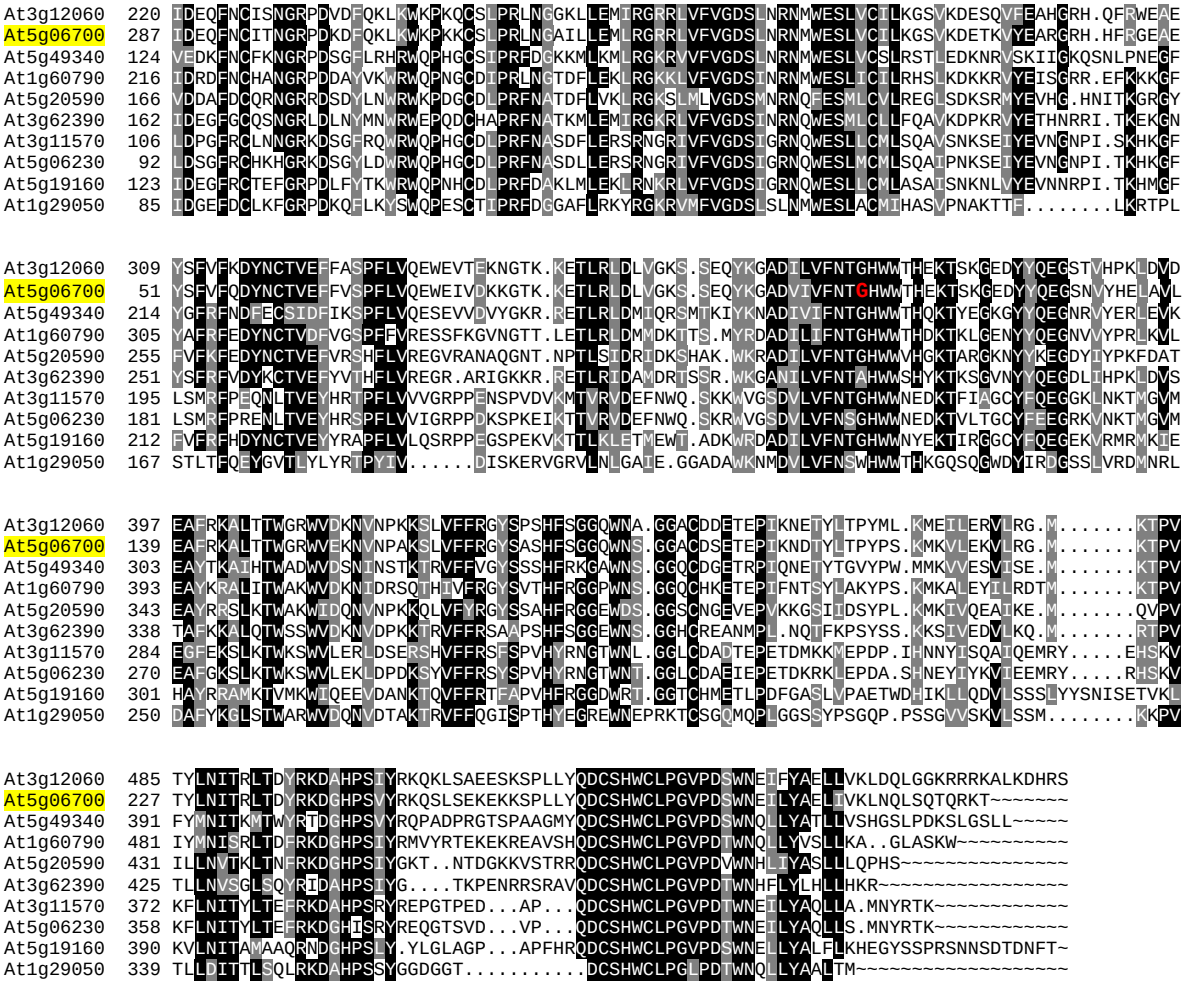

B

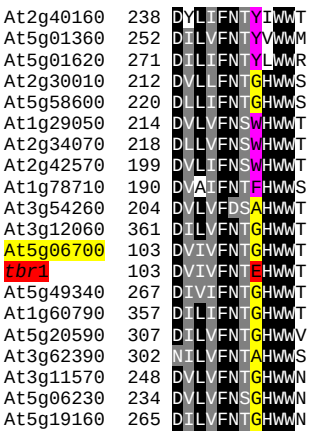

Figure 24: A) Alignment of the C-terminal region of *TBR1* homologues in *Arabidopsis thaliana*. The aminoacid change in the *tbr1* mutant is marked in red color**. B) The amino acid exchange in** *tbr1* (G to E), marked in red color, introduces a negatively charged residue into a highly conserved motif.

Figure 25. Segmental duplications between chromosomes III and V of *Arabidopsis thaliana* including the *TBR* gene and its closest homolog, and the similarity in the gene structure between *TBR* and its duplicated homolog.
A) *TBR* homolog –gene At3g12060, is a segmental duplication of *TBR* (At5g06700) on chromosome III. The numbers below the chromosome bars indicate the respective chromosome number; B) panel shows a schematic representation (to scale) of *TBR* and its duplicated homolog displaying their high similarity. Exons are indicated as grey boxes, introns as the fragments between exons, and UTRs are also indicated on the figure (grey oblique shading). The location of the mutation in *tbr1* mutant is indicated by a black asterisk on the figure.

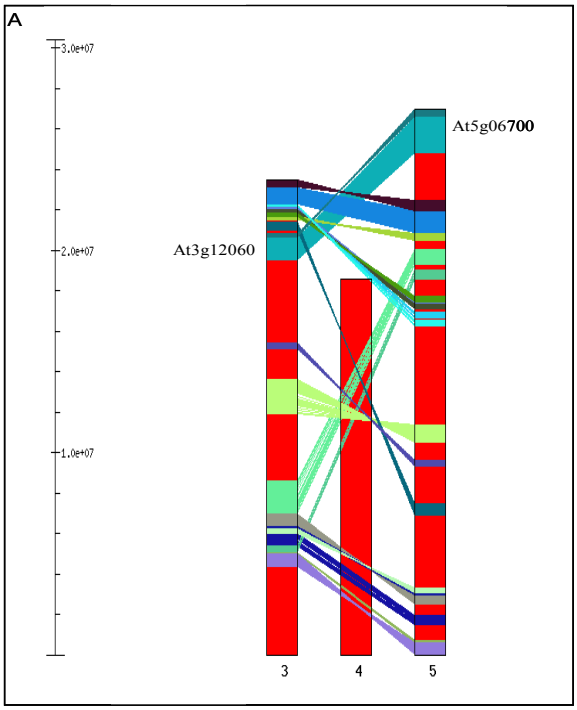

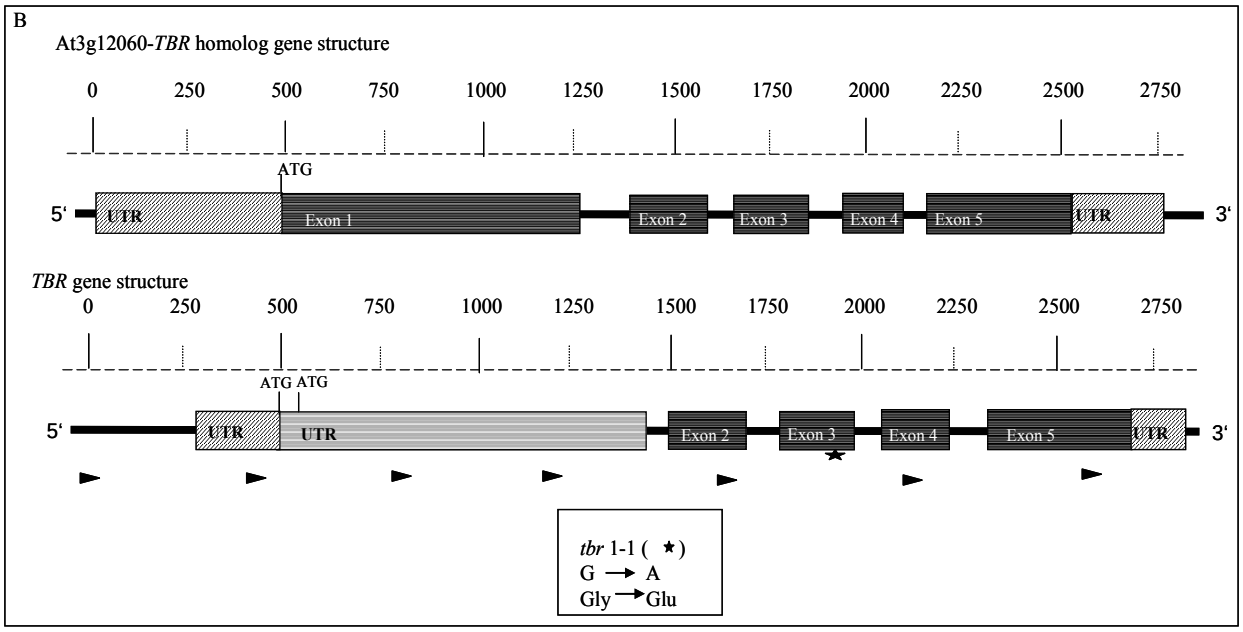

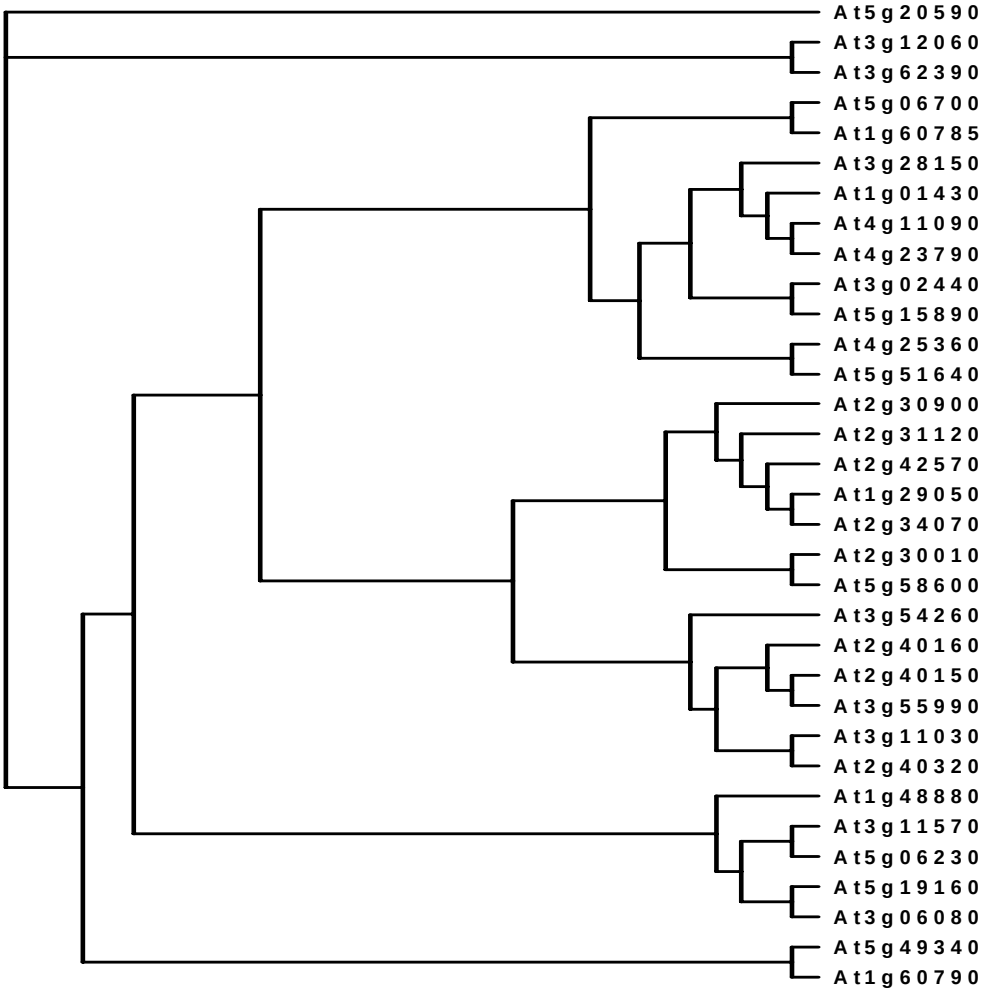

Figure 26. Phylogenetic tree of *TBR* homologous genes in *Arabidopsis thaliana*. The phylogenetic tree was constructed using the deduced protein sequences of all members, using ClustalW program.

3.3 COMPLEMENTATION OF THE *TBR1* MUTANT USING EITHER THE SUGGESTED, OR ANNOTATED GENE FRAGMENT

3.3.1 Complementation of *tbr1* mutant using the suggested gene fragment

With respect to a confirmation of the real length of the identified *TBR* gene, two different mutant complementation experiments were designed involving both, the annotated and the suggested longer gene fragment. Finding which one is able to rescue the mutant phenotype reveals whether the upstream gene sequence is it a coding or non-coding region and what is the start codon.

A genomic DNA fragment of suggested *TBR*, including the entire data-base annotated gene sequence together with the missing fragment, suspected to be part of the gene, was cloned into a binary vector to complement the mutation. The primers used to amplify this insert were placed as follow: the forward one starts at 80 bases upstream of the first non-annotated ATG-start point, and the reverse one, 191 bases downstream of the stop codon TAA (Figure 27, panel A). The amplified PCR product was 2444 bp long, containing *BamHI/SalI* restriction sites at the ends to make it suitable for cloning into the MCS (multiple cloning site) of the pBINAR vector (12 kb, kanamycin resistance gene).

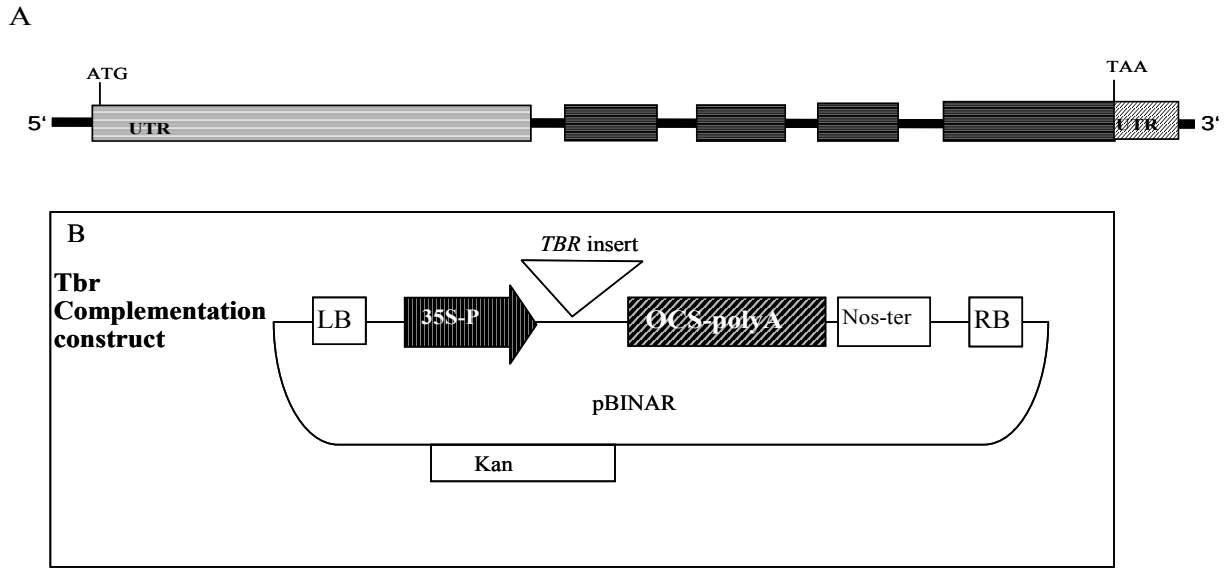

Figure 27. Generated construct for *tbr1* mutant complementation, using the suggested gene fragment**.** A) –Representation of the amplified gene sequence (not to scale) used for *tbr1* complementation; B) –The construct resulted by inserting the *TBR* fragment into the pBINAR vector; 35S-P represents CAMV 35S promoter; OCS-poly A indicates the polyadenylation signal sequence of octopine synthase and Nos ter- the nopaline synthase terminator. Left border and right border are also indicated as LB and RB, respectively.

The constructed plasmid was introduced into *E. coli* strain *DH5α*, by chemical transformation, then transferred into electrocompetent *Agrobacterium tumefaciens* strain *GV 3101* and finally, introduced into *tbr1* mutant plants, by the floral dip (infiltration) method.

The transformed plants were selected on medium agar plates, containing the right selection marker, (kanamycin). The mature resistant plants were further checked for the presence of the *tbr1* phenotype, i.e. lack of trichome birefringence under polarized light.

All the resistant plants displayed a wild type phenotype, (in terms of trichome birefringence, density of trichomes, growth rate and leaf phenotype), leading to the conclusion

that the mutation was successfully complemented by the suggested longer gene fragment (Figure 28, panel B and D).

Figure 28. Phenotype of complemented *tbr1* plants when using the suggested (longer) *TBR* gene fragment. A) –Wild type Col-0 plants; B) –Complemented *tbr1* plants; C) –*tbr1* plants; D) –Trichomes phenotype of the complemented *tbr1* plants. The resistant plants display the strong birefringence under polarized light, characteristic of wild type trichomes.

3.3.2 *tbr1* mutant complementation using the annotated gene coding region

A second experiment was designed to test whether the annotated gene coding sequence could complement the mutant plant, and whether the annotated open reading frame encodes the full-length functional protein, or not. A genomic fragment of 1235 bp in size was amplified, including the entire annotated *TBR* gene, plus 65 bases upstream of ATG, and ending with 30 bases downstream of the stop codon (TAA) (Figure 29).

Figure 29. Representation of the database annotated *TBR* gene fragment (not to scale) **used for mutant complementation.**

The PCR amplified insert was containing the right restriction sites at the ends necessary for ligation into the binary vector.

The cloning strategy was similar to the first *TBR* gene complementation experiment (pBINAR vector was used and the *BamHI/SalI* restriction sites for inserting the gene fragment into the vector). The selection of progeny and the microscopic phenotype analysis under polarized light was done in the same way as described above. All selected transgenic plants clearly showed the mutant phenotype, i.e. lack of trichome birefringence, variation in growth rate, low trichome

density, therefore, the mutation was not complemented by the selected short genomic fragment based on the annotation of the *TBR* gene in the public database (Figure 30). This indicates that the 5' sequence is required to yield a functional gene product.

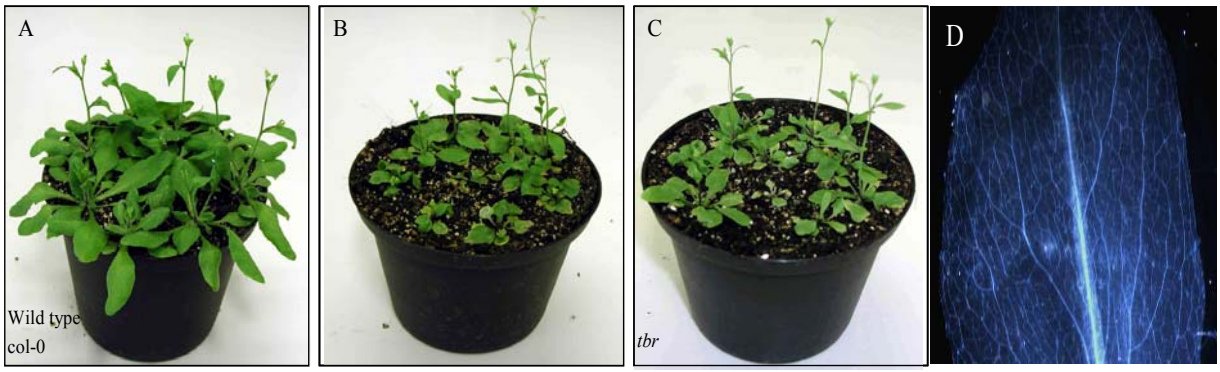

Figure 30. Phenotype of *tbr1* plants transformed with a construct containing the database annotated gene fragment. A) –Wild type Col-0 plants; B) –Transformed *tbr1* plants; C) –*tbr1* plants; D) –Trichome phenotype of the complemented *tbr1* plants observed under polarized light. Transformed *tbr1* plants display no birefringence of the trichomes observed under polarized light.

The *TBR* transcript presence was also checked in *tbr1* plants transformed with the construct containing the annotated gene fragment by RT-PCR, using a pair of primers spanning the annotated transcript fragment, giving a product of 72 bp length, to rule out the possibility that the construct is not expressed.

The inability of the shorter *TBR* gene fragment, based on the annotation of the gene in the public database, to complement the mutation, showed that the annotation is likely to be incorrect. The RAFL16-77-N09 cDNA clone indicates that the annotated gene is missing an exon from the 5'-end of the protein coding region. This was confirmed by the ability of the longer, suggested fragment of the gene to complement the *tbr1* mutant. Therefore, the extended part of the transcript, suggested to belong to it, has a role in the protein function.

3.4 *TBR* GENE EXPRESSION ANALYSIS

3.4.1 RT-PCR expression analysis of *TBR* and two close homologues in wild type *Arabidopsis thaliana* plants

Real time RT-PCR analysis was used to investigate expression patterns of the identified *TBR* gene in different parts of the *Arabidopsis thaliana* plant. RNA was extracted from various tissues from wild type Col-0 plants, at different developmental stages: roots, rosette leaves, cauline leaves, shoot apex, stems, flowers, green siliques and mature seeds, and cDNA was prepared and further used as a template for the real time RT-PCR analysis. RT-PCR primers designed from the sequences of *TBR* and two close homologues (*TBL1*- At3g12060 and *TBL2*- At1g60790) were used to check the expression level of the corresponding genes. From the RT-PCR data, threshold cycle number values (Ct) were calculated based on the average of three technical replications for each of *TBR* and the two homologous gene, previously normalized according to the values of a housekeeping gene, ubiquitin (Ubq 10)-At4g05320 used as a control.

The RT-PCR results indicate that the *TBR* gene and the tested homologues *TBL1* and *TBL2* as well, are expressed in most of the analyzed tissues, and at different developmental stages of the plant. The highest level of expression seems to be in flowers and green siliques (Figure 31, panel A, B and C).

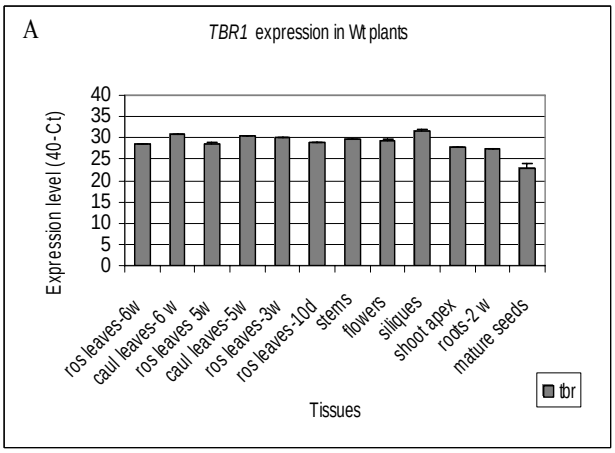

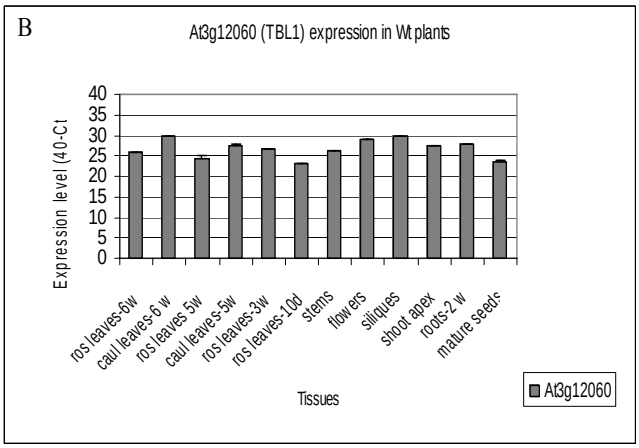

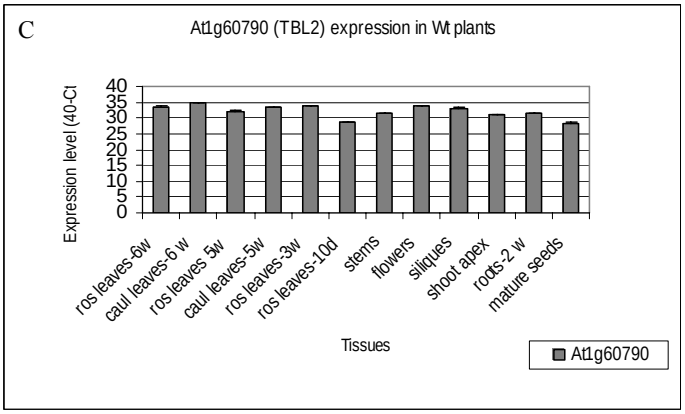

Figure 31. RT-PCR expression analysis of *TBR* and two close homologues *TBL1* and *TBL2*, in wild type *Arabidopsis thaliana* Col-0 plants, in different tissues, at various developmental stages. The results represent the average of three technical replications. Standard deviation is represented on the graphs. Ct values were first normalized against the Ubq 10 housekeeping gene -At4g05320. w-week; A) –*TBR* expression; B) –*TBL1* (At3g12060) homolog expression C) –*TBL2* (At1g60790) homolog expression. *TBR* and its close homologues, *TBL1* and *TBL2* are expressed in all analyzed tissues.

3.4.2 Expression Analysis using ATH1 arrays

The AtGenExpress data-base provides a collection of Affymetrix ATH1 array data from different developmental stages and environmental stresses in *Arabidopsis thaliana* (http://arabidopsis.org/info/expression/ATGenExpress.jsp). Additional ATH1 array data from Max-Planck-Institute of Molecular Plant Physiology includes data from different nutrient and diurnal responses in *Arabidopsis thaliana*. The expression data of *TBR* extracted from these data are given in figure 32. They revealed that *TBR* has a higher expression in rosette leaves (Figure 32-A 12-17), cauline leaves (26), stems (27) and flowers (37), compared to other organs at various developmental stages (Figure 32-A). The expression of *TBR* is elevated in shoots and roots under cold conditions (4 ^{0}C) (Figure 32-B, C). The treatment with abscisic acid (ABA) results in *TBR* repression (Figure 32-D), but addition of indoleacetic acid (IAA) leads, after three hours, to an increase in the expression level. When different nutrient conditions were tested, *TBR* expression was slightly increased upon PO_4 readdition and carbon starvation. Regarding diurnal responses, *TBR* expression is increased during extended night (Figure 32-F). The expression of *TBR* is slightly affected by different light qualities (Figure 32-G). Different pathogen treatments of *Arabidopsis thaliana* plants result in increases of the expression level of *TBR* (Figure 32-H).

The AtGenExpress data of the *TBR* close homologues, *TBL1 (*At3g12060) and *TBL2* (At1g60790), are given in Appendix 2.

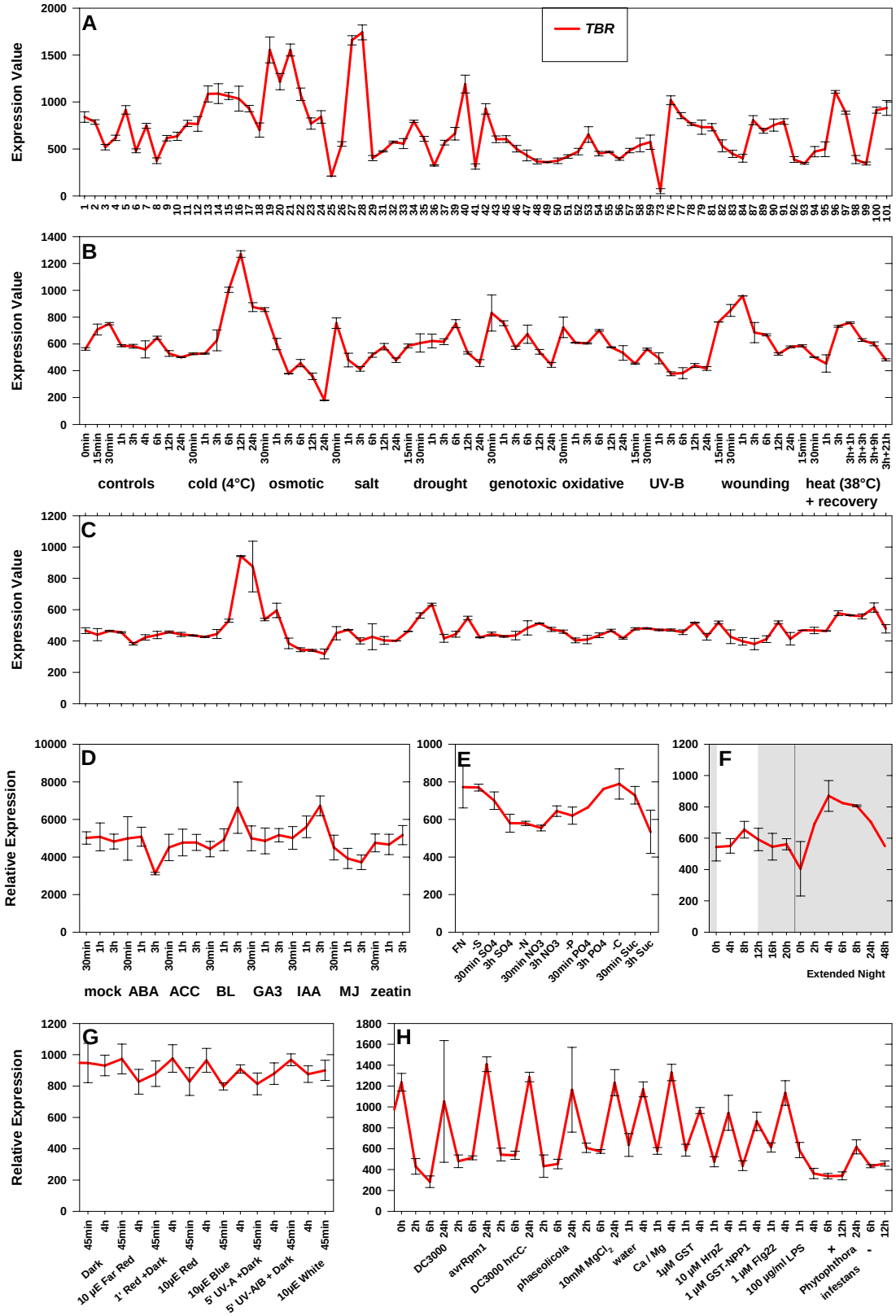

Figure 32. ATH1 gene chip expression profile of *TBR*

(A) Developmental series. A full description of samples 1-101 is available at http://www.weigelworld.org/resources/microarray/AtGenExpress/.

(B,C) Abiotic stress series for (B) shoots and (C) roots. A more detailed description of the samples is available at http://web.uni-frankfurt.de/fb15/botanik/mcb/AFGN/atgenextable2.htm.
(D) Hormone series. Wild type Col-0 seedlings were grown in liquid MS medium for seven days at 23°C treated with IAA, zeatin, GA3, ABA, MJ, ACC or BL for 30 minutes, 1 or 3 hours.

(E) Nutrient starvation and re-addition series. Wild type Col-0 seedlings were grown as described in Scheible *et al*. (2004). Full nutrition (FN); Sulfur, nitrogen, phosphorus or carbon starvation (-S, -N, -P, -C, respectively); 30 min or 3 h. sulfate (SO4), nitrate (NO3), phosphate (PO4) or sucrose (suc) re-addition.

(F) Diurnal series / extended night / *pgm* mutant. Wild type Col-0 (black line) or *pgm* mutant (gray line) were grown and harvested as described in Bläsing *et al*. (2005).

(G) Light series. A detailed description of the samples is available at http://web.uni-frankfurt.de/fb15/botanik/mcb/AFGN/atgenextable3.htm.

(H) Biotic stress series. A detailed description of the samples is available at
http://web.uni-frankfurt.de/fb15/botanik/mcb/AFGN/atgenextable3.htm.
http://arabidopsis.org/info/expression/ATGenExpress.jsp

3.4.3 Promoter GUS (β-glucuronidase) expression analysis of *TBR* and the two close homologues, *TBL1* and *TBL2*

In order to obtain information about the expression of *TBR* and two of the closest homologues, *TBL1* (At3g12060) and *TBL2* (At1g60790) throughout the plant, the promoters of the genes of interest were fused with the GUS reporter gene. The encoded β-glucuronidase enzyme from *E. coli* has been well documented to provide desirable characteristics as an expression marker in the transformed plants. The GUS reporter gene has many advantages including stable expression of the *E. coli* GUS enzyme, no interference with normal plant metabolism, and low intrinsic GUS activity in higher plants.

Promoter fragments of the *TBR* gene, *TBL1* (At3g12060) and *TBL2* (At1g60790) respectively, were amplified by PCR, using primers designed to introduce appropriate restriction sites to become suitable for cloning into binary vector pBI101.1 (Figure 33). The vector (12.2 kb size) is a low copy plasmid and contains a kanamycin resistance gene as selectable marker. The cloned *TBR* gene promoter was 1639 bp long, including the extended promoter region suggested and experimentally proved to belong to the gene, and was cloned into *BamH1/ Sal1* restriction sites of the vector.
The amplified promoter region of the *TBL1* homolog, was 2053 bp in length and was cloned also into the *BamH1/ Sal1* restriction sites of the pBI101.1 multiple cloning site. The second analyzed homolog, promoter region of the *TBL2* gene, was 2079 bp in length and was cloned into the *SalI/SmaI* sites of same vector (Figure 33).

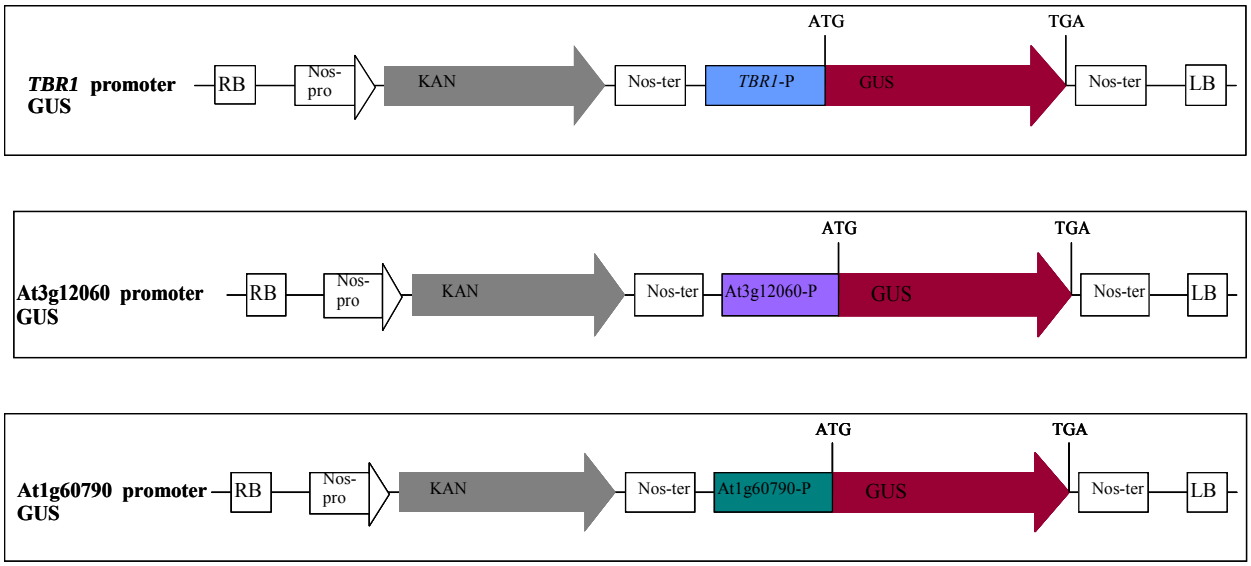

Figure 33. Representations (not to scale) of *TBR*, *TBL1* and *TBL2* promoter-*GUS* gene fusion constructs. *TBR* (*TBL1*-At3g12060, *TBL2*-At1g60790)-P: *TBR* (homologues) promoter sequence; *GUS*: β-glucuronidase coding region; Nos ter: polyadenylation signal from the nopaline synthase gene; kan: kanamycin resistance gene coding region; RB: right border; LB: left border.

Each of the three generated GUS constructs was cloned first in *E. coli* strain *DH5α*, chemical competent cells. The plasmids were purified and partially sequenced to check that the promoter regions were in the correct frame fusion with the *GUS* gene and that there were no mutations in the promoter sequence. In the next step, the confirmed plasmids were introduced into *Agrobacterium tumefaciens GV3101* cells by electroporation, and finally these were used to transform wild type *Arabidopsis thaliana* Col-0 plants, using the floral dip infiltration method. Transformed plants were selected on kanamycin containing agar-medium plates and then transferred to soil. In order to check the expression pattern, the plants were immersed in GUS staining solution, containing X-Gluc (5-bromo-4-chloro-3-indolyl glucuronide) as a substrate for the β-glucuronidase enzymatic reaction, and subsequently examined for the presence of the blue GUS signal of the reaction product. Plants at different developmental stages were subjected to the assay, to determine the expression patterns occurring during growth and development.

The *TBR* promoter is active, as expected, in leaves and stem trichomes (Figure 34, panels A, B, C, D, and E). In agreement with the previous RT-PCR expression analysis, it shows expression in many other organs: root, stem, rosette leaves, cauline leaves, flowers and green siliques (Figure 34).

At a very early developmental stage (five days old seedlings), the GUS staining appears in the whole plant, suggesting the possibility that *TBR* plays a general role in cell expansion (Figure

34, panel A) and raises the question whether TBR might be involved in the primary wall synthesis. The expression level in all tissues decreases with plant age (Figure 34, panels F, G, H, I, and J).

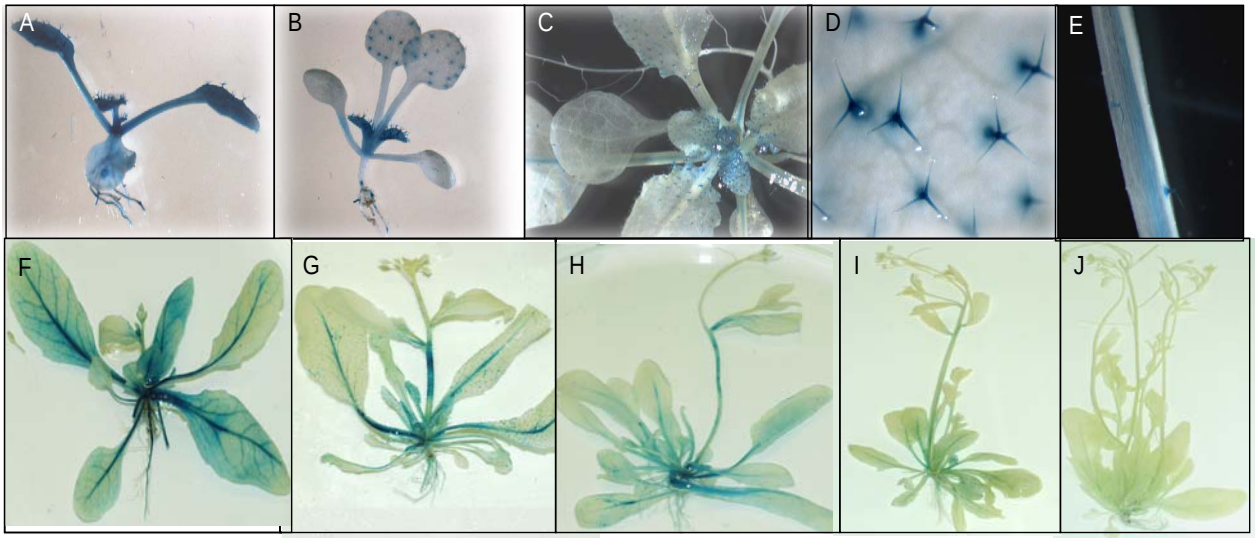

Figure 34. GUS expression signal in transgenic *Arabidopsis thaliana* Col-0 plants, carrying a *TBR* promoter-*GUS* fusion construct. A) –The expression pattern in five days old seedlings; B) –Seven days old seedlings; C) –Two weeks old plants; D) –Expression signal present in the leaves trichomes; E) –Expression in stem and stem trichomes; F) –Three weeks old plant; G) –Four weeks old plant; H) –Four and a half weeks old plant; I) –Five weeks old plant; J) –Six weeks old plant.

The *TBR* promoter is also strongly active in the anthers and pistils of the flowers (Figure 35, panel A and B). The expression also occurs in the green siliques, but only at the dehiscence zone (Figure 35, panel C).

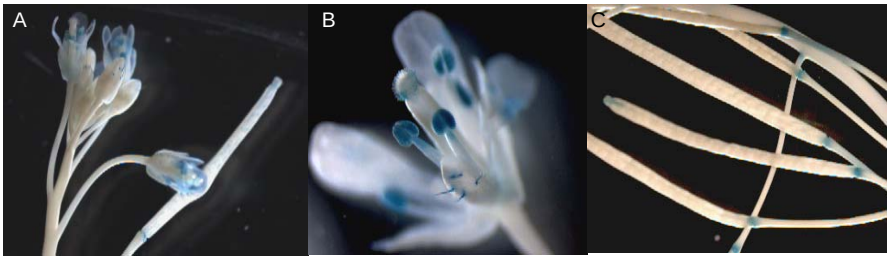

Figure 35. GUS expression analysis of the *TBR* promoter in *Arabidopsis thaliana* Col-0 transformed plants. A), B) –Flowers (anthers and pistil) and C) –Green siliques expression at dehiscence area.

In the roots, the promoter activity varies during development, resulting in a strong, ubiquitous GUS staining in the young seedling roots (Figure 36, panel A), but the staining was restricted to the root primordia in the case of one and two weeks old plants (Figure 36, panel B and C). In the mature plants (older than three weeks) the expression signal is present

throughout most of the root, but at a much lower level (by the intensity of blue GUS signal) (Figure 36, panel D and E).

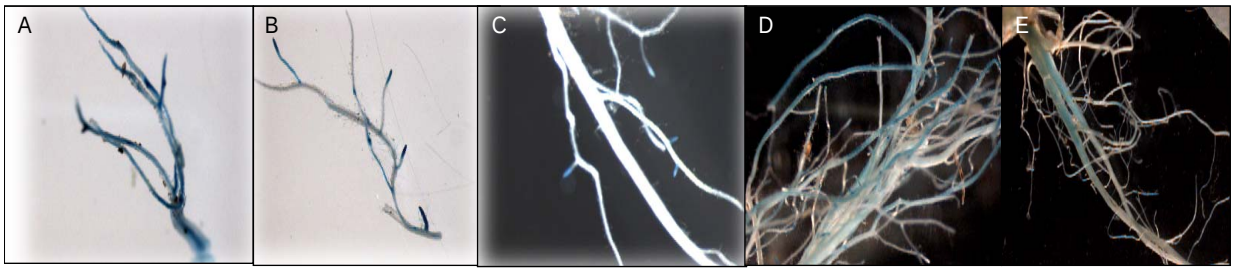

Figure 36. Expression of *TBR* promoter-GUS gene fusion in roots of *Arabidopsis thaliana* Col-0 transformed plants, at different developmental stages; A) – The root of five days old seedlings; B) – One week old roots; C) –Two weeks old roots; D) –Four weeks old roots; E) –Six weeks old plant roots.

The *TBL1* homolog (At3g12060) gene promoter *GUS* fusion revealed the expression in the leaf petioles and root (main root and root primordia of the young plants) (Figure 37, panel B and C). Later on, during the developmental process, it appears in stems, flowers (anthers and pistils) (Figure 37, panel F and G) and green siliques, at the stem emergence point and dehiscence (Figure 37, panel H), maintaining a similar expression pattern to that of *TBR* promoter. In older leaves the expression is restricted to the vascular tissue, at a low level (by the GUS signal intensity).

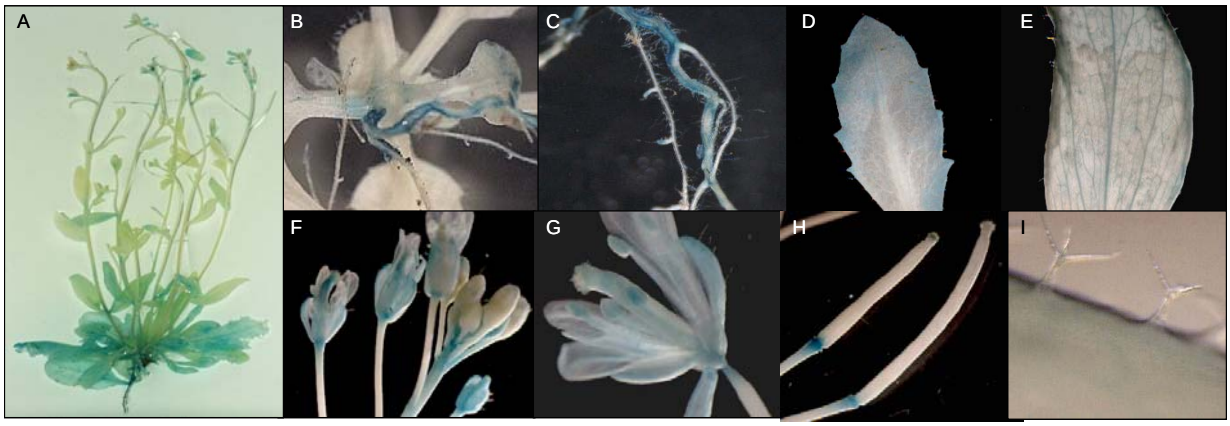

Figure 37. GUS expression analysis of *TBL1* homolog (At3g12060) promoter in *Arabidopsis thaliana* Col-0 transformed plants: A) –Six weeks old plants; B) –Expression in young seedlings (two weeks) roots and petioles; C) –Expression in the main root and root primordia of two weeks old plants; D) –Young leaf (two weeks old); E) –Six weeks old leaf; F), G) –Flowers anthers and pistil; H) –Green siliques; I) –No signal of expression was detected in trichomes.

The expression of the second analyzed *TBL2* homolog gene (At1g60790) promoter-GUS fusion showed a different pattern than that of the *TBR* and *TBL1* genes. It is active in the

very young leaves, mostly in the petioles (Figure 38, panel B). In mature plants, expression is maintained in the petioles (Figure 38, panel C) and it also occurs in the stem and in green siliques, but the level is clearly lower than that of *TBR* (Figure 38, panel A and D). The expression pattern and level does not vary too much during plant growth.

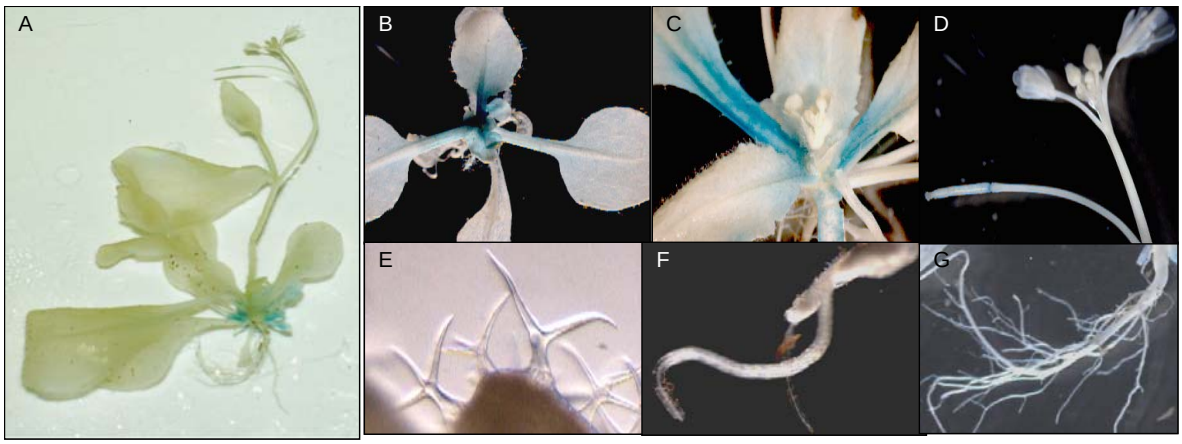

Figure 38. GUS expression analysis of *TBL2* (At1g60790) promoter in *Arabidopsis thaliana* Col-0 transformed plants: A) –Four weeks old plant expression signal; B) –Two weeks old; C) –Three weeks old; D) – Expression in green siliques, at the dehiscence ; E) –No expression signal was detected in trichomes as well as in F), G) –Young and mature roots, respectively.

3.4.4 Studying the root phenotype of the *tbr1* mutant

Observing the strong GUS expression signal of the *TBR* promoter appeared in the young roots of transformed wild type plants, *tbr1* mutant roots were visually inspected for phenotypes. For this purpose, wild type Col-0 and *tbr1* seeds were germinated on vertical agar medium plates. The plants were daily-observed and the roots length measured (both primary and secondary roots) to detect any differences in root development and appearance.

The *tbr1* plants develop more root hairs and have slightly longer root hairs when compared to wild type plants. These differences were visible during the first week of growth (Figure 39). Later on, the roots become similar to wild type, with no obvious visible differences. The average number of lateral roots was similar in both genotypes, and there were no significant differences in root growth, either.

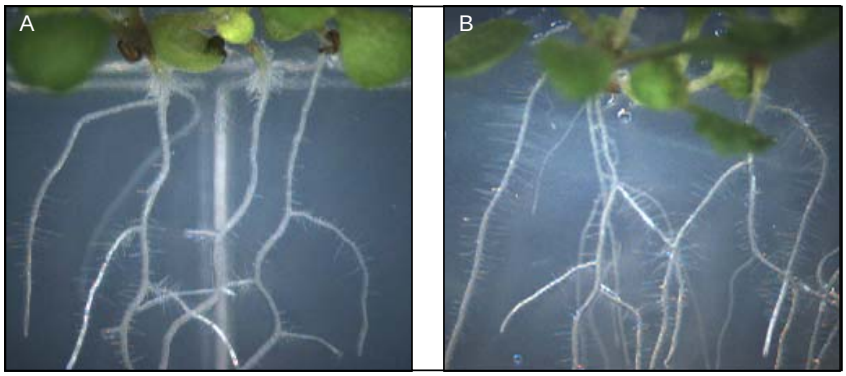

Figure 39. Roots of one week old seedlings grown on agar plates medium. The plants were one week old, grown in normal conditions (light and temperature) in a growth chamber. A) –Wild type Col-0 and B) –*tbr1* young seedlings. Mutant plants display more and longer root hairs than the wild type plants, during the first week of growth.

3.5 STUDY OF T-DNA INSERTION LINES OF THE *TBR* GENE AND ITS HOMOLOGUES, *TBL1* AND *TBL2*

From the initial screen by Potikha and Delmer (1995), only one mutant allele *tbr1* was available. As the mutation causes a single amino acid change it was not clear whether this leads to a complete or only a partial loss of function. Further more, no mutants were available for any of its close homologues. In order to investigate the consequences of knock-out mutations, T-DNA insertion lines available for *TBR* and for the two close homologues, *TBL1* (At3g12060), and *TBL2* (At1g60790) were studied.

T-DNA insertion lines were ordered from the Salk and Sail collections for each of *TBR* gene and the homologues, *TBL1* (At1g60790) and *TBL2* (At3g12060).

For the *TBR* gene, three T-DNA insertion lines were ordered: Salk_058509, Salk_134014 and Salk_134006, all of them carrying the insertion in the extended region suggested and experimentally shown to be required for the functionality of the gene product (Figure 40, panel A). An additional line, Sail 707D07, was also studied, having the insertion in the first database annotated exon of the gene. In the case of first analyzed homolog, *TBL1* gene (At3g12060), two Salk lines: Salk_069441 and Salk_135222 were chosen and ordered for analysis. The insertion in both lines occurred in the first exon region of the gene (Figure 40, panel B). For the second homolog, *TBL2* (At1g60790), also two lines: Salk_065990 and Salk_020184, carrying the insertions in different exons (in the first and in the last) (Figure 40, panel C), were analyzed.

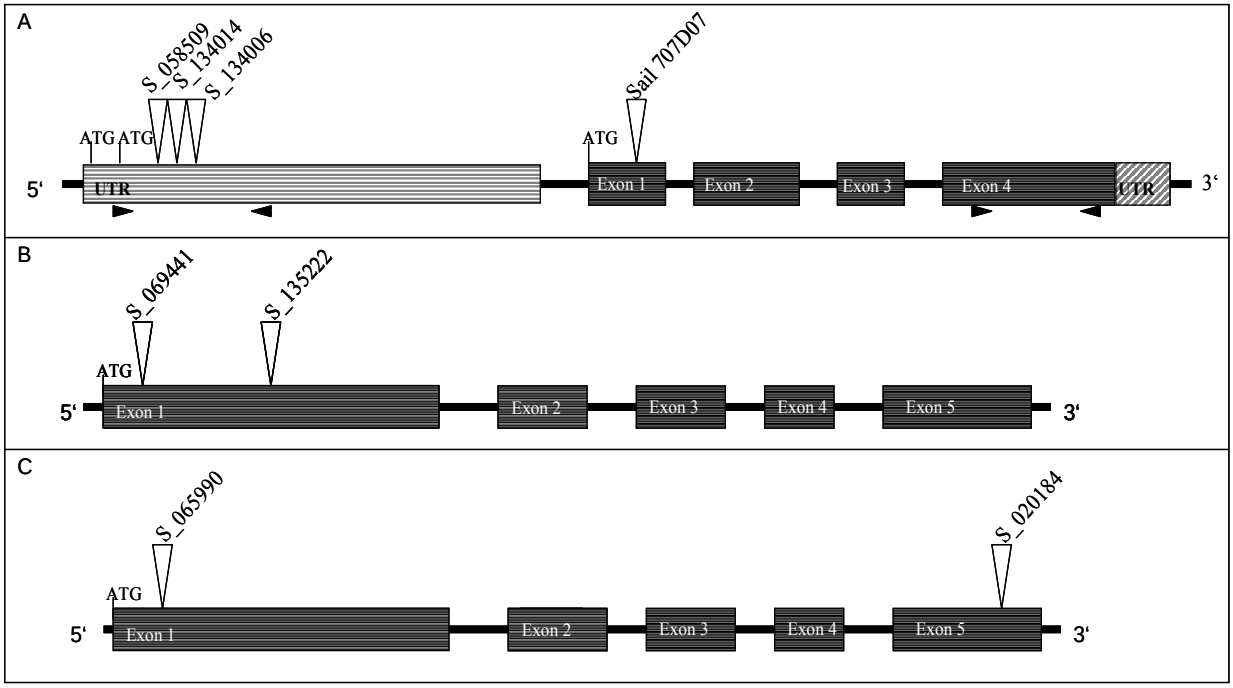

Figure 40. T-DNA insertion lines for the *TBR* gene and close homologues *TBL1* (At3g12060) **and *TBL2*** (At1g60790). A) –*TBR* gene insertion lines. The black arrows indicate the primers pairs used to amplify specific DNA probes used in RNA blot experiment; B) –Insertion positions in *TBL1* – At3g12060 T-DNA lines; C) –Insertion positions in *TBL2* –At1g60790 T-DNA lines.

All the insertion lines were screened by PCR reaction. The isolated genomic DNA of each T-DNA insertion plant was tested using either a pair of primers amplifying a specific wild type product, or primers to yield a product specific for the T-DNA insertion, with the aim of identifying homozygous insertion plants. The plants were also observed for the presence of the trichome related phenotype and/or any other visible alteration. Homozygous insertion plants were found in the T-DNA lines of *TBL1* (At3g12060) and *TBL2* (At1g60790), but these showed no visible phenotypic changes. No homozygous T-DNA insertion plants were identified from screening of the three Salk insertion lines in the *TBR* gene.

An RNA blot experiment was designed using two DNA probes, one in the extended UTR, suggested to belong to the gene structure (420 bp- PCR product length), and one in the last exon (PCR product of 284 bp) (Figure 40, panel A). The probes were DIG (digoxigenin) labeled and used to hybridize RNA that was isolated from *TBR* Salk plants that were identified to be heterozygous when screened by PCR. There was no visible signal on the blotted membrane. Wild type Col-0 RNA, that was used as control, showed no signal detection either. This result could be due to a low level of expression of the *TBR*.

Expression of the *TBR* gene was investigated in heterozygous Salk plants by RT-PCR. cDNA was synthesized based on the RNA isolated from the *TBR* Salk plants detected as heterozygous by PCR screening, and used as a template to check the expression level of *TBR* gene by RT-PCR. The RT-PCR expression experiment was carried out using two pairs of primers spanning 1) the extended region of the (longer) gene structure, and 2) a junction of two exons of the *TBR* transcript, amplifying short fragments of 65 and 72 bp, respectively (Figure 41).

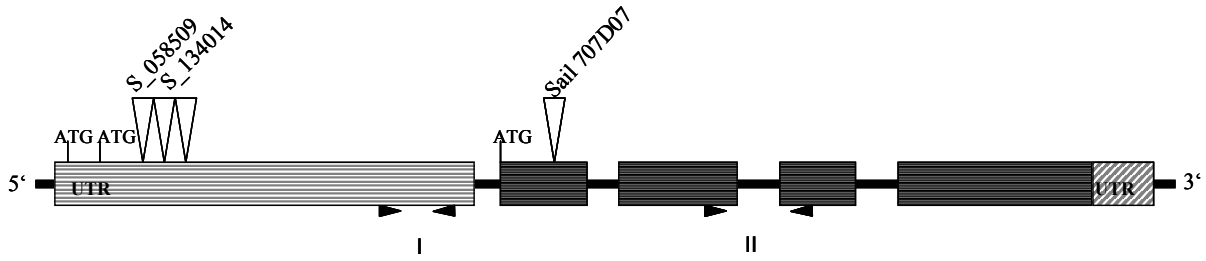

Figure 41. RT-PCR primer pairs localizations. The exons are marked as dark boxes and introns as the spaces between exons**.** The first pair of primers (I) spans the front region of *TBR,* and a second pair (II) amplifies a product at a junction of two exons of the transcript**.**

The expression values found are similar to wild type plants (Figure 42).

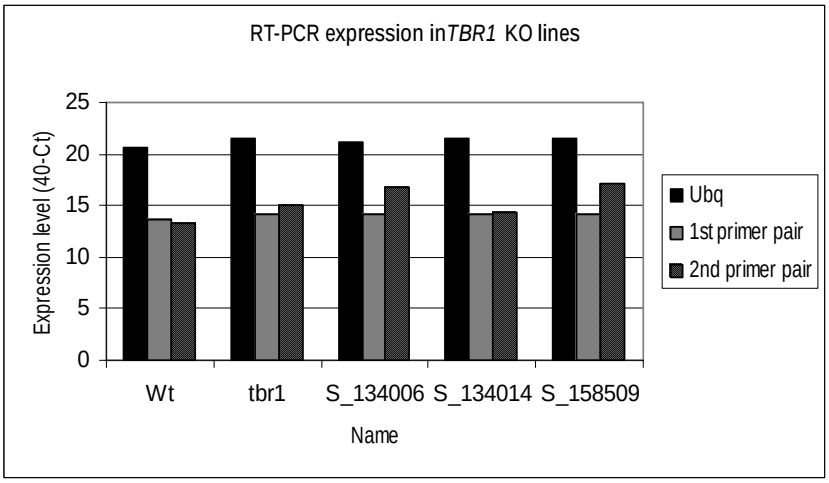

Figure 42. RT-PCR analysis expression level of *TBR* transcript in the *TBR* T-DNA insertion plants that were detected as heterozygous by PCR screening. The plants were four weeks old grown in the greenhouse conditions. RNA used as template for the cDNA synthesis was isolated from flowers, because of the high RNA yield and the high expression level of *TBR* when checked by promoter gene *GUS*-fusion assay and by RT-PCR analysis in wild type Col-0 plants.

Moreover, the silique phenotype and seed segregation were checked in the progeny of the plants identified as heterozygous for T-DNA insertion in the *TBR* gene when screened by PCR. Mature green siliques were opened and observed under the microscope, and compared

with wild type siliques (Figure 43). The siliques from *tbr1* mutant plants were also opened for comparison (Figure 43, B).

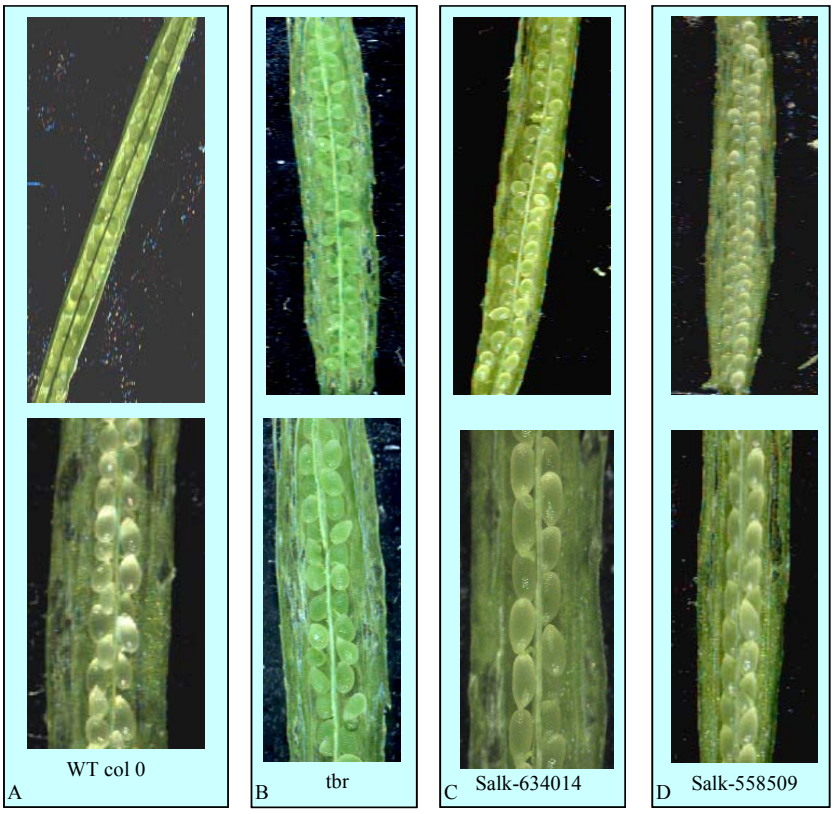

Figure 43. Opened siliques to observe seeds segregation effect in *TBR* T-DNA insertion plants identified as heterozygous for the insertion. A) –Wild type Col-0; B) –*tbr1*; C), D) –*TBR* T-DNA insertion plants identified as heterozygous for the insertion. There is no alteration in seed development observed in the opened siliques of the heterozygous T-DNA insertion plants progeny, compared to wild type.

There was no apparent alteration in seed development in the opened green siliques of plants heterozygous for the T-DNA insertion in the *TBR* gene.

The *TBR* insertion line -Sail 707D07- was also screened by PCR to look for homozygous plants. All the plants subjected to the analysis (total number of 135) displayed a heterozygous signal. However, some showed a visible phenotype, having fewer and smaller rosette leaves and very early flowering process (Figure 44, panel B). Some others displayed more rosette leaves, but these were smaller than the leaves of wild type plants (Figure 44, panel C).

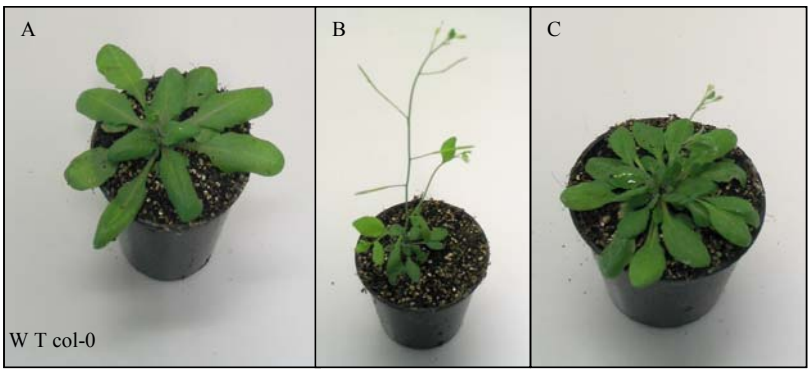

Figure 44. Phenotype of heterozygous plants from *TBR* insertion line -Sail 707D07. The plants were 20 days old, grown in the greenhouse. A) –Wild type Col-0 plant; B) –Early flowering phenotype; C) –Phenotype showing higher number of rosette leaves which were smaller than the leaves of wild type plants at the same age.

3.6 GFP (GREEN FLUORESCENT PROTEIN) TBR PROTEIN FUSION ANALYSIS

To elucidate the subcellular localization of TBR, a GFP fusion experiment was performed in which the *TBR* full length cDNA (isolated from the cDNA clone RAFL16-77-N09) was fused in frame with a *GFP* reporter gene. Both N- and C- protein terminal fusions were accomplished.

The *TBR* coding region of the suggested longer gene structure was PCR amplified from the cDNA clone, RAFL16-77-N09, and first subcloned into an intermediary cloning system - TOPO pENTR/SD/D (Invitrogen). The insert was then transferred into the GATEWAY destination vectors, pK7FWG2 and pK7WGF2 (11.8 kb, spectinomycin and streptomycin resistance in bacteria; kanamycin in plants). The resulting GFP constructs were transferred into *Agrobacterium tumefaciens GV3101* by electroporation and then into wild type *Arabidopsis thaliana* Col-0 plants. The constructs were previously sequenced to check that the TBR and GFP coding regions were in the correct frame fusion, and the absence of any mutation.
Transgenic (T1) plants were selected by growing on kanamycin agar plates. In the case of the N-terminal GFP fusion construct, 146 resistant plants were analyzed for GFP signal presence. Transformation of wild type plants with the GFP C-terminal fusion construct yielded 76 transgenic kanamycin resistant plants. None of the kanamycin resistant plants resulted from the N- or C- protein terminal fusion constructs displayed GFP fluorescence signal when analyzed under the confocal microscope.

Transient expression was also performed with the generated GFP constructs (both N-, or C-terminal fusion), by bombarding wild type *Arabidopsis thaliana* Col-0 leaves with microcarrier gold particles carrying the DNA plasmid. Leaves were also bombarded with the empty vector as a negative control.
No GFP characteristic fluorescence signal was detected when bombarded leaves were inspected under confocal microscope.

The GFP fusion constructs were also introduced into *tbr1* mutant plants by *Agrobacterium tumefaciens GV 3101* mediated transformation, and in both cases (N- and C-protein terminal fusion constructs) the mutant phenotype was rescued as the selected transgenics showed normal trichome birefringence, therefore the generated constructs were functional.

3.7 EXPRESSION OF DEFENCE RELATED GENES IN *TBR1* MUTANT

In previous studies on the primary cell wall mutants, higher expression of some defence gene pathways was observed (Ana Cano-Delgado *et al.,* 2003). It was also found that reduced levels of cellulose synthesis lead to lignin synthesis mediated in part by the jasmonic acid (JA), ethylene and other signaling pathways. Defence proteins involved in JA- and ethylene mediated signaling pathways were tested. The vegetative storage protein1 (*VSP1)* is induced in vegetative tissues by jasmonic acid alone, while expression of a plant defensin protein (*PDF1.2)* requires the action of both, JA- and ethylene-dependent signal pathways. *VSP1* was expressed at a high level in *rsw1*, while *PDF1.2* was expressed at very low levels in these conditions. Both, *PDF1.2* and *VSP1* were expressed at a high level in *eli1-1* seedlings and in wild type plants treated with isoxaben (a cellulose synthesis inhibitor) (Ana Cano-Delgado *et al.,* 2003).
The expression of defence genes in the tested plants, primary cell wall mutants and plants treated with cellulose synthesis inhibitor, suggested that reduced cellulose synthesis leads to cellular responses, some of which are regulated via JA- and ethylene mediated pathways. The delayed expression of VSP1 in the *cev1* mutant compared to the rapid responses of these genes to direct JA treatment suggests that defence gene expression is an indirect effect of reduced cellulose synthesis (Ellis *et al.,* 2002).

To check whether the defects in the secondary cell wall synthesis can trigger defence responses, the expression level of some known defence genes was investigated in the *tbr1* mutant, using RT-PCR tools.

RT-PCR specific primers were designed for twelve different genes involved in different defence pathways, as follow: 1) vegetative storage protein1-At5g24770; 2) vegetative storage protein2-At5g2470; 3) plant defence protein-At5g44420; 4) basic endochitinase activity (endomembrane system)-At3g12500; 5) defence response thionin-At1g72260; 6) glucuronosyl transferase family protein-At4g34135; 7) a member of the Fe(II) ascorbate oxidase gene family (senescence related protein)-At1g17020; 8) pathogenesis related protein1-At2g14610; 9) pathogenesis related protein5 (endomembrane system)-At1g75040; 10) cinnamoyl-CoA reductase (involved in lignin biosynthesis)-At1g80820; 11) an oxidoreductase from oxygenase family protein-At4g10500; 12) chitinase-At2g43570. The expression levels of all twelve genes were investigated in *tbr1* and *rsw1* plants, and related to the expression level in wild type Col-0 plants. Expression was also investigated in *irx3* mutant and compared with wild type Ler plants, as the *irx3* mutation is in a Ler background. The *irx3* was involved as comparison element, as this is also a well characterized secondary cell wall mutant (Turner and Somerville, 1997). The *rsw1* mutant, which is a primary cell wall mutant, was used as a positive control.

The concentrations of cDNA used as a template were previously normalized according to threshold cycle number (Ct value) of ubiquitin -At4g05320, housekeeping gene.

In the case of *rsw1*, the experimental results confirmed the reported induction of vegetative storage protein1 -At5g24770 and to a lower level the induction of the plant defensin protein -At5g44420. There is a slight increase of the vegetative storage protein1 -At5g24770 and thionin defence genes -At1g72260, the same was observed for pathogenesis related protein1 -At2g14610 and cinnamoyl-CoA reductase -At1g80820. No remarkable alteration in the expression of the other tested defence genes was detected (Figure 45).

In the *tbr1* mutant plants there was no significant change for any of the twelve investigated defence genes (Figure 45).

The *irx3* shows a high expression level of the vegetative storage protein 2 and plant defensin protein, and slightly higher levels of the senescence related protein (SRG1), both pathogenesis related proteins and the cinnamoyl-CoA reductase, involved in lignin biosynthesis (Figure 45).

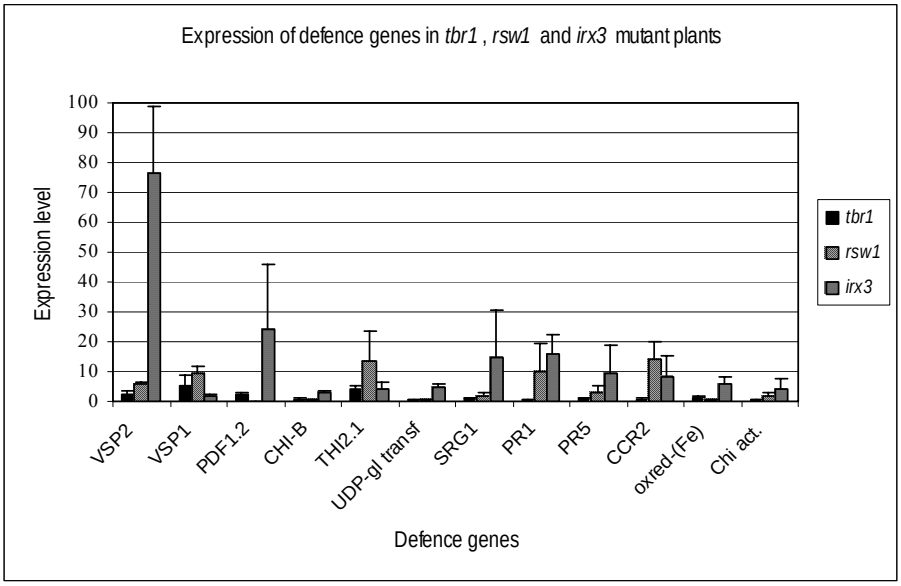

Figure 45. Expression level of defence related genes in *tbr1*, *rsw1* and *irx3* mutant plants. The defence genes tested: 1) VSP1 vegetative storage protein1-At5g24770; 2) VSP2 vegetative storage protein2-At5g2470; 3) PDF1.2 plant defence protein-At5g44420; 4) CHI-B basic endochitinase activity (endomembrane system)-At3g12500; 5) THI2.1 defence response thionin-At1g72260; 6) UDP-gl transf. glucuronosyl transferase family protein-At4g34135; 7) SRG1 a member of Fe(II) ascorbate oxidase gene family (senescence related protein)-At1g17020; 8) PR1 pathogenesis related protein1-At2g14610; 9) PR5 pathogenesis related protein5 (endomembrane system)-At1g75040; 10) CCR2 cinnamoyl-CoA reductase (involved in lignin biosynthesis)-At1g80820; 11) oxred-(Fe) an oxidoreductase from oxygenase family protein-At4g10500; 12) Chi act. chitinase-At2g43570.
The results are the average of three biological replicates and two technical replicates performed for each of the biological replica. Standard deviation bars are indicated on the figure.

3.8 BIOCHEMICAL CHARACTERIZATION OF THE *TBR1* MUTANT

3.8.1 Biochemical analysis of wild type and *tbr1* mutant cell wall

3.8.1.1 Gas-chromatography analysis

The *tbr1* mutant was identified to be a cell wall deficient mutant. The cell wall composition in the mutant plants was checked by biochemical analyses to discover any additional phenotype features, and whether the changes caused by reduction of cellulose content leads to other (compensatory) changes in other cell wall polymers and composition.
The cell walls of *tbr1* and wild type plants were analysed by GC (Gas-Chromatography) and MALDI-TOF (Matrix Assisted Laser Desorption Ionization Time-of Flight) mass spectrometry. The cell wall material was prepared from both, leaves and trichomes of *A. thaliana* plants, at different developmental stages, starting from two, three, four, up to five weeks old plants.

GC analysis separates all of the components in a sample and provides a representative spectral output. Each component ideally produces a specific spectral peak. GC method provides qualitative details about matrix polysaccharides composition and also crystalline cellulose microfibrils composition. Since the *tbr1* mutation affects the secondary cell wall biosynthesis, it was possible that the mutant could be distinguished from wild type by analysing cell wall components.

However, the results exhibited no significant differences in the relative amounts of cell wall components from mutant leaves, compared to those of wild type in both, matrix polysaccharide and in crystalline cellulose analyses (Figure 46). Hence the *TBR1* gene product does not seem to be required for the deposition of cellulose and other cell wall polymers in leaves. However, an effect in specific cell types cannot be ruled out.

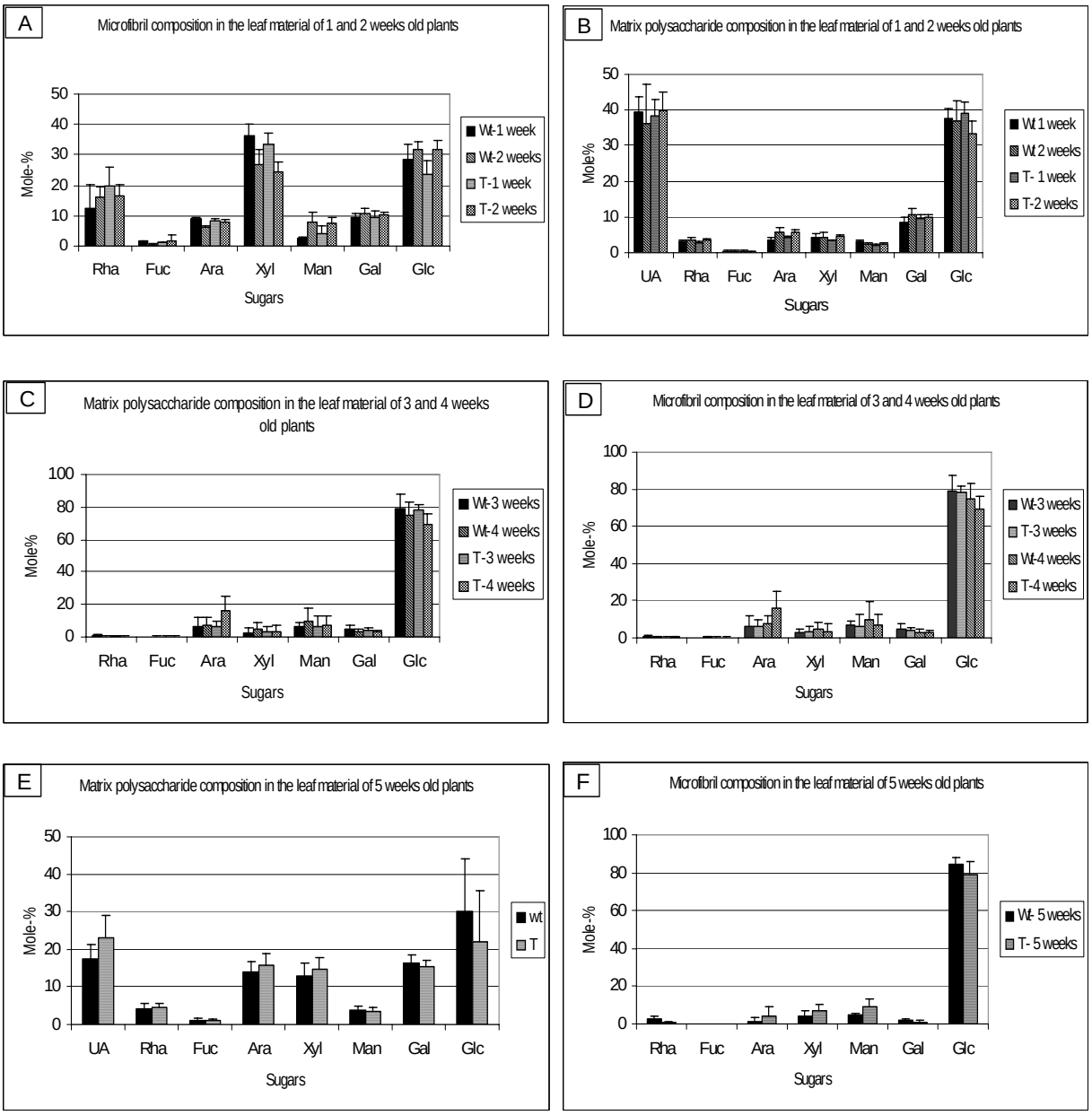

Figure 46. GC analysis of wild type *Arabidopsis thaliana* Col-0 and *tbr1* leaf cell wall material, extracted from plants of different ages (from one to five weeks old)**.** A); C), E) –Show matrix polysaccharide composition. B); D); F) –Display microfibril components, crystalline cellulose fraction. The values are the mean of five biological replications for each developmental stage The standard deviation is indicated on the graphs. There are no significant changes between wild type and mutant plants leaves in the cell wall composition. T denotes the *tbr1* plants.

GC analysis was also performed on wild type and *tbr1* trichomes (harvested from three week old plants). The results showed a slightly elevated uronic acid fraction in the *tbr1* trichomes, in comparison with wild type trichome analysis (Figure 47). Accumulation of pectic substances like uronic acid has previously been found in plants with inhibited cellulose synthesis (Burk *et al.,* 1999; Sato *et al.,* 2001; Scheible *et al.,* 2003).

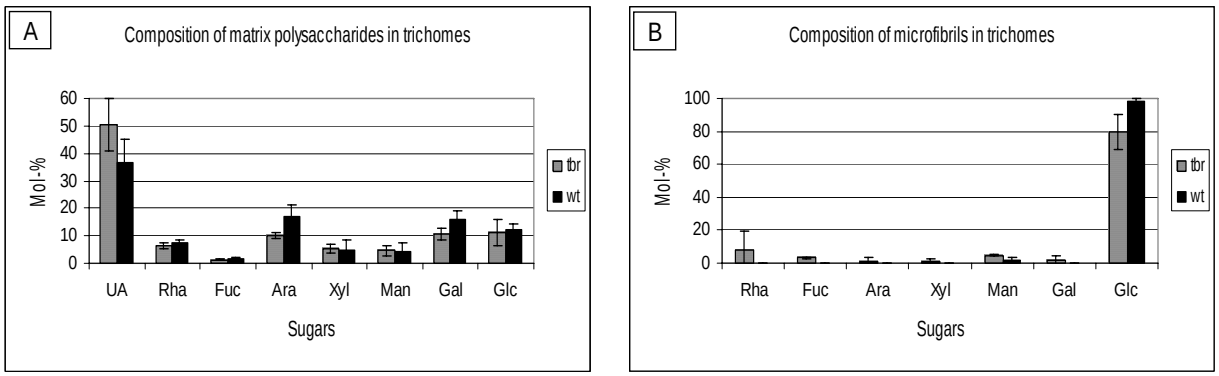

Figure 47. GC analysis of cell wall in wild type *Arabidopsis thaliana* Col-0 and *tbr1* trichomes: A) –Matrix polysaccharides and B) –Microfibrils components. The plants were three weeks old when the leaf trichomes were harvested for the analysis. A slight increase in uronic acids content in the matrix polysaccharides fraction of *tbr1* trichomes compared to wild type can be observed. The values represent the mean of three biological replications; the standard deviations are indicated on the figures.

3.8.1.2 MALDI-TOF analysis

MALDI-TOF mass spectrometry has become a popular tool for large and small molecule analyses, using a matrix to embed the sample. MALDI-TOF analysis was performed on cell wall fraction digested with xyloglucanendoglucanase to display changes in the components of the cell wall xyloglucan (XG) fraction.

Endoglucanases (EGs) represent a class of hydrolytic enzymes that can hydrolyze glycosidic bonds inside a glucan chain of XGs (Figure 48). There are many different endoglucanases with several known substrate specificities. One group of enzymes hydrolyzes β-1,4-linkages recognized in ß-1,4-glucan chains in both polymers, xyloglucan and cellulose. Most EGs can hydrolyse cellulose as well as XG, but some EGs have been shown to be XG specific (Edwards *et al.*, 1986; Tabuchi *et al.*, 1997; Matsumoto *et al.,* 1997; Pauly *et al.*, 1999).

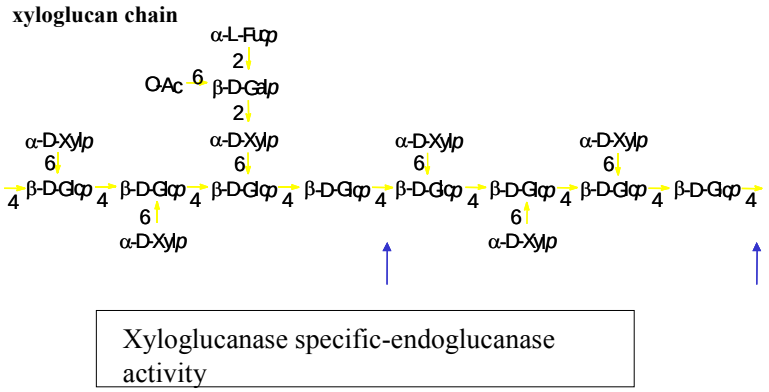

Figure 48. Endo-1,4-β-glucanases hydrolyses 1,4-linkages in xyloglucan.
In plants, xyloglucan rather than cellulose is the likeliest target for these enzymes, although it is possible that they could hydrolyse some surface 1,4-β-glucan chains that are in the amorphous regions of the cellulose microfibril (Hayashi *et al.*, 1984; Hayashi, 1989). The enzyme cleaves the xyloglucan chain into specific products, which can then be identified in MALDI-TOF spectra.

MALDI-TOF analysis was first applied to wild type and *tbr1* leaf cell wall material digested with xyloglucanase. However, no major differences could be detected in the relative abundance of xyloglucan fragments (Figure 49).

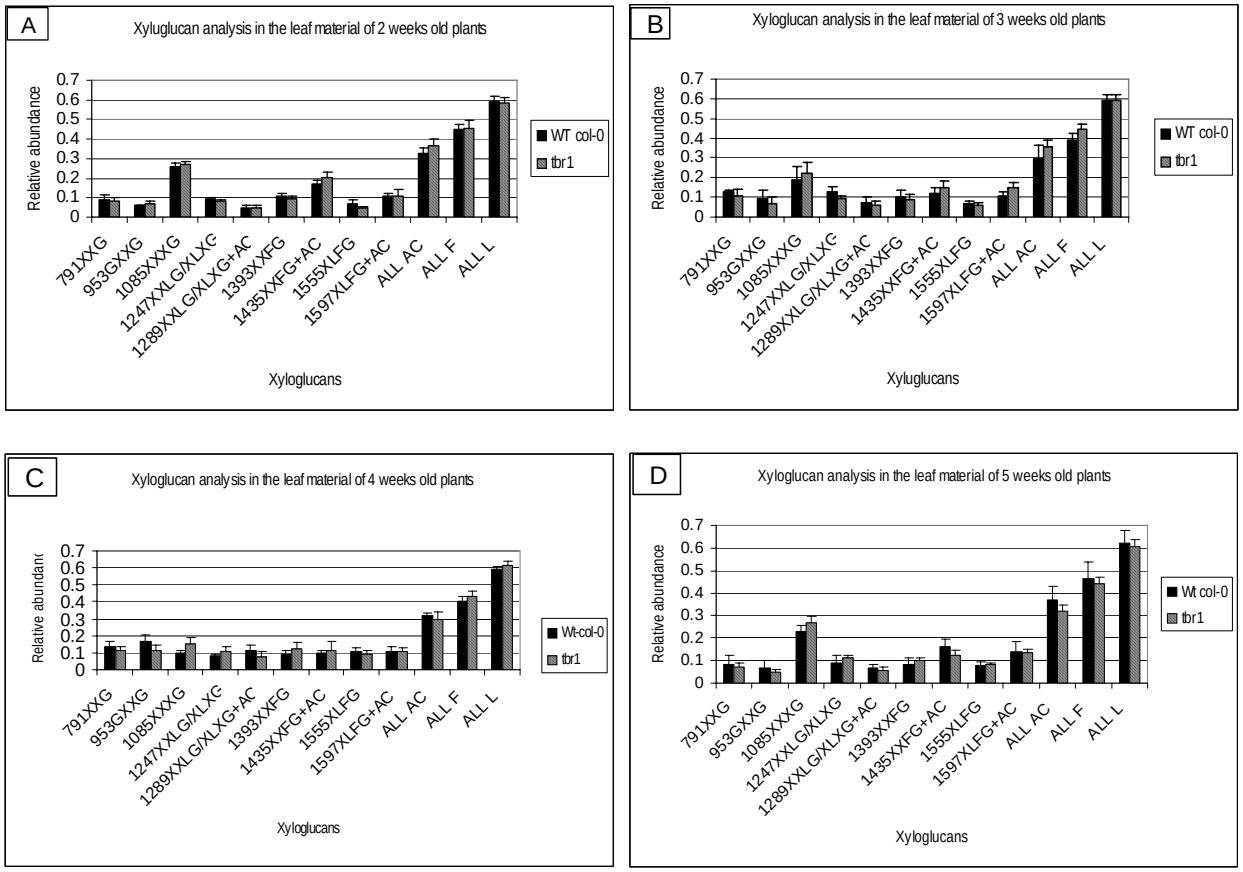

Figure 49. MALDI-TOF analysis of the xyloglucan fraction in wild type Col-0 and *tbr1* leaf cell wall material, isolated from plants of different ages. A) –Two weeks old leaves; B) –Three weeks old leaves; C) –Four weeks old leaves and D) –Five weeks old leaves. The values are the mean of five biological replications considered for the experiment. The standard deviation is indicated on the figures. The numbers under the XG fraction indicates the molecular weight of the respective product. The nomenclature is given in the introduction part (section 1.1). AC –Indicates acetiolated fraction resulted from XG enzymatic digestion; ALL AC –Represent the sum of all acetilolated resulted products; ALL F –Represent the sum of all fucosylated resulted products; ALL L –Represent the sum of all galactosylated analyzed fractions of the XG. There are no major differences in the xyloglucan composition between wild type and *tbr1* mutant.

MALDI-TOF analysis was also applied to trichome samples from both, wild type and *tbr1* mutant leaves to investigate changes in cell wall composition in trichomes. No significant differences were observed between wild type and mutant plants (Figure 50).

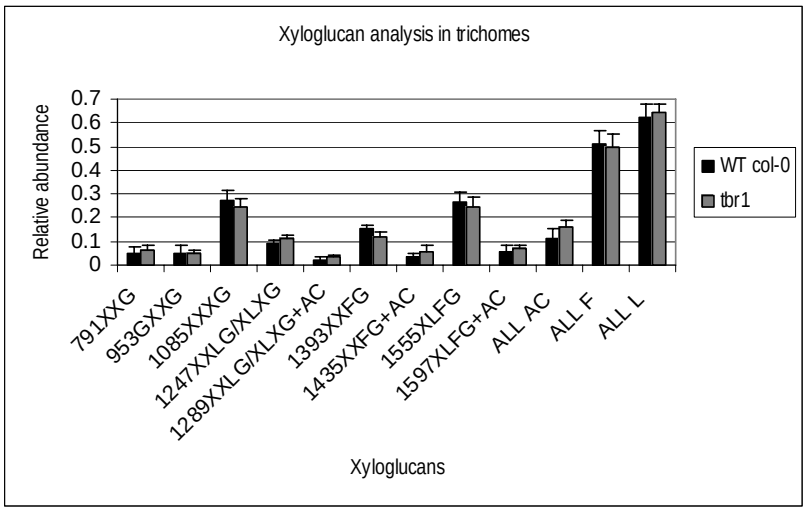

Figure 50. MALDI-TOF analysis of the xyloglucan fraction from the cell wall of *tbr1* trichomes in comparison to wild type trichomes. The leaf trichomes were harvested from the plants more than three weeks old in the greenhouse. The values are the mean of five biological replications and standard deviation is shown on the figure. The nomenclature is given in the introduction part (section 1.1). AC – Indicates acetiolated fraction resulted from XG enzymatic digestion; ALL AC –Represent the sum of all acetilolated resulted products; ALL F –Represent the sum of all fucosylated resulted products; ALL L – Represent the sum of all galactosylated analyzed fractions of the XG.

3.9 COMPARISON OF *TBR1* AND WILD TYPE TRICHOMES BY SCANNING ELECTRON MICROSCOPY ANALYSIS

Electron microscopy method allows examination of objects at very fine scale, yielding information about topography and morphology.

Trichomes from both, wild type Col-0 and *tbr1* plants over three weeks old were harvested and subjected to scanning electron microscopy analysis which revealed some differences. On the wild type trichome branch surface, the calcium-containing papillae are present, which are typical for the mature secondary cell wall trichomes (Marks, 1997) (Figure 51, panel B). In contrast, they are completely absent from the surface of the *tbr1* trichomes (Figure 51, panel D).

This result confirmed the *tbr1* phenotype characterization of Potikha and Delmer (1995). Moreover, the epidermal cells that build up the base of a wild type trichome are not observed in

the mutant (Figure 51, panel C). The absence of epidermal cells from the base of the trichome was also reported before (Potikha and Delmer, 1995).

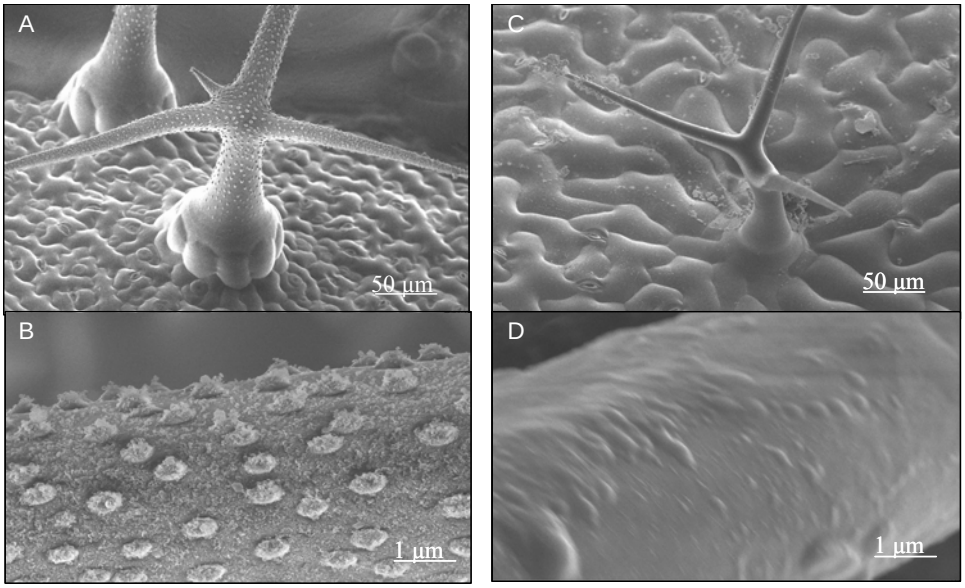

Figure 51. Scanning electron micrographs of wild type and *tbr1* trichomes. A) –Wild type trichome (magnitude 330X); B) –Papillae presence on the branch surface of a wild type trichome (magnitude18000X); C) *–tbr1* trichome lacks the epidermal basal cells compared to wild type (magnitude 330X); D) *–tbr1* trichome branches display a smooth surface without papillae (magnitude 18000X).

Electron microscopy analysis of trichome cross-sections revealed a clear difference in structure of the mutant trichome (Figure 52, panel C and D) when compared to wild type (Figure 52, panel A and B). The wild type trichomes appeared to be "empty" inside, while the cross-section in *tbr1* mutant trichome displays a kind of matrix deposition which fills the trichome inside (Figure 52, panel A and C). The wild type trichome cell wall is much thicker than the mutant trichome cell wall (Figure 52, panel B and D). The secondary cell wall cellulose is not deposited in the mutant trichomes (Figure 52, panel D).

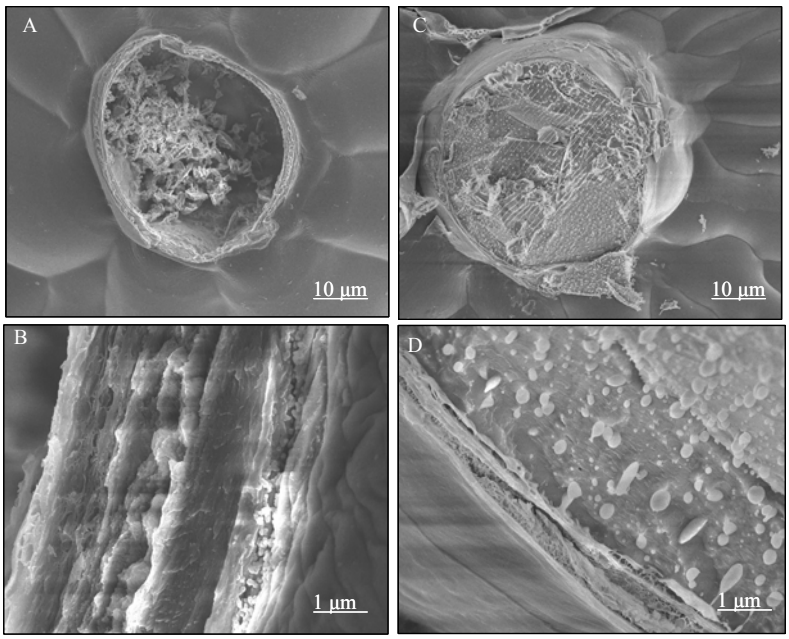

Figure 52. Scanning electron micrographs of wild type and *tbr1* trichomes cross-sections. A) – Wild type trichome cross-section (magnitude 700X); B) –Wild type trichome cross-section, internal structure view (magnitude 15000X); C) –*tbr1* trichome cross-section (magnitude 1000X); D) –*tbr1* trichome cross-section, internal structure view (magnitude 10000X).

3.10*LM5* AND *JIM5* ANTIBODY IMMUNOLABELING OF CELL WALL POLYSACCHARIDES IN *TBR1* AND WILD TYPE TRICHOMES

The use of defined antibodies is one of the most direct approaches available to gain insight into the molecular composition of cell walls.

The major components of the cell wall pectic matrix are homogalacturonan (HG), rhamnogalacturonan I (RG-I), and rhamnogalacturonan II (RG-II).

Antibodies for specific labeling of cell wall sugars epitopes have been developed, for example: CCRC-R1 (specific for RGII monomer), CCRC-M1 (specific for xyloglucan α-fucose (1-2) linked to D-galactosyl), LM5 and LM6 (specific for RGI/(1-5)α-L-arabinan), JIM5, etc (Wilats and Knox, 2003).

JIM5 is an antibody specific for homogalacturonan from the pectin fraction of primary cell wall, that recognizes methyl-esterified homogalacturonan (VandenBosch *et al.,* 1989; Knox *et al.,* 1990). Wild type trichomes showed clearly labeling by the *JIM5* antibody, displayed by the presence of a strong green fluorescence (Figure 53, panel A). In contrast, *tbr1*

trichomes totally lacked the fluorescence signal when labeled with *JIM5* antibody (Figure 53, panel B).

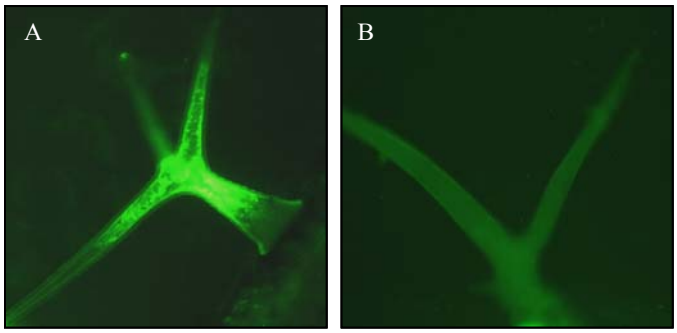

Figure 53. *JIM5* antibody labeling of trichome cell wall polysaccharides. The trichomes were four weeks old, in the greenhouse. A) –Wild type trichome showing the fluorescence signal and B) *–tbr1* trichome. Mutant trichome shows no labeling.

The *LM5* antibody is specific for rhamnogalacturonan I, recognizing β 1,4-D-galactose oligomers. It binds to four residues of (1-4)-β- galactan (Jones *et al.,* 1997; Willats *et al.,* 1997). This antibody showed a difference in fluorescence labeling between wild type and *tbr1* trichomes, with the fluorescence signal being detected in the wild type (Figure 54, panel A) but not in the *tbr1* mutant case (Figure 54, panel B).

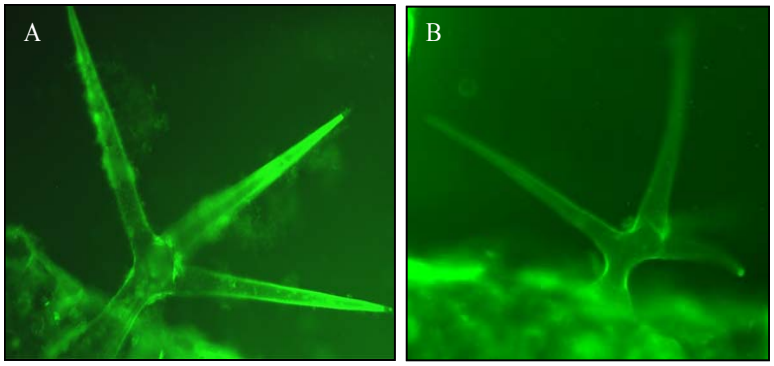

Figure 54. *LM5* antibody labeling of trichome cell wall polysaccharides. The trichomes were four weeks old, in the greenhouse A) –Wild type trichome displays a labeling fluorescence signal and B) – *tbr1* trichome. No labeling was detected in the mutant trichomes.

4. CHAPTER: DISCUSSION

Future advances in our understanding of cellulose biosynthesis process in higher plants will make possible the manipulation of cellulose production for human benefit. The cellulose synthesis complex can be divided into two main parts: one comprises the members that have a role in initiation and polymerization (cellulose synthase complex), and the second part comprises various regulatory components.

The members of the cellulose synthase complex have been identified mostly from study of cell wall mutants, as well as some of the additional components that play different roles in cellulose synthesis. However, there are probably many other components still to be identified, particularly those involved in regulation of cellulose synthesis process.

4.1 PRELIMINARY CHARACTERIZATION OF *TBR1* REVEALED ADDITIONAL PHENOTYPIC FEATURES

The *tbr1* mutant was identified because of lacking trichome birefringence when observed under polarized light. Birefringence is a characteristic of ordered cellulose fibrils deposited in the secondary cell wall (Potikha and Delmer, 1995).

It was observed that *tbr1* plants show some additional phenotypes, other than those described when isolated the mutant, by Potikha and Delmer (1995). Mutant plants grown in the greenhouse display a wide range of growth rates. Also the leaves are more rounded in shape, with shorter petioles than those of wild type plants. Stems of the mutant plants appear to be thinner and shorter than those of wild type. Measurements of stem diameter, at both, upper and lower parts resulted in a wide variation in mutant plants of the same age. However, stained stem cross-sections revealed no tissue morphological phenotype when observed under the microscope.

This confirms the result of the previous analysis in which the cellulose content in *tbr1* stems, was found to be essentially the same as in wild type stems (Potikha and Delmer, 1995).

The *tbr1* mutant was identified as a secondary cell wall mutant, with the phenotype being displayed in trichomes, by lacking the birefringence, when observed under polarized light. This phenotype is due to deficiency in cellulose microfibril deposition in the secondary cell wall (Potikha and Delmer, 1995).

The *irx* mutants (*irx1* and *irx3*) were also identified as secondary cell wall deficient mutants, with a significant decrease in the cellulose content of the secondary cell wall. They show a strong phenotype, namely collapsed xylem and weak xylem walls (Turner and Somerville, 1997; Taylor *et al.,* 1999). Since lack of trichome birefringence was characteristic phenotype of *tbr1*, which is also a secondary cell wall mutant, this phenotype was therefore checked in the *irx* mutants.

Both the *irx1* and *irx3* mutants displayed strong trichome birefringence under polarized light, as observed in wild type plants. Therefore, it seems that lack of trichome birefringence is not necessarily a characteristic result of a general deficiency in secondary cell wall cellulose deposition. An alternative explanation is that there are different levels of secondary cellulose deposition in the secondary cell walls, and the *irx* mutants deposit still enough secondary cellulose in order to show trichome birefringence. Maybe a double mutant *irx1irx3* would have a higher deficiency in the cellulose deposition and would show a lack of birefringence when observed under polarized light. A further possibility is that some other cellulose synthase-like genes are involved in producing the cellulose deposited in secondary cell walls in trichomes and they are affected in the *tbr1*, but not in the *irx* mutants.

4.2 *TBR* ENCODES A PUTATIVE PROTEIN OF UNKNOWN FUNCTION

Positional (or map-based) cloning techniques are widely used in the forward genetics approaches to identify the protein products of genes defined by mutation and described phenotype (Lukowitz *et al.,* 2000). Map-based cloning procedure resulted in the localization of the *TBR* gene on the top of chromosome V of *Arabidopsis thaliana*. Over 2100 F2 plants of the mapping population *tbr1* x Ler were subjected to genotyping by PCR screening with flanking genetic markers from the chromosomal area, in order to select enough recombinants to define the interval containing the mutation. The genetic interval of interest was narrowed down to 45 kb by analyzing a sufficient number of genetic markers from the respective region. It was also a necessary step to phenotype the selected recombinant plants in the next generation to confirm the presence of the recombination. The gene responsible for the lack of trichome birefringence phenotype in the *tbr1* mutant was finally identified by cosmid complementation experiment performed for the selected interval, by transforming mutant plants with selected overlapping cosmid clones. Only one of the cosmid clones complemented the mutant plants, pointing to the one complete gene sequence in the cosmid clone, as the best candidate. Supportive evidence

was obtained from DNA sequencing, which revealed a point mutation in the mutant plant, in the same candidate gene.

At the time of identification, the annotation of the *TBR* gene structure in public databases comprised four exons and three introns. However, evidences pointed to the gene being larger than the annotated version, comprising five exons and five introns. First, the identification of a cDNA clone (RAFL16-77-N09) that was sequenced and shown to include a non-annotated exon that extended the protein sequence at the 5'-end. Secondly, the extended N-terminus of the deduced protein sequence shows similarity with that of the close homolog *TBR*-like1 (*TBL1(trichome birefringence like1)*-At3g12060) supporting the suggestion that the *TBR* gene is actually longer than the annotated sequence in the public available databases. The *TBL1* gene was found to be a segmental duplication of *TBR,* localized on chromosome III.

In order to test the revised model of the *TBR* gene structure experimentally, to find out if the extended fragment from 5'-end is it a coding region and what is the start codon, two different *tbr1* mutant complementation experiments were performed. One complementation approach used the database annotated version of the gene, and the second complementation involved the longer form (including the non-annotated part). Only the longer form of the gene was able to rescue the mutant phenotype. The kanamycin resistant plants from transformation with the full length gene (genomic sequence) when checked for trichome birefringence under polarized light and for their growth rates were comparable to wild type.
Attempted mutant complementation involving only the database annotated version of the *TBR* gene, resulted in kanamycin resistant plants that showed the variation in growth rates, leaf phenotype and no trichome birefringence, which are characteristic of the mutant phenotype.

From these different mutant complementation experiments it was concluded that the non-annotated fragment of the *TBR* gene (suggested to be actually part of the gene), is essential for *TBR* gene function and therefore, the longer, revised gene structure is correct.

The gene encodes a putative protein of unknown function, which is predicted to be a plasma membrane protein. It contains a transmembrane spanning domain (region between amino acid residues 39 and 56, based on computer program prediction). Some of the closest homologues in the phylogenetic tree of related sequences are also predicted to be plasma membrane proteins, in agreement with the suggestion when the mutant was initially isolated (Potikha and Delmer, 1995), that TBR might play a role as a component of cellulose synthesis machinery.

The database annotation of the *TBR* gene was recently modified, and now agrees with our suggestion for a longer fragment for the gene model.

4.3 EXPRESSION ANALYSIS OF *TBR* AND TWO CLOSE HOMOLOGUES *TBL1* AND *TBL2*

The expression patterns of the *TBR* gene and two of its closest homologues *TBL1* (At3g12060) and *TBL2* (At1g60790) were investigated by Real Time RT-PCR, and analysis of gene promoter fusions with the GUS reporter gene for tissue localization details. The results of RT-PCR were confirmed, indeed, by promoter-*GUS* fusion analysis. The *TBR* gene was found to be expressed in most of the analyzed tissues, at different developmental stages: roots, rosette leaves of different ages, cauline leaves, stem, flowers and green siliques.

In the leaf and stem trichomes, the expression is maintained from the early stages of growth, up to later developmental stages, slightly decreasing with the age of the plant. Similar case was observed in stem and leaf vascular tissue. The expression in leaf vasculature was not a surprising event, because the cellulose content of this tissue in the *tbr1* mutant was found to be decreased when compared with wild type (Potikha and Delmer, 1995). The expression pattern changes during plant development in the sense that it decreases in all tissues the older the plant becomes (by the intensity of GUS expression signal). A high, ubiquitous expression was found in the very young seedlings, suggesting an involvement in the cell elongation process and, therefore, in the primary cell wall synthesis.

The expression pattern in roots changes during development. In the roots of very young seedlings (five days old), *TBR* is highly expressed in the main root and in secondary roots. In the next developmental stage, in two to three weeks old plants, the expression was observed only in the root primordia. In older plants of four to six weeks old, the expression is present throughout the whole root, main roots and secondary roots, but at a low level. However, there was no obvious root morphological phenotype when the growth and development of roots in mutant young seedlings were compared to wild type.

The homologues of *TBR*, *TBL1* (At3g12060) and *TBL2* (At1g60790) are also expressed in most of the analyzed tissues, but at a lower level than *TBR*. The expression pattern is slightly different between the two homologues. It is important to mention that, GUS promoter analysis revealed no expression signal of either homologue in the leaves, or stem trichomes, at any developmental stages. This suggests that *TBR* and these two homologues, at least, are not

functionally redundant. It is also worth noting that the blue signal characteristic of GUS expression appeared only after overnight incubation of plant tissues with the substrate, suggesting that the expression of *TBR,* together with the two analyzed homologues, is not very high.

The AtGenExpress data from Affymetrix ATH1 microarrays results in agreement with the RT-PCR expression profiles and promoter-*GUS* fusion analysis data. *TBR* expression is increased by indoloacetic acid (IAA) addition, and is repressed by abscisic acid (ABA) treatment. Phosphate resupply and Carbon starvation also leads to a slight increase in *TBR* expression level. Extended night also results in a higher expression. Most of the pathogen treatments increase *TBR* expression.

The study of different T-DNA K.O. lines found in the Signal available database, for *TBR* and two close homologous genes, *TBL1* and *TBL2* did not succeed in identifying a second allele of *tbr1*. Two different insertion lines were analyzed for each of the homologues and four different lines were checked for *TBR* gene. Homozygous plants were identified in the case of T-DNA lines of *TBR* homologues, but none of them displayed either the lack of trichome birefringence phenotype, or any other visible phenotype.

TBR Salk T-DNA lines screening did not result in identification of any homozygous plant, or plants with a visible phenotype that could be observed. RT-PCR analysis using specific primers, spanning both, the annotated and the extended part of the transcript, revealed expression values similar to wild type, showing that *TBR* transcript is still present in the heterozygous insertion plants. Studying of plants from a fourth *TBR* T-DNA line from the Sail collection resulted in identification only of heterozygous plants by PCR screening, but some visible phenotype was already observed when the plants were grown in the greenhouse. Some of the plants had fewer rosette leaves, and these were much smaller than those of wild type. The plants also showed very early flowering. A number of different plants from the same T-DNA population displayed more rosette leaves, but these were still smaller in size than in wild type. No missing trichome birefringence phenotype was detected. Further analyses are required of the next generation of the heterozygous Sail line.

The biological function of the TBR protein is still unknown. In spite of using several different approaches, the information regarding the subcellular localization of the protein is still lacking. Expression of the GFP-TBR fusion protein (N- and C-terminal fusion) resulted in

no fluorescence specific signal detected, even though the generated constructs successfully complemented the *tbr1* mutant phenotype, proving that they were functional. It is possible that TBR is a scaffolding protein, specifically expressed in trichomes. Possible use of antibodies that recognise the GFP protein would provide information about intracellular localization of the GFP-TBR fusion protein.

4.4 EXPRESSION OF DEFENCE RELATED GENES IN THE *TBR1* MUTANT

The expression of defence related genes has previously been studied in the primary cell wall deficient mutants, in particular in relation to jasmonic acid, ethylene, and lignin production pathways. The expression of defence-related genes in the *eli1* mutant, in cellulose synthase inhibitor-treated plants and in other plants with a deficiency in cellulose synthesis, suggested that reduced cellulose synthesis involves many different cellular responses which are regulated via JA- and ethylene-mediated pathways (Christine Ellis *et al.*, 2002). Lignification is also induced during inhibiting pathogen ingress, as a defence response (Vance *et al.*, 1980). In the *cev1* mutant, a constitutive expression of stress response genes and enhanced resistance to fungal pathogens was observed, establishing a link between cellulose synthesis, jasmonate, and ethylene responses. It was found that the *cev1* mutant phenotype could be reproduced by treating wild type plants with cellulose biosynthesis inhibitors (Ellis *et al.*, 2002).
Reduced cellulose synthesis has an indirect effect on defence gene expression. The corresponding mutant plants have an increase in jasmonate (JA) and ethylene production.
These studies provide further evidence that there may be a close link between pathogen attack and altered cell wall properties.

To date, defence gene expression has not been studied in any of the secondary cellulose deficient mutants. In order to find out if the secondary cell wall deficiency also leads to increase defence responses, the expression of twelve defence genes involved in different defence pathways was therefore investigated in the *tbr1* mutant, together with *irx3* another secondary cell wall mutant, and *rsw1*, a primary cell wall mutant, used as a control. Real-time RT-PCR was involved as analytical tool to follow the expression, using primers specific for the tested defence genes. No significant change was observed in *tbr1* mutant plants for any of the twelve checked defence genes, leading to the conclusion that there is no major activation of defence pathways in *tbr1* plants. In contrast, the *irx3* mutant shows high induction level of the

vegetative storage protein 2 (VSP2) and plant defensin protein (PDF1.2), and higher transcript levels of the senescence related protein (SRG1), both pathogenesis related proteins (PR), and cinnamoyl-CoA reductase (CCR2), which is involved in lignin biosynthesis.
In *rsw1,* a primary cell wall mutant used as a control, induction of vegetative storage protein1 (VSP1) and lower level for plant defensin protein (PDF1.2) was observed, confirming the previous report (Ana Cano-Delgado *et al.,* 2003). The pathogenesis related protein (PR) and cinnamoyl-CoA reductase (CCR2) showed a slight induction level along with the vegetative storage protein1 (VSP1) and thionin defence gene (THI2.1). No remarkable induction of the other of the defence genes tested was observed.

4.5 BIOCHEMICAL CHARACTERIZATION OF *TBR1* CELL WALL MUTANT

Gas-chromatography analysis of cell walls in leaves of mutant and wild type plants, revealed no significant differences in the matrix polysaccharide fraction or microfibril components. However, a change in the relative abundance of the components in the cell wall composition cannot be excluded.
When trichome material was analyzed, a slight increase in uronic acid content was found in the *tbr1* plants. A similar result has been found before in other cellulose synthesis mutants (Burk *et al.,* 1999; Sato *et al.,* 2001; Scheible *et al.,* 2003). MALDI-TOF analysis of the xyloglucan fraction of cell wall material from either leaves, or trichomes, resulted in no significant differences in the mutant plants compared to wild type. Therefore, GC and MALDI-TOF analyses did not identify any mutant plant phenotype in relation to changes in the cell wall components.

The scanning electron microscopy analysis of *tbr1* mutant trichomes in comparison to wild type trichomes revealed more details about their structure than previously described. In addition to the known lack of epidermal basal cells and of the branch surface papillae (Potikha and Delmer, 1995), the cross-sections displayed a clear difference in the internal structure of mutant trichomes, compared to wild type. The cell wall of wild type trichome is much thicker and more dense than in the mutant trichome. It appears that the secondary cell wall cellulose is missing in the *tbr1* mutant trichome, although this method does not provide further information about the materials deposited there. The analysis of trichomes cross-section reveals that the

wild type trichome is “empty” inside, but the mutant trichome deposited a kind of matrix that fills the trichome.

Labelling with polysaccharide specific antibodies can provide information about cell wall structure and function (Willats *et al.,* 2000), in contrast to other techniques, like mass-spectroscopy or NMR, electrophoresis, that involve the destruction of the cellular order. Monoclonal antibodies such as: JIM5, JIM7, PAM1, and LM7 approaches were successfully used to compare the degree of methyl esterification in the cell walls, indicating a significant difference in the homogalacturonans between different plant lines (Wiethölter *et al.,* 2003).

Application of the cell wall polysaccharide specific antibodies showed differences between *tbr1* trichomes and wild type. Two different antibodies, specific for different components of the pectin fraction, were used. The pectic network of the cell wall is complex and consists of structurally and functionally distinct domains: homogalaturonan (HG), rhamnogalacturonan-I (RG-I), and rhamnogalacturonan-II (RG-II) (Carpita and Gibeaut, 1993).

JIM5 is a specific antibody for homogalaturonan, that can bind to unesterified oligomers of galactan, but optimal binding is achieved when some methyl-ester groups are present (VandenBosch *et al.,* 1989; Knox *et al.,* 1990).

LM5 is specific for rhamnogalacturonan-I fraction. It binds to four residues of 1,4-β-galactan from the pectin fraction which was shown to be restricted to a thin recently deposited layer of primary cell wall, adjacent to the plasma membrane in resin embedded sections of pea cotyledons (Jones *et al.,* 1997; Willats *et al.,* 1997). Such observations indicate that the differing structures in the side chains of pectins are likely to have specific properties and functions in the primary cell walls (Willats *et al.,* 2000).

From *JIM5* labelling wild type trichomes displayed a strong fluorescence, but the *tbr1* trichomes mutant did not. The same result was obtained with the *LM5* antibody, with the *tbr1* mutant trichomes showing no fluorescence signal. The *tbr1* trichomes seem to lack these pectin components, recognized by the two antibodies, therefore there seems to be also an alteration in the pectic deposition of the cell wall.

5. CHAPTER: EXPERIMENTS IN PROGRESS

5.1 TBR PROTEIN TAGGING EXPERIMENT

The biological function of the TBR protein and its interacting partners remain unknown. Therefore, a protein tagging experiment was planned, to obtain some information in this respect. N- and C-terminal fusion constructs were generated. The TBR cDNA sequence was cloned into PENTR/SD/D/TOPO (Invitrogen), and the destination vectors, pGWB17 and pGWB18, were used to generate Myc protein fusions. The expression in these vectors is driven by a 35S promoter.

The resulted constructs (Figure 55) were first cloned in *E. coli DH 5α* and then transferred to *Agrobacterium tumefaciens GV 3101*, by electroporation. Further on, wild type Col-0 and *tbr1* mutant plants were transformed.

The constructs rescued mutant phenotype. Resistant plants were showing normal trichome birefringence under polarized light. Transformed wild type plants were transferred to the greenhouse, and rosette and stem material was harvested from mature plants. The total protein will be extracted from these samples and the tagged TBR protein will be purified using commercially anti-MYC antibodies. The co-purified proteins will be analyzed by mass-spectrometric methods (MALDI-TOF MS) to find TBR interacting partners.

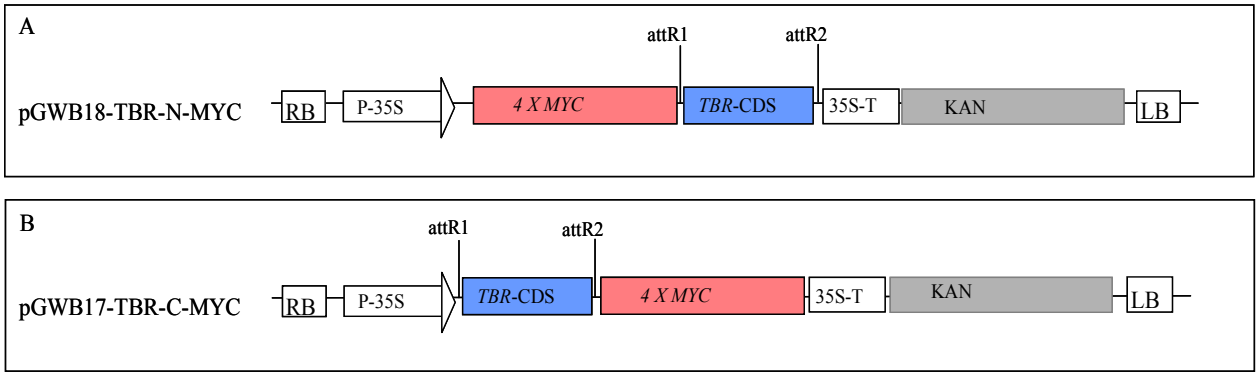

Figure 55. **Representation (not to scale) of the generated constructs used for epitope tagging**.
N: N-terminal fusion; C: C-terminal fusion; P-35S: the promoter of cauliflower mosaic virus; 35S-T: terminator of 35S cauliflower mosaic virus; TBR-CDS represents the TBR cDNA fragment; KAN: coding region of kanamycin resistance gene; attR1, attR2: GATEWAY DNA recombination sites: RB and LB: right and left T-DNA border.

REFERENCES

Amor, Y., Haigler, C. H., Johnson, S., Wainscott, M., Delmer, D. P. (1995). A membrane associated with sucrose synthase and its potential role in synthesis of cellulose and callose in plants. Proc Natl Acad Sci USA. **92**, 9353-9357.

Ana Cano-Delgado, Karin Metzlaff and Michael W. Bevan. (2000). The *eli1* mutation reveals a link between cell expansion and secondary cell wall formation in *Arabidopsis thaliana*. Development. **127**, 3395-3405.

Arioli, T., Peng, L., Betzner, A. S., Burn, J., Wittke, W., Herth, W., Camilleri, C., Hoefte, H., Plazinski, J., Birch, R., Cork, A., Glover, J., Redmond, J., and Williamson, R. E. (1998). Molecular analysis of cellulose biosynthesis in *Arabidopsis*. Science **279,** 717-720.

Atalla, R. H., Hackney, J. M., Uhlin, I., Thompson, N. S. (1993). Hemicelluloses as structure regulators in the aggregation of native cellulose. Int. J. Biol. Macromol. **15**, 109-112.

Bacic, A., Harris, P. J., Stone, B. A. (1998). Structure and function of plant cell walls. The biochemistry of plants (ed. Press, J.). Academic Press. London. **14**, 297-371.

Baskin, T. I. (2001). On the alignment of cellulose microfibrils by cortical microtubules: a review and a model. Protoplasma. **215**, 150-171.

Brown, R.M. (1996). The biosynthesis of cellulose. J. Macromol. Sci. Pure Appl. Chem. **A33,** 1345–1373.

Brown, R. M. (1996). Cellulose biosynthesis in higher plants. Trends Plant Sci. **1**, 149-155.

Brookes, A.J. (1999). The essence of SNPs. Gene. **23,** 177-186.

Cano-Delgado, A., Penfield, S., Smith, C., Catley, M., Bevan, M. (2003). Reduced cellulose synthesis invokes lignification and defence responses in *Arabidopsis thaliana*. Plant Journal. **34(3)**, 351-362.

Cantatore, J. L., Murphy, S. M., and Lynch, D. V. (2000). Compartmentation and topology of glucosylceramide synthesis. Biochem. Soc. Trans. **28**, 748-750.

Carpita, N. C., Gibeaut, D.M. (1993). Structural models of primary cell walls in flowering plants: consistency of molecular structure with the physical properties of the walls during growth. Plant Journal. **3,** 1-30.

Christine Ellis, Ioannis Karafyllidis, Claus Wasternack and John G. Turner. (2002). The

Arabidopsis mutant *cev1* links cell wall signalling to jasmonate and ethylene responses, The Plant Cell. **14**, 1557-1566.

Christine Ellis and John Turner. (2001). The Arabidopsis mutant *cev1* has constitutively active jasmonate and ethylene signal pathways and enhanced resistance to pathogens, The Plant Cell. **13**, 1025-1033.

Chris Somerville, Stefan Bauer, Ginger Brininstool, Michelle Facette, Thorsten Hamann, Jennifer Milne, Erin Osborne, Alex Paredez, Steffan Persson, Ted Raab, Sonja Vorwerk, Heather Youngs. (2004). Toward a systems approach to understanding plant cell walls. Science. **306**, 2206-2211.

Clough, S. J., and Bent, A. F. (1998). Floral dip: a simplified method for *Agrobacterium*-mediated transformation of *Arabidopsis thaliana*. Plant Journal. **16**, 735-743.

Daniel J. Cosgrove. (1997). Assembly and enlargement of the primary cell wall in plants. Annu. Rev. Cell Dev. Biol. **13**, 171-201.

Darvill, A. G., McNeill, M., Albersheim, P., Delmer, D. (1980). The primary cell wall of flowering plants. In Tolbert, N. (ed.). The biochemistry of plants. Academic Press. London **1**, 91-162.

Delmer, D. P. (1999). Cellulose biosynthesis: exciting times for a difficult field of study. Annu. Rev. Plant. Physiol. Plant Nol. Biol., **50**, 245-276.

Delmer, D. P., and Amor, Y. (1995). Cellulose biosynthesis. Plant Cell. **7**, 987-1000.

Delmer, D. P. and Stone, B. A. (1988). Biosynthesis of plant cell walls. The biochemistry of Plants. **14**, Academic Press, San Francisco, 373-420.

Edwards, M., Dea, I. C. M., Bulpin, P. V., and Reid, J. S. G. (1986). Purification and properties of a novel xyloglucan-specific endo-(1→4)-ß-D-glucanase from germinated *Nasturtium* seeds (Tropaeolummajus L). Journal of Biological Chemistry. **261(20)**, 9489-9494.

Ellis, C., Karafyllidis, I., Wasternack, C., and Turner, J. G. (2002). The *Arabidopsis* mutant *cev1* links cell wall signalling to jasmonate and ethylene responses. Plant Cell. **14**, 1557-1566.

Elbein, A. D., Forsee, W. T. (1975). Biosynthesis and structure of glycosyl diglycerides, steryl glucosides, and acylated steryl glucosides. Lipids. **10(7)**, 427-36.

Emons, A. M. C., Derksen, J., Sassen, M. M. A. (1992). Do microtubules orient plant cell wall microfibrils?. Plant Psysiol. **84**, 486-493.

Fagard Mathilde, Thierry Desnos, Thierry Desprez, Florence Goubet, Guislane

Refregier, Gregory Mouille, Maureen McCann, Catherine Rayon, Samantha Vernhettes, and Herman Höfte. (2000). *PROCUSTE1* Encodes a cellulose synthase required for normal cell elongation specifically in roots and dark-grown hypocotyls of *Arabidopsis*. Plant Cell. **12(12)**, 2409–2423.

Folkers, U., Berger, J., and Hülskamp. (1997). Cell morphogenesis of trichomes in *Arabidopsis* differential control of primary and secondary branching by branch initiation regulators and cell growth. Development. **124**, 3779-3786.

Fry, S. C. (1988). The growing plant cell wall: chemical and metabolic analysis. Essex: Longman, Scientific &Technical.

Fry, S. C., York, W. S., Albersheim, P., Darvill, A., Hayashi, T., Joseleau, J. P., Kato, Y., Lorences, E. P., Maclachlan, G. A., McNeil, M., Mort, A. J., Reid, J. S. G., Seitz, H. U., Selvendran, R. R., Voragen, A. G. J., and, White, A. R. (1993). An umbiguous nomenclature for xyloglucan derived oligosaccharides. Physiologia Plantarum. **89**, 1-3.

Gibeaut, D. M. and Carpita, N. C. (1994). Improved recovery of (1,3),(1,4)-β-D-glucan synthase activity from Golgi apparatus of *Zea mays* using differential flotation centrifugation. Protoplasma. **180**, 92-97.

Gilmor, C. S., Poindexter, P., Lorieau, J., Palcic, M. M. and Somerville, C. (2002). A Glucosidase I is required for cellulose synthesis and morphogenesis in *Arabidopsis*. J. Cell Biol. **156**, 1003-1013.

Haigler, C. H. and Brown, R. M. Jr. (1986). Transport of rosettes from the Golgi apparatus to the plasma membrane in isolated mesophyll cells of *Zinnia elegans* during differentiation to tracheary elements in suspension culture. Protoplasma **134,** 111–120.

Haigler, C. H., White, A. R., Brown, R. M. Jr., Cooper, K. M. (1982). Alteration of in vivo cellulose ribbon assembly by carboxymethylcellulose and other cellulose derivatives. J. Cell Biol. **94**, 64-69.

Hartley, J. L., Temple, G. F., and Brasch, M. A. (2000). DNA cloning using *in vitro* site-specific recombination. Genome Research **10**, 1788-1795.

Haughn, G. W., Somerville, C. R. (1988). Genetic control of morphogenesis in *Arabidopsis*. Dev. Genet. **9**, 73-89.

Hayashi, T., Marsden, M. P. F., Delmer, D. P. (1987). Pea xyloglucan and cellulose V. xyloglucan-cellulose interactions in vitro and in vivo. Plant Physiol. **83**, 384-389.

Hayashi, T., Owaga, K., and Mitsuishi, Y. (1994). Characterization of the adsorption of xyloglucan and cellulose. Plant Cell Physiol. **35**, 1199-1205.

Hayashi, T., Wong, Y.S., and Maclachlan, G. (1984). Pea Xyloglucan and cellulose. II Hydrolysis by pea endo-1,4-ß-glucanases. Plant Physiol. **75**, 605-610.

His, I., Driouich, A., Nicol, F., Jauneau, A., Hofte, H. (2001). Altered pectin composition in primary cell walls of *korrigan,* a dwarf mutant of *Arabidopsis* deficient in a membrane-bound endo-1,4-β-glucanase. Planta. **212**, 348-358.

Hooykaas, P. J. J. and Shilperoort, R. A. (1992). *Agrobacterium* and plant genetic engineering. Plant Molecular Biology. **19**, 15-38.

Hülskamp, M., Misera, S., and Juergens, G. (1994). Genetic dissection of trichome cell development in *Arabidopsis*. Cell. **76**, 555-566.

Jones, L., Seymour, J. B., and Knox, J. P. (1997). Localization of pectic galactan in tomato cell walls using a monoclonal antibody specific to 1,4-ß-D-galactan. Plant Physiology. **114**, 1123-1133.

Knox, J. P., Linstead, P. J., King, G., Cooper, C., and Roberts, K. (1990). Pectin esterification is spatially regulated both within cell walls and between developing tissues of root apices. Planta. **181**, 512-521.

Inoue, H., Nojima, H., and Okayama, H. (1990). High efficiency transformation of *Escherichia coli* with plasmids. Gene **96,** 23-28.

Jander, G., Norris, S. R., Rounsley, Bush, D. F., Levin, I. M., and Last, R. L. (2002). *Arabidopsis* map-based cloning in the post-genome era. Plant Physiol. **129**, 440-450.

Jefferson, R. A., Burgess, S. M., Hirsh, D. (1986). β-glucuronidase from *E. coli* as a gene fusion marker. Proc. Natl. Acad. Sci. **83**, 8447-8451.

Jefferson, R. A. (1987). Assaying chimeric gene in plants: the *GUS* gene fusion system. Plant Mol. Biol. **5**, 387-405.

Joanne E. Burn, Charles H. Hocart, Rosemary J. Birch, Anna C. Cork and Richard E. Williamson. (2002). Functional analysis of the cellulose synthase genes *CesA1, CesA2* and *CesA3* in *Arabidopsis.* Plant Physiology. **129 (2)**, 797-807.

Karimi, M., Inze, D., and Depicker, A. (2002). GATEWAY vectors for *Agrobacterium* mediated plant transformation. Trends Plant Sci. **7**, 193-195.

Kiefer, L. L., York, W. S., Darvill, A. G., and Albersheim, P. (1989). Structure of plant cell walls XVII. Xyloglucan isolated from suspension-cultured sycamore cell walls is *O*-acetylated. Phytochemistry **28**, 2105-2107.

Kimura, S., Laosinchai, W., Itoh, T., Cui, X., Linder, C. R., and Brown, R. M. Jr. (1999). Immunogold labelling of rosette terminal cellulose-synthesizing complexes in the vascular plant *Vigna angularis*. Plant Cell **11,** 2075–2085.

Klimyuk, V.I., Carroll, B. J., Thomas, C. M., Jones, J. D. G. (1993). Alkali treatment for rapid preparation of plant material for reliable PCR analysis: technical advance. Plant Journal **3,** 493–494.

Koncz, C. and Schell, J. (1986). The promotor of TL-DNA gene 5 controls the tissue-specific expression of chimeric genes carried by a novel type of *Agrobacterium* binary vector. Mol. Gen. Genet. **204,** 383-396.

Konieczny A. and Ausubel F. M. (1993). A procedure for mapping *Arabidopis* mutations using co-dominant ecotype-specific PCR-based markers. Plant Journal. **4**, 403-410.

Koornneef, M., Dellaert, S. W. M., and Van der Veen, J. H. (1982). EMS-and radiation-induced mutation frequencies at individual loci in *Arabidopsis thaliana.* Mutat. Res. **93**, 109-123.

Landy, A. (1989). Dynamic, structural, and regulatory aspects of λ site-specific recombination Ann Rev Biochem. **58**, 913-949.

Lapasin, R., Pricl, S. (1995). The Rheology of Industrial Polysaccharides. Theory and Applications.

Levy, S., Maclachlan, G., and Staehelin, L.A. (1997). Xyloglucan side chains modulate binding to cellulose during in vitro binding assays as predicted by conformational dynamics simulations. Plant Journal. **11**, 373-386.

Lukowitz, W., Nickle, T. C., Meinke, D. W., Last, R. L., Conklin, P. L. and Somerwille, C. R. (2001). *Arabidopsis cyt1* mutants are deficient in a mannose-1-phosphate guanylyltransferase and point to e requirement of N-linked glycosylation for cellulose biosynthesis. Proc. Natl. Acad. Sci. USA. 98, 2262-2267.

Harvey Lodish, Arnold Berk, Lawrence S. Zipursky, Paul Matsudaira, David Baltimore, James Darnell. (2000). The dynamic plant cell wall. Molecular cell biology-fourth edition.

Harris, P. J., Kelderman, M. P., Kendon, M. F., and McKenzie, R. J. (1997). Monosaccharide compositions of unlignified cell walls of monocotyledons in relation to the occurrence of wall-bound ferrulic acid. Biochem. Syst. Ecol. **25,** 167-179.

Marks, M. D. (1997). Molecular genetic analysis of trichome development in *Arabidopsis*, Annu. Rev. Plant Physiol. Plant. Mol. Biol. **48**, 137-168.

Marie-Ann Ha, Iain M. MacKinnon, Adriana Sturcova, David C. Apperley, Maureen C. McCann, Simon R. Turner and Michael C. Jarvis. (2002). Structure of cellulose-deficient secondary cell walls from the *irx3* mutant of *Arabidopsis thaliana,* Phytochemistry. **61**, 7-14.

Matsumoto, T., Sakai, F., and Hayashi, T. (1997). A xyloglucan-specific endo-1,4-ß-glucanase isolated from auxin-treated pea stems. Plant Physiology. **114(2)**, 661-667.

Mayer, U., Torres-Ruiz, R. A., Berleth, T., Misera, S. and Jürgens, G. (1991). Mutations affecting body organization in the developing *Arabidopsis* embryo. Nature. **353,** 402-407.

McCann, M. C., Wells, B., Roberts, K. (1990). Direct visualization of cross-links in the primary plant cell wall. J Cell Sci. **96**, 323–334.

Michael, M. Neff., Edward Turkand and Michael Kalishman. (2002). Web-based primer design for single nucleotide polymorphism analysis. Trends in Genetics. 1-3.

Monika S. Doblin, Isaac Kurek, Deborah Jacob-Wilk and Deborah P. Delmer. (2002), Cellulose biosynthesis in Plants: from genes to Rosettes, Plant and Cell Physiology, **12**, 1407-1420.

M. David Marks. (1997). Molecular genetic analysis of trichome development in *Arabidopsis*. Annu. Rev. Plant. Physiol Plant. Mol. Biol. **48**, 137-163.

Nagel, R., Elliot, A., Masel, A., Birch, R. G., and Manners, J. M. (1990). Electroporation of binary Ti plasmid vector into *Agrobacterium tumefaciens* and *Agrobacterium rhizogenes*. FEMS Microbiology letters. **67**, 325-328.

Neil G. Taylor, Wolf-Rüdiger Scheible, Sean Cutler, Chris R. Somerville and Simon R. Turner. (1999). The irregular xylem3 locus of *Arabidopsis* encodes a cellulose synthase required for secondary cell wall synthesis. The plant cell. **11**, 769-779.

Nickle, T. **C. and Meinke, D. W.** (1998). A cytokinesis-defective mutant of *Arabidopsis* (cyt1) characterized embryonic lethality, incomplete cell walls, and excessive callose accumulation. Plant Journal. **15**, 21-332.

Nicol, F., His, I., Jauneau, A., Vernhettes, S., Canut, H., Höfte, H. (1998). A plasma membrane-bound putative endo-1,4-β-D-glucanase is required for normal wall assembly and cell elongation in *Arabidopsis*. EMBO J. **17**, 5563-5576.

Nicholas Carpita, Maureen McCann. (2000). The cell wall. Biochemistry and Molecular Biology of Plants, 52-75.

Nishitani, K. and Matsuda, Y. (1983). Auxin induced changes in the cell wall xyloglucans: effects of auxin on the two different subfractions of xyloglucans in the epicotyl cell wall of *Vigna angularis*. Plant Cell Physiol. **24**, 345-355.

Oppenheimer, D. G., Pollok, M. A., Vacik, J., Szymanski, D. B., Ericson, B., Feldmann, K., Maks, M. D. (1997). Essential role of a kinesin-like protein in *Arabidopsis* trichome morphogenesis. Proc. Natl. Acad. Sci. USA. **94**, 6261-6266.

Pagant, S., Bichet, A., Sugimoto, K., Lerouxel, O., Desprez, T., McCann, M., Lerouge, P., Vernhettes, S., and Höfte, H. (2002). KOBITO encodes a novel plasma membrane protein necessary for normal synthesis of cellulose during cell expansion in *Arabidopsis*. Plant Cell. **14**, 2001-2013.

Patricia L. Herman, and M. David Marks. Trichome development in *Arabidopsis thaliana* II. isolation and complementation of the *GLABROUSI* gene. The Plant Cell. **1**, 1051-1055.

Pauly, M., Andersen, L.N., Kauppinen, S., Kofod, L.V., York, W.S., Albersheim, P., and Darvill, A. (1999). A xyloglucan-specific endo-ß-1,4-glucanase from *Aspergillus aculeatus*: expression cloning in yeast, purification and characterization of the recombinant enzyme. Glycobiology. **9(1)**, 93-100.

Pear, J. R, Kawagoe, Y., Schreckengost, W. E., Delmer, D. P., Stalker, D. M. (1996). Higher plants contain homologs of the bacterial *celA* genes encoding the catalytic subunit of cellulose synthase. Proc. Natl. Acad Sci. USA. **93**, 12637-42.

Peng, L., Kawagoe, Y., Hogan, P., Delmer D. (2002). Sitosterol-β-glucoside as primer for cellulose synthesis in Plants. Science. **295**, 147-150.

Perrin, R., Wilkerson, C., Keegstra, K. (2001). Golgi enzymes that synthesize plant cell wall polysaccharides: finding and evaluating candidates in the genomic era. Plant. Mol. Biol. **47**, 115-130.

Potikha Tamara and Deborah P. Delmer. (1995). A mutant of *Arabidopsis thaliana* displaying altered patterns of cellulose deposition. The Plant Journal. **7(3)**, 453-460.

Potikha, T. S., Collins, C. C., Johnson, D. I. Delmer, D. P., and Levine, A. (1999). The involvement of hydrogen peroxide in the differentiation of secondary walls in cotton fibres. Plant Physiol., **119**, 849-858.

Ramakers, C., Ruijter, J. M., Deprez, R. H., and Moorman, A. F. (2003). Assumption-free analysis of quantitative real-time polymerase chain reaction (PCR) data. Neurosci Lett. **339**, 62-66.

Rerie, W. G., Feldmann, K. A., and Marks, M. D. (1994). The *GLABRA2* gene ancodes a homeo domain protein required for normal trichome development in *Arabidopsis.* Genes Dev. **8**, 1388-1399.

Ridley, B. L., O'Neill, M. A., and Mohnen, D. (2001). Pectins: structure, biosynthesis, and oligogalacturonide-related signaling. Phytochem. **57**, 929-967.

Ringli, C., Keller, B., Ryser, U. (2001). Glycine-rich proteins as structural components of plant cell walls. Cell Mol Life. Science. **58**, 1430-41.

Salnikov, V. V., Grimson, M. J., Delmer, D. P., Haigler, C. H. (2001). Sucrose synthase localizes to cellulose synthesis sites in tracheary elements. Phytochemistry. **57**, 823-33.

Sambrook, J., Fritsch, E. F., and Maniatis, T. (1989). Molecular cloning a laboratory manual, Second edition. Cold Spring harbor laboratory press, New York.

Sato, S., Kato, T., Kakegawa, K., Ishii, T., Liu, Y-G., Awano, T., Takabe, K., Nishiyama, Y., Kuga, S. (2001). Role of the putative membrane-bound endo-1,4-β-D-glucanase KORRIGAN in cell elongation and cellulose synthesis in *Arabidopsis thaliana*. **42**, 251-263.

Saxena,. I.M., K. Kudlicka, K. Okuda, and R. M. Brown, Jr. (1994). Characterization of genes in the cellulose synthesizing operon (acs operon) of *Acetobacter xylinum:* Implications for cellulose crystallization. J. Bacteriology. **176**, 5735-5752.

Saxena, I.M., Brown, R.M., Fevre, M., Geremia, R.A., and Henrissat, B. (1995). Multidomain architecture of β-glycosyl transferases: Implications for mechanism of action. J. Bacteriol. **177,** 1419–1424.

Saxena Inder M., Malcolm Brown Jr. (1997). Identification of cellulose synthase(s) in higher plants: Sequence analysis of processive β- glycosyltransferases with the common motif "D,D,D35Q(RQ)XRW". Cellulose. **4**, 33-49.

Scheible, W. R., Eshet, R., Richmond, T., Delmer, D., and Somerville, C. (2001). Mutations in cellulose synthase confer resistance to isoxaben and thiazolidinone herbicides in the *Arabidopsis ixr*1 mutants. Proceedings of the National Academy of Science USA 98, 10079-10084.

Scheible, W. R., Törjek, O., and Altmann, T. (2004). From markers to cloned genes: map-based cloning. Biotechnology in agriculture and forestry. **55**, 55-86.

Silvere Pagant, Adeline Bichet, Keiko Sugimoto, Olivier Lerouxel, Thierry Desprez, Maureen McCann, Patrice Lerouge, Samantha Vernhettes and Herman Höfte. (2002). *KOBITO1* encodes a novel plasma membrane protein necessary for normal synthesis of cellulose during cell expansion in *Arabidopsis.* The Plant Cell. **14**, 2001-2013.

Showalter, A. M. (1993). Structure and function of plant cell wall. Plant cell **5**, 9-23.

Szyjanowicz, P. M., McKinnon, I., Taylor, N. G., Gardiner, J., Jarvis, M. C., Turner, S. R. (2004). The *irregular xylem 2* mutant is an allele of *korrigan* that affects the secondary cell wall of *Arabidopsis thaliana*. Plant Journal. **37**, 730-740.

Silk. (1984). Quantitative description of development. Annu. Rev. Plant. Physiol. **35**, 479-518.

Simon Turner and Chris R. Somerville. (1997). Collapsed xylem phenotype of *Arabidopsis*

identifies mutants deficient in cellulose deposition in the secondary cell wall. Plant cell. **9,** 689-701.

Staehelin, L. A. and Moore, I. (1995). The plant Golgi apparatus: structure, functional organization and trafficking mechanism. Annu. Rev. Plant. Physiol. Plant Mol. Biol. **46**, 261-288.

Steve M. Read and Tony Bacic. (2002). Prime time for cellulose. Science. **295**, 59-60.

Tabuchi, A., Kamisaka, S., and Hoson, T. (1997). Purification of xyloglucan hydrolase/endotransferase from cell walls of azuki bean epicotyls. Plant and Cell Physiology. **38(6)**, 653-658.

Taylor, N.G., Scheible, W.-R., Cutler, S., Somerville, C.R., and Turner, S.R. (1999). The irregular xylem3 locus of *Arabidopsis* encodes a cellulose synthase required for secondary cell wall synthesis. Plant Cell. **11,** 769–779.

Taylor, N. G., Laurie, S. and Turner, S. R. (2000). Multiple cellulose synthase catalytic subunits are required for cellulose synthesis in *Arabidopsis*. Plant Cell. **12**, 2529-2539.

Taylor, N. G., Howells, R. M., Huttly, A. K., Vickers, K. and Turner, S. R. (2003). Interactions between three distinct CesA proteins essential for cellulose synthesis. Proceedings of the National Academy of Sciences of the USA. **100**, 1450-1455.

Tire, C., De Rycke, R., De Loose, M., Inze, D., Van Montagu, M., Engler, G. (1994). Extensin gene expression is induced by mechanical stimuli leading to local cell wall strengthening in *Nicotiana plumbaginifolia*. Planta. **195,** 175-181.

Todd Richmond. (2000). Higher plant cellulose synthases. Genome Biology. **I(4)**, 3001.1-3001.6.

Turner S. R., and Somerville C. R. (1997). Collapsed xylem phenotype of *Arabidopsis* identities mutants deficient in cellulose deposition in the secondary cell wall. Plant Cell. **9**, 689-701.

Vance, C. P., Kirk, T. K., and Sherwood, R. T. (1980). Lignification as a defence mechanism of disease resistance. Annu. Rev. Phytopathol. **18**, 259-288.

VandenBosch, K. A., Bradley, D. J., Knox, J. P., Perotto, S., Butscher, G. W., and Brewin, N. J. (1989). Common components of the infection thread matrix and the intercellular space identified by immunocytochemical analysis of pea nodules and uninfected roots. EMBO J. **8**, 335-342.

Wiethölter, N., **Graessner, B., Mierau, M., Mort, A. J., Moerschbacher, M.** (2003). Differences in the methyl ester distribution of homogalacturonans from near-isogenic what lines resistant and susceptible to the wheat rust fungus. MPMI. **16 (10)**, 945-952.

Willats, W., Steele King, G. S., Markus, S. E., Knox, J. P. (2002). Antibodies techniques. Molecular Plant Biology 2, Theoretical Approach. **254**, 199-219.

Willats, W. G. T., Steele-King, C. G., Marcus, S. E., and Knox, J. P. (1999). Side chains of pectic polysaccharides are regulated in relation to cell proliferation and cell differentiation. Plant J. **20**, 619-628.

William G.T. Willats and J. Paul Knox. (2003). Molecules in context: probes for cell wall Analysis. The plant cell wall, 92-110.

William G. T., Clare G. Steel-King, Lesley McCartney, Caroline Orfila, Susan E. Marcus, J. Paul Knox. (2000). Making and using antibody probes to study plant cell walls. Plant Physiol. Biochem. **38 (1/2)**, 27-36.

Williamson RE, Burn JE, Hocart CH. (2001). Cellulose synthesis: mutational analysis and genomic perspectives using *Arabidopsis thaliana*. Cellular and Molecular Life Sciences **58**, 1475-1490.

W**olfgang Lukowitz, C. Stewart Gillmor and Wolf- Rüdiger Scheible**. (2000). Positional Cloning in *Arabidopsis*. Why it feels good to have a genome initiative working for you. Breakthrough Technologies. **123**, 795-805.

W.-R. Scheible, R. Eshet, T. Richmond, D. Delmer, and C. Somerville. (2001). Mutations in cellulose synthase confer resistance to isoxaben and thiazolidinone herbicides in the *Arabidopsis ixr*1 mutants. Proceedings of the National Academy of Science USA **98**, 10079-10084.

APPENDIX I

Sequence and length of the DNA probes used in the cosmid complementation of *tbr1* mutant:

Probe A:

GATTCTGGATTCTTAGCTCGTTGTTACTCTGAAATTTTCATAGATAACTTCAATGCTCTGATGTAGTG
GTGTTGTTTTCAGTTCGTTTGATGAGAAACACTTTCAAAGTTTCGAGTTTTGAGTTTTCTTCTAGTATG
AGGTTTGGATTTGGATCCCTTAACATGATCTACTCCTTTTCAAATTCAGTCTTGATTATTGTGTGTTCA
AGTCCTTTTCATATGCTTTGACATCTTTCTAATCATTTGTACACCAAAAGGCTTGAGTTTTCATGCGT
ATGGATTGTTTGGAGACTGAAATGAGAGGTTAGTGAAAGATGTAGGTAATAAGAGTACACATGGAT
AGGGTTTTGTCAAGTGTAATGGGTAAGTTACAGAGAGGCTCAGGTCATATCCTCAGCAATGTA
Product length: 403 bp

Probe B:

AGGCCATAGCGTAAGCACCAAAATATACAAAATTAGTAGTACTACATTTTAAGCATCCAACAATTTG
TGACCTCCAATGGTGATCATTCCAAGAAACTTCTTTAGGAATAGTTTTTATAACCACAGCAAATTAA
ACTACTAACACCTCCTTAAGTTATTTGATAAGCGCAATAACAGTGCATGGTACATTTGATTATAACA
TGAGTTCATCAAAGTCTTCATTCCTAATGAGAAGTTAATGACTTAAGACTTGGGAAAGTTATGAGAA
ATTTGCGATTTTCTGACGGAAATGAATGAAATC
Product length: 301 bp

Probe C:

AACTCTCCACTGCGATCTGAGCGCTTCTGTGATATTTTTCGATCGTAAAAAATTAGGTTAAAATGACT
GACTTAGCCACCTTGGTCACACCACTAACTTTTTTTATTCACGGTAAAAAAAAAAAAAAATCATGCA
TATAACACAATATGCTTAGTTCATTAGTCCTAAGTAAAATACATACCGCCTTTATTCTTCCTTGTTTTT
TGTTTTTCTTTTTTTGATAAACATTTATTCTTCCTTGTTGCTTGAAATTATAGTTCTTCATCTTCCTCAC
TGGACATATCTCAATTTTACTTTATATGTAAAGTTTCAAAAACTTCCCCAATATTATTCTTTTTCTATC
CTTGGTCAAGCGTC
Product length: 357 bp

Probe D:

GCTCATGCGAATACGGTTCTTCTCCATCTGGTTCACCAGCACAAATTATGTTGTTGTTAGTGATCTTA
GTGCATGACAAATAGAAATAAACAAAGGCCGCTGTTCACATTTATTACCGCTTTCGTAATCAGAAGC
ATCCGTAAGCCTTGCAATGGCAGCAATAAGCGCCTGTTCATGTTCCTATATCATCCAATAACAACAA
CACCAAGTTTCACTTCACTGTTTCTTTCAATCGATATCTCGTCACAAAGTTCTTATCAATTATCATATC
GCTCACCTTGAGTAGCTTCTTGGCCTTATCAAGCTCATGTGGATCAGGAAGGTTTGAATCAAAAACT
CTCTCGACCTAATGCGAAAGATTTCGACATCAAAAACCCTTTTTGCCTAAAGAGAAACAAAATGCAG

AGAGATAGAGATACCTACCTCTTTCACAAGTGAGTCTGTGTTGAACAATTCAATCTCACCGAAAAAC
TTCCTCCCACCACCGTTTTCCGTTGCTAAATGT

Product length: 505 bp

APPENDIX II

AtGenExpress data of *TBR* homolog gene, *TBL2* (At1g60790):

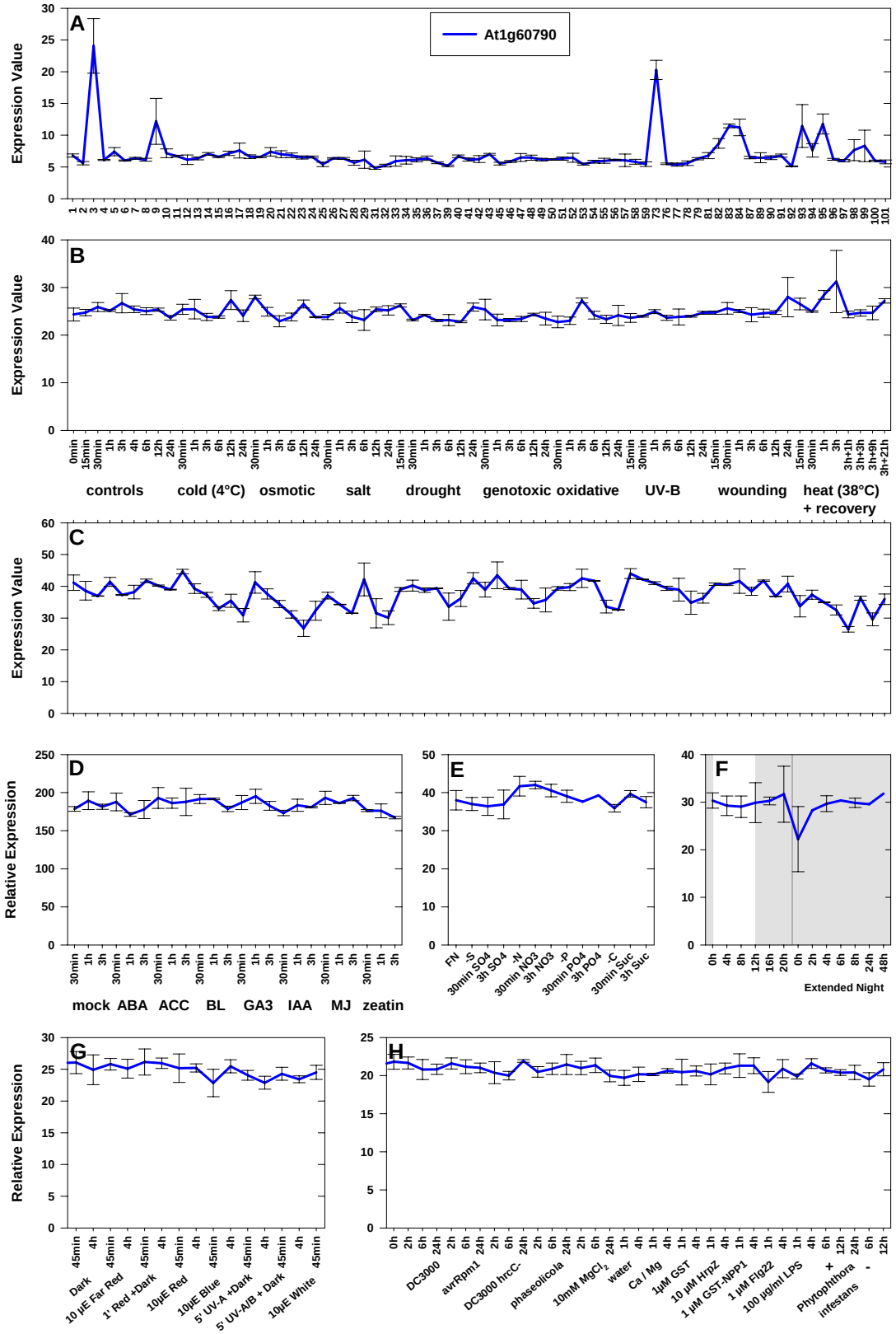

AtGenExpress data of *TBR* homolog gene, *TBL1* (At3g12060):